

**CHARACTERISTIC PROPERTIES AND  
RECYCLABILITY OF ALUMINIUM BEVERAGE  
CANS AND COFFEE CAPSULES**

**A Thesis Submitted to  
the Graduate School of  
İzmir Institute of Technology  
in Partial Fulfillment of the Requirements for the Degree of  
MASTER OF SCIENCE  
in Material Science and Engineering**

**by  
Rabia ÖNEN**

**June 2022  
İZMİR**

## ACKNOWLEDGMENTS

I would like to thank my thesis advisors, Dr. Mertol GÖKELMA and Dr. Aziz GENÇ for their constant support, fatherly patience, guidance and encouraging approach through the learning and writing process of my master thesis.

More, I would like to thank all the members of Gökelman-Lab for their friendship, support and assistance throughout the life of my master's degree.

I wish to thank my family who deserves the better expression of my gratefulness for their endless support and prayers. This thesis is dedicated to my dear fiancé Fırat TÜZGEL who always support and directed me for success. Also, I would like to express gratitude to my dear father, Ali ÖNEN who supported me and affectionately raised me for the whole of my life. I would like to thank my mother, Songül ÖNEN, is the person who always helped and stands behind me.

Last but not least, very special thanks go to the many others that go unmentioned but have contributed in one way or another to the successful outcome of this work.

## ABSTRACT

### CHARACTERISTIC PROPERTIES AND RECYCLABILITY OF ALUMINIUM BEVERAGE CANS AND COFFEE CAPSULES

Recycling is an effective way to reduce environmental pollution. Recycled aluminium uses 95% less energy than primary production. Therefore, there is a high demand for more efficient recovery technologies. Aluminium is used in transportation, consumer products, and electronics. Short life cycles, thin walls, and surface coatings make aluminium recycling difficult. This study focuses on UBCs and coffee capsules' properties and recyclability (CCs). A lab-scale electrical resistance heating chamber furnace was used for the de-coating and remelting experiments. The coatings were characterized using Scanning Electron Microscopy with Energy Dispersive Spectroscopy (SEM/EDS). As a result of the study, it was found that thermal pre-treatment temperature is more critical for alloys that have high Mg content due to their oxidation tendency. Suitable thermal pre-treatment temperature was observed between 520 to 550 °C for the samples. On the other hand, when the volatile organic content of the scraps was analyzed, it was observed that clean UBCs and CCs contain 2.2% and 9% volatile organic content, respectively, but it can be increased with increasing drink rest inside of it. A result of these experiments shows that the metal yield can differ up to 3.5% due to the drink residues (sugar). Also, it was observed that high-density pressing of the samples prior to the de-coating process increases the amount of the entrapped carbonaceous materials and decreases the de-coating efficiency. Finally, it was observed that samples with low wall thicknesses should be remelted under a salt flux to prevent oxidation and allow coalescence.

## ÖZET

### ALÜMİNYUM İÇECEK KUTULARININ VE KAHVE KAPSÜLLERİNİN KARAKTERİSTİK ÖZELLİKLERİ VE GERİ DÖNÜŞTÜRÜLEBİLİRLİĞİ

Geri dönüşüm, çevre kirliliğini azaltmanın etkili yollarından biridir. Alüminyum geri dönüşümü, birincil üretime kıyasla enerji tüketimini %95'e kadar azaltabilir. Bu nedenle, daha verimli kurtarma teknolojilerine yüksek talep var. Alüminyum tüketimi ulaşım, tüketim ürünleri ve elektrikli ekipmanlar gibi birçok sektörde artış göstermiştir. Ambalaj ürünlerinde kullanılan alüminyumun geri dönüşümü, kısa yaşam döngüleri, düşük duvar kalınlıkları ve yüzeydeki kaplama malzemeleri nedeniyle zor olabilir. Kaplamalar, kaplama malzemesine ve baz alaşımına bağlı olarak farklı etkilere sahip olabilir. Bu çalışma, alüminyum içecek kutuları ve kahve kapsüllerinin karakteristik özelliklerine ve geri dönüştürülebilirliğine odaklanmaktadır. Kaplama çözme ve yeniden eritme deneyleri için laboratuvar ölçeğinde bir elektrik dirençli ısıtma odası fırını kullanıldı. Kaplamalar, Enerji Dağılım Spektroskopisi (SEM/EDS) kullanılarak karakterize edildi. Çalışma sonucunda, oksidasyon eğiliminden dolayı yüksek Mg içeriğine sahip alaşımlar için ısıl ön işlem sıcaklığının daha kritik olduğu tespit edilmiştir. Deneylerde kullanılan numuneler için uygun ısıl ön işlem sıcaklığı 520 ile 550 °C arasında gözlemlenmiştir. Öte yandan hurdaların uçucu organik içeriği incelendiğinde, temiz UBC'lerin ve CC'lerin sırasıyla %2,2 ve %9 uçucu organik içerik içerdiği, ancak içindeki içecek artıklarının artmasıyla artırılabilceği görülmüştür. Bu deneyler sonucunda, içecek artıkları (şeker) nedeniyle metal veriminin %3.5'e kadar değişebileceğini göstermektedir. Ayrıca numunelerin kaplamadan arındırma işleminden önce yüksek yoğunlukta preslenmesinin, tutulan karbonlu malzeme miktarını arttırdığı ve kaplama verimini azalttığı görülmüştür. Son olarak, oksidasyonu önlemek ve kaynaşmayı sağlamak için düşük duvar kalınlıklarına sahip numunelerin bir tuz akışı altında yeniden eritilmesi gerektiği gözlemlendi.

# TABLE OF CONTENTS

LIST OF FIGURES .....	vii
LIST OF TABLES .....	xi
CHAPTER 1. INTRODUCTION .....	1
CHAPTER 2. LITERATURE REVIEW .....	3
2.1. Aluminium Production.....	3
2.1.1. Primary Production of Aluminium .....	3
2.1.2. Secondary Production of Aluminium .....	8
2.1.3. Environmental and Economic Comparison between Primary and Secondary Production of Aluminium .....	10
2.2. Usage Areas and Properties of Aluminium .....	13
2.3. Aluminium Packaging Products .....	16
2.4. Environmental and Economic Effects of Beverage Cans and Coffee Capsules .....	18
2.5. Industrial Recycling Techniques.....	20
2.5.1. Pre-Treatment Methods .....	22
2.5.2. Remelting Methods.....	26
2.5.3. Metal Losses During Recycling.....	33
CHAPTER 3. MATERIALS, CHARACTERIZATION, AND METHODS .....	35
3.1. Materials .....	35
3.2. Experimental Setup.....	35
3.3. Experimental Procedure.....	37
3.3.1. Thermal Pre-Treatment Experiments.....	37
3.3.2. Remelting Experiments.....	39
CHAPTER 4. RESULT AND DISCUSSION .....	42
4.1. Characterization Results .....	42

4.1.1. Used Beverage Cans .....	42
4.1.2. Coffee Capsules .....	44
4.2. Thermal Pre-Treatment Results .....	49
4.2.1. Used Beverage Cans .....	49
4.2.2. Coffee Capsules .....	62
4.3. Re-melting Results .....	66
4.3.1. Used Beverage Cans .....	66
4.3.2. Coffee Capsules .....	70
CHAPTER 5. CONCLUSIONS .....	73
CHAPTER 6. FUTURE WORKS .....	74
REFERENCES .....	75
ATTACHMENT .....	82

# LIST OF FIGURES

<b><u>Figure</u></b>	<b><u>Page</u></b>
Figure 2.1. Bayer Process Steps <sup>6</sup> .....	4
Figure 2.2. Summary of the Bayer Process <sup>10</sup> .....	6
Figure 2.3. Schematic representation of Hall–Héroult process. ....	7
Figure 2.4. Primary aluminium production from raw material <sup>15</sup> .....	8
Figure 2.5. Typical recycled Al production pathways <sup>19</sup> .....	10
Figure 2.6. Carbon footprint Primary vs. Recycled Aluminium <sup>24</sup> .....	11
Figure 2.7. Red mud waste <sup>25</sup> .....	11
Figure 2.8. Comparison of primary and secondary aluminium production <sup>30</sup> .....	13
Figure 2.9. Usage areas of aluminium and Global recycled scrap by market <sup>32</sup> .....	14
Figure 2.10. Coating layers of beverage can and CC. ....	17
Figure 2.11. Coffee capsules machines market graph <sup>46</sup> .....	18
Figure 2.12. Global Beverage Cans Market <sup>50</sup> .....	19
Figure 2.13. Greenhouse Gas Emissions from replacing wasted containers, 2010 (million MTCO <sub>2</sub> E) <sup>23</sup> .....	20
Figure 2.14. Energy savings from different metals based on production route and recycled portion <sup>54</sup> .....	21
Figure 2.15. Flow chart of secondary production of aluminium <sup>54</sup> .....	22
Figure 2.16. Illustration of de-coating of a coated metal substrate under an O <sub>2</sub> gas <sup>60</sup> ....	24
Figure 2.17. Suitability of the sample for thermal pre-treatment process according to its VOC. ....	25
Figure 2.18. TGA curve of the epoxy-based coating with different heating rates under nitrogen gas <sup>61</sup> .....	25
Figure 2.19. Melting furnace selection criteria for Al recycling <sup>54</sup> .....	27
Figure 2.20. Functional diagram of a rotary furnace <sup>69</sup> .....	28
Figure 2.21. Tilt rotary furnace <sup>70</sup> .....	29
Figure 2.22. Schematic diagram of electric arc furnace <sup>75</sup> .....	29
Figure 2.23. The reduction in the number of Al droplets (coalescence) with time for different fluoride additions <sup>80</sup> .....	31
Figure 2.24. Equilibrium ternary diagram of CaF <sub>2</sub> -NaCl-KCl <sup>88</sup> .....	32

<b><u>Figure</u></b>	<b><u>Page</u></b>
Figure 2.25. NaCl KCl binary phase diagram <sup>88</sup> .....	32
Figure 2.26. The relationship between metal loss and CaF <sub>2</sub> addition for different salt/Al ratios <sup>87</sup> .....	33
Figure 3.1. (a) Memmert drying oven (b) Protherm laboratory-scale electrical resistance chamber furnace (c) Protherm tiltable casting furnace. ....	36
Figure 3.2. Set up of re-melting procedure. ....	37
Figure 3.3. Summary of the experimental procedure. ....	41
Figure 4.1. Mass Distribution of UBC component. ....	42
Figure 4.2. SEM image of the cross-section of a beverage can. ....	43
Figure 4.3. EDS result of the body part of a beverage can sample which held in the furnace at 500 °C for 90 minutes. ....	44
Figure 4.4. Mass distribution of CC component. ....	44
Figure 4.5. SEM image of the cross-section of a CC. ....	45
Figure 4.6 EDS result of the red coating material of CCs. ....	46
Figure 4.7 EDS result of the orange coating material of CCs. ....	46
Figure 4.8 EDS result of the purple coating material of CCs. ....	47
Figure 4.9 EDS result of the brown coating material of CCs. ....	47
Figure 4.10. VOC of cleaned coffee capsule and beverage can samples. ....	49
Figure 4.11. Pressed and unpressed UBC samples after thermal pre-treatment. ....	50
Figure 4.12. The inner surface of the UBC samples after thermal pre-treatment (a) Unpressed and (b) Pressed. ....	51
Figure 4.13. EDS result of UBC sample kept in the oven from 520 to 550 °C for 90 minutes. ....	51
Figure 4.14. EDS result of the sample taken from the body of the UBC which was kept in the oven at 615-630 °C for 30 minutes. ....	52
Figure 4.15. EDS result of lid alloy of a UBC, which was kept in the oven at 615-630 °C for 30 minutes. ....	53
Figure 4.16. Thermal pre-treatment behaviour of different alloys on the UBC sample a) Body b) Base. ....	54
Figure 4.17. Mass loss of UBC sample at 550 and 600 °C. ....	54
Figure 4.18. Mass loss of pressed, unpressed, and industrial pressed UBC samples. ....	55
Figure 4.19. Mass loss of pressed and unpressed UBC samples at different temperatures. ....	56



<b><u>Figure</u></b>	<b><u>Page</u></b>
Figure 4.20. Mass loss comparison of UBC samples which have a sugar-free and sugared drink.....	57
Figure 4.21. Mass Loss comparison of UBC samples which have different brands and different drink residue.....	57
Figure 4.22. TGA analysis of UBC-body sample (international brand) under nitrogen gas.....	58
Figure 4.23. TGA analysis of UBC-body sample (international brand) under oxygen gas.....	59
Figure 4.24. TGA analysis graph of UBC- lid sample (international brand) under oxygen gas.....	60
Figure 4.25. TGA analysis of UBC-body sample (local brand) under oxygen gas.....	61
Figure 4.26. TGA analysis of UBC-lid sample (local brand) under oxygen gas.....	61
Figure 4.27. Coffee capsule samples after pre-heat treatment at 350, 400, 450, 500, 550, and 600 °C (from left to right).....	62
Figure 4.28. Mass loss of thermally pre-treated coffee capsule samples at different temperatures and holding times.....	62
Figure 4.29. EDS result of CC sample kept in the oven from 520 to 550 °C for no-holding time.....	63
Figure 4.30. EDS result of CC sample kept in the oven from 520 to 550 °C for 15 minutes.....	64
Figure 4.31. Mass loss of cleaned and uncleaned CC samples.....	64
Figure 4.32. TGA analysis of CC sample under oxygen gas.....	65
Figure 4.33. TGA analysis of CC sample under nitrogen gas.....	66
Figure 4.34. Flame observation during the burning of organics on the sample surface.....	67
Figure 4.35. Steps of the slow heating of the UBC samples.....	67
Figure 4.36. Coagulation of aluminium droplets in salt flux.....	68
Figure 4.37. Slag mass after direct melting of UBC samples which have different conditions and heating rates.....	68
Figure 4.38. Effect of heating rate on metal yield for unpressed and pressed UBC samples.....	69
Figure 4.39. The metal yield of different brand UBC samples.....	70
Figure 4.40. Coagulated coffee capsule samples after re-melting under salt flux.....	71

**Figure**

**Page**

Figure 4.41. Metal yield comparisons of different pre-treated and melting combinations of CC samples..... 71

## LIST OF TABLES

<b><u>Table</u></b>	<b><u>Page</u></b>
Table 1. Comparison of Primary and Secondary Aluminium Production Process <sup>26</sup> .....	12
Table 2. Chemical and Physical Properties of Aluminium <sup>1,31</sup> .....	13
Table 3. Experimental parameters of thermal pre-treatment trials of CCs.....	38
Table 4. Experimental parameters of thermal pre-treatment trials of UBCs.....	38
Table 5. Remelting Experiments and Sample Definitions for Coffee Capsule.....	40
Table 6. Remelting Experiments and Sample Definitions for UBC.....	41
Table 7. Mass of organic coating and metal for CC.....	48
Table 8. Experimental parameters and results of thermal pre-treatment trials of CCs...	82
Table 9. Experimental parameters and results of thermal pre-treatment trials of UBCs.	82

# CHAPTER 1

## INTRODUCTION

Aluminium is used in a wide range of products, from food packaging to spacecraft. This is due to its unique characteristics. It has a low density, is non-toxic, has good thermal conductivity, has excellent corrosion resistance, and is easy to cast, machine, and form<sup>1</sup>.

The Hall-Héroult method and Bayer process are used for the primary production of aluminium. Electrolytic reactions occur during the primary production of aluminium, and it emits carbon dioxide, which contributes to climate change, and the process consumes a huge amount of electrical energy<sup>2</sup>. Aluminium production consumes 5% of all electricity generated in the United States<sup>3</sup>. This indicates that recycling as a more energy-efficient method must be applied. Recycling is one of the most effective strategies to reduce pollution in the environment. When compared to primary production, aluminium recycling can save up to 95% of the energy. For instance, aluminium cans are also 100% recyclable, and they can be put back on the shelf in just 60 days<sup>4</sup>. Therefore, there is a high demand for more efficient recovery technologies. When it is compared with primary and secondary production, it can be said that secondary production significantly reduces the environmental impact, and it also reduces to use of primary sources. Because of this reason, alternative ways of producing aluminium should be investigated. Post-consumer products are one of the significant usage areas of aluminium. They are being used continuously in the world. Because of this reason, recycling supplies significant benefits to both economic and environmental aspects. If post-consumer aluminium packaging products can be recycled, it can provide less energy and primary source consumption.

However, recycling aluminium used in packaging products can be challenging due to short life cycles, low wall thicknesses, and coating materials on the surface<sup>5</sup>. The coatings might have different effects depending on the material of the coating and the base alloy. Post-consumer aluminium packaging products mainly consist of organic and inorganic substances. Organic pigments are compounds based on carbon chains and rings. Organic pigments are generally used for coating the packaging products, and some

packaging products introduce organic parts inside of the scrap, such as coffee in coffee capsule (CC), drink in used beverage can (UBC), etc. Organic substances of scraps lead to exothermic reactions due to combustion; because this reason, it leads to more oxidation during direct re-melting of the scraps; it also causes carbide formation due to high soluble carbon in aluminium. It causes melt quality issues. Its solution is thermal pre-treatment which prevents loss of aluminium and melt quality. Because the molten aluminium reactivity is more than solid aluminium, therefore when samples are thermally pre-treated in solid-state, it is going to be oxidized less than direct re-melting.

Therefore, understanding the coating of the samples which is going to be recycled is significant in increasing the efficiency of the recyclability. In this study, the characteristic properties and recyclability of aluminium beverage cans and CCs were investigated.

## CHAPTER 2

### LITERATURE REVIEW

#### 2.1. Aluminium Production

##### 2.1.1. Primary Production of Aluminium

Primary aluminium production is a two-step process. Firstly, alumina is refined and then reduced to metallic aluminium. Bauxite is an ore with a high concentration of aluminium hydroxide minerals (>35%), and it is the starting material for almost the entire alumina manufacture<sup>6</sup>. Alumina production starts with the mining of the bauxite ore, a hydrated aluminium oxide principally consisting of alumina ( $\text{Al}_2\text{O}_3$ ) with trace quantities of iron, silicon, and titanium. The Bayer process is used to convert bauxite into alumina. The Hall-Heroult process is used to convert alumina to aluminium metal electrolytically<sup>6</sup>. Roughly 4 t of bauxite is required to make 2 t of alumina, and almost 2 t of alumina is required to produce 1 t of aluminium metal via the Hall–Heroult process. Bauxite and used energy are the two most expensive components of Bayer's operational expenses per ton of alumina<sup>7</sup>.

##### **Bayer Process**

Bauxite is processed to produce Alumina, which has a melting point of 2040 °C and a boiling temperature of 2980 °C. Aluminium oxide, more commonly referred to as alumina, is a kind of amphoteric oxide composed of aluminium and oxygen. Bauxite contains silica, iron oxides, and titanium dioxide in addition to 30-60 wt.% of aluminium oxide. The Bayer process is the most often used method for converting bauxite into alumina.

The Bayer alumina manufacturing method consists of four steps that are digestion, filtration, precipitation, and calcination. The Bayer process steps are summarized in Figure 2.2.

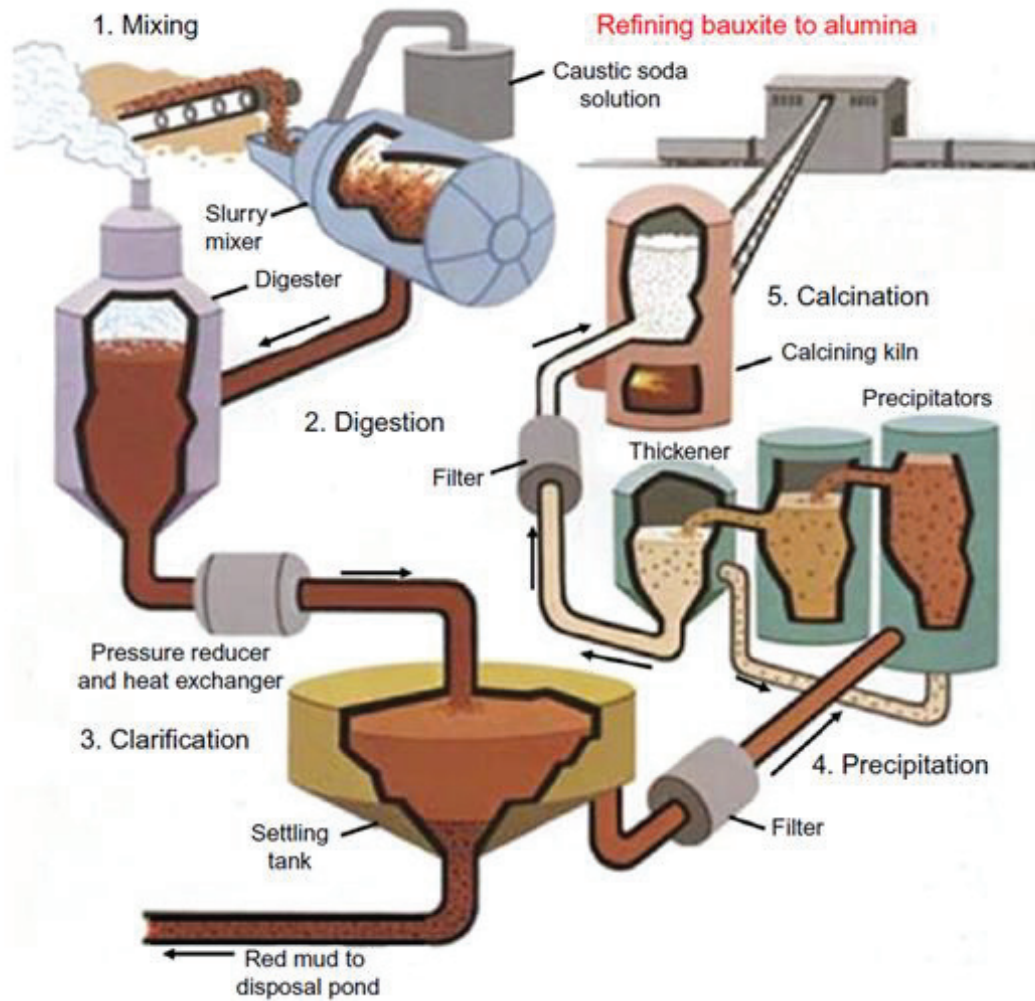
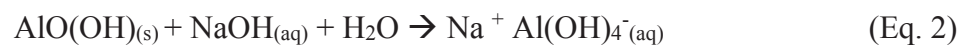


Figure 2.1. Bayer Process Steps<sup>6</sup>.

**Digestion:** This step of the Bayer process involves crushing for size reduction, which increases the digestion kinetics, and heating bauxite ore with sodium hydroxide at a temperature of around 150-200 °C to separate impurities from aluminium oxide in bauxite. Under these conditions aluminium-containing species in ore can be dissolved. Sodium hydroxide interacts with bauxite's aluminous minerals to generate sodium aluminate. Insoluble impurities, called red mud (RM), remain in suspension and are separated in filtration<sup>8</sup>. The reactions in digestion are:



**Filtration:** This step refines the solution that comes from the digestion process to remove insoluble impurities. Apart from alumina and silica, the remaining components of bauxite are insoluble. The undissolved solids sink to the bottom, forming red mud. A rotary sand trap is frequently used to separate this red mud from the solution.

**Precipitation:** Heat exchangers are used to cooling the remaining clear liquid before adding it to precipitators. It cooled to decrease the solubility of sodium aluminate solution and obtain a precipitate of aluminium hydroxide crystals. To speed up the crystal separation, aluminium hydroxide crystals are added to the precipitator solution. Seed crystals attract other crystals and create agglomerates, which are divided into product-sized and recycled seeds. Aluminium hydroxide crystal agglomerates are filtered and washed to remove the caustic solution. The precipitation occurs with the following equation<sup>9</sup>:



**Calcination:** The final step of the Bayer process is the calcination of aluminium hydrate. Aluminium hydroxide ( $\text{Al}(\text{OH})_3$ ) is converted to alumina ( $\text{Al}_2\text{O}_3$ ) through a calcination process conducted at roughly 1100 °C in rotary kilns<sup>8</sup>. The calcination reaction is given below.



After  $\text{Al}(\text{OH})_3$  is produced, it is used as the input material of Hall-Heroult Process to produce aluminium<sup>11</sup>.



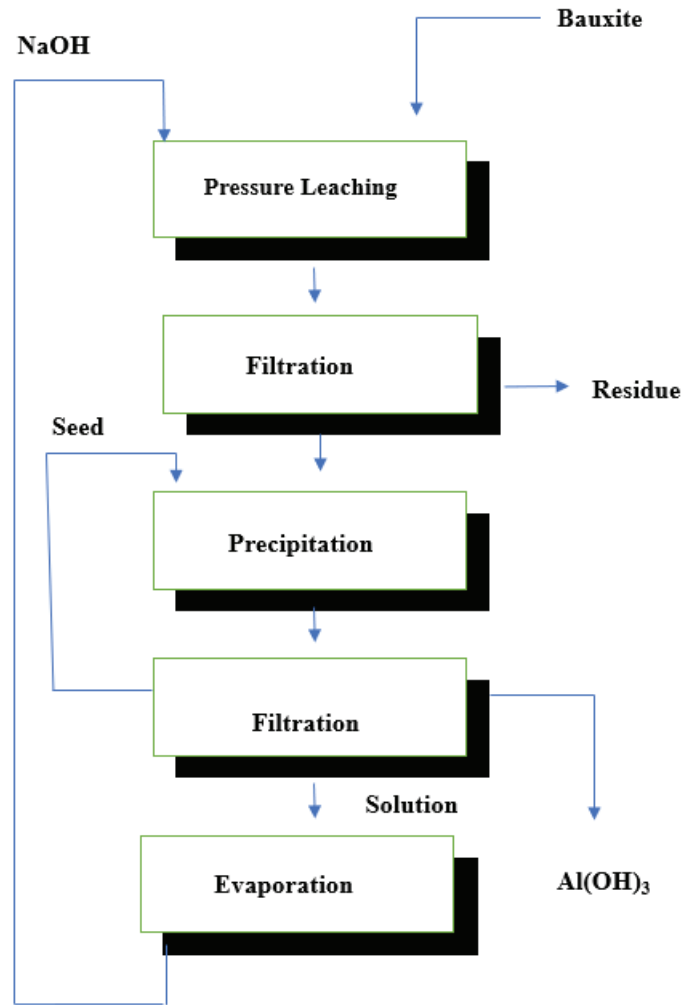


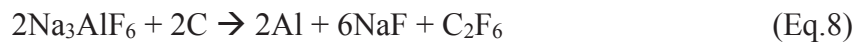
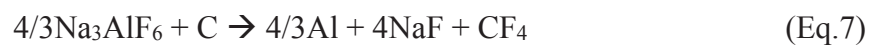
Figure 2.2. Summary of the Bayer Process<sup>10</sup>.

### Molten Salt Electrolysis (Hall–Héroult process)

The Hall–Héroult process is the most prevalent industrial method for aluminium smelting. The process involves dissolving aluminium oxide in molten cryolite and electrolyzing the molten salt solution, often in a specialized cell. Pure cryolite melts at 1009 °C. When alumina is added, its melting point falls to about 1000 °C. Cryolite is a good electrolyte because the electrolyte dissolves alumina, conducts electricity, and dissociates electrolytically at a higher voltage than alumina<sup>6</sup>.

Most electrolytes include aluminium fluoride (AlF<sub>3</sub>). With AlF<sub>3</sub>, the cryolite ratio, which is known as the molar ratio of sodium fluoride to aluminium fluoride, may be increased to 2–3 and the melting point lowered, allowing electrolysis at 940–980 °C. Liquid aluminium has a density of 2.3 g/ml between 950 and 1000 °C. The electrolyte

must be less than 2.1 g/ml in density for molten aluminium to separate from the electrolyte and settle in the cell bottom<sup>6</sup>. To electrolyze the mixture, a low voltage direct current of 100–300 kA is used. The oxygen released by the breakdown of alumina during the process reacts with the anode carbon, and the reactions which are shown below are observed<sup>6, 12</sup>. This process uses 6.23 kWh/(kg of Al); however, it typically requires 15.37 kWh<sup>13</sup>.



On an industrial scale, the Hall–Héroult technique produces 99.5–99.8% pure aluminium at 940–980 °C. Recycled aluminium is not utilized in this method since it does not need electrolysis<sup>14</sup>. The process of primary production of aluminium produces a significant amount of carbon dioxide, which contributes to global warming, and requires a large amount of electrical energy<sup>2</sup>. Figure 2.3 shows the schematic representation of Hall–Héroult process. Figure 2.4 shows the relevant material consumption and emissions of primary production.

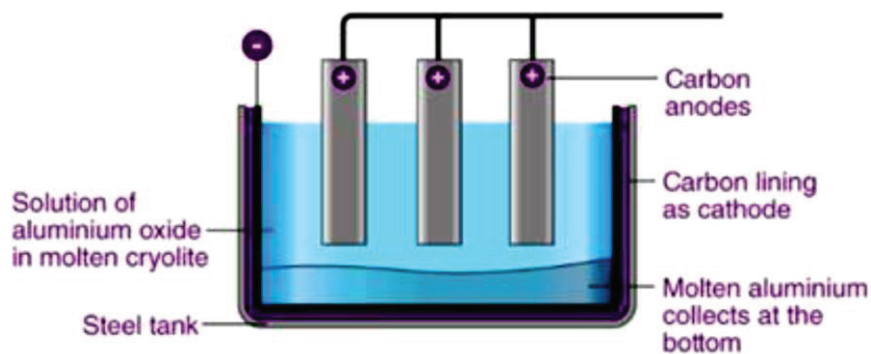


Figure 2.3. Schematic representation of Hall–Héroult process.

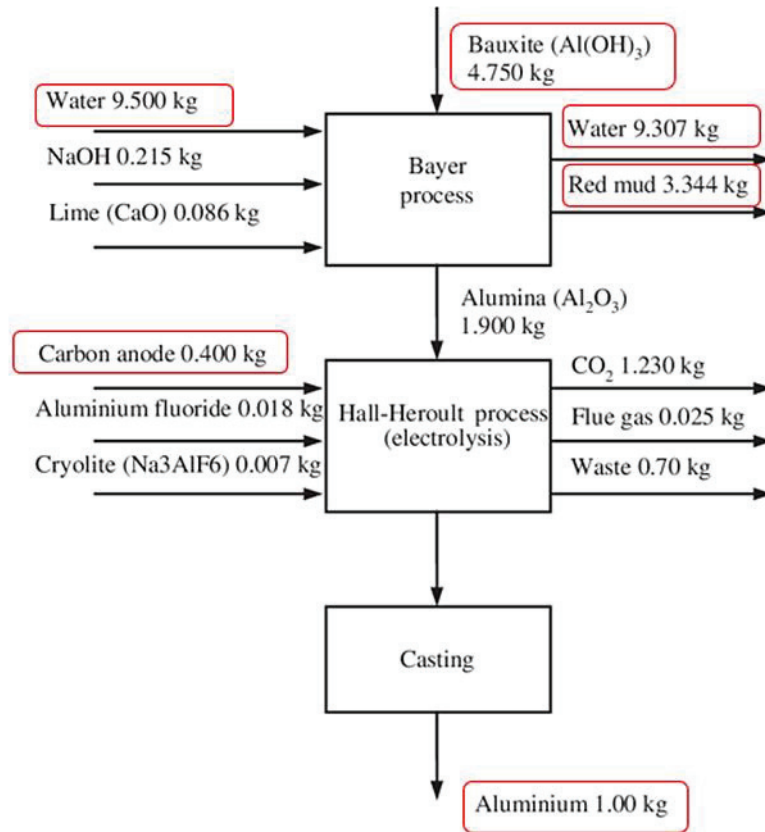


Figure 2.4. Primary aluminium production from raw material<sup>15</sup>.

### 2.1.2. Secondary Production of Aluminium

Secondary aluminium production refers to aluminium that is produced by using aluminium from different forms of aluminium waste and scraps, such as production off-cuts, machining chips, dross, and end-of-life aluminium products. Frequently, aluminium scraps are categorized as old, new, and dross. In a furnace, scrap (recycled) metal is remelted and cast into relevant forms.

#### Old Scrap

Old scrap is defined as a product after been used by consumers. When compared to other sorts of scraps, this form of scrap is more difficult to sort due to the fact that its composition and manufacturer are unknown as well as the complexity of their forms<sup>6</sup>. The reasons for the complexity can be products with a thin wall thickness, coating, or residue. Aluminium that is attached to plastic or paper (aluminium composite materials) might also cause recycling difficulties as well as the requirement of high-cost processes.

## **New Scrap**

In manufacturing, aluminium products are frequently trimmed to the required shape; this is referred to as AI cuts or trims as scrap. Additionally, new scrap components may be products with defects. Today, most of the new scraps can be effectively recovered since their composition is widely recognized and collection is not complicated<sup>6</sup>.

## **Dross**

Dross is a by-product/waste of the primary or secondary remelting processes. Dross contains less aluminium than both old and new scrap. To recover aluminium from dross, numerous process steps are required, and in some cases, the expenses exceed the revenue. However, as more nations implement regulations in response to environmental concerns over dross, the incentive to recover dross grows.

## **Sorting and Collecting of Scraps**

Sorting and collecting the scraps are significant steps in a recycling procedure. Scraps can be collected with the deposit or separation during the collecting procedure. There are different alloys that have different qualities in old scraps; therefore, sorting is necessary for old scraps to increase the yield of the recycling. Sorting methods can be classified into two groups depending on the used techniques: manual and automated sorting.

Manual sorting, also called hand sorting, is the basic sorting that does not require any facilities, and it is a useful alternative to separate scrap by categorizing their density and shapes using hands.

Automated sorting methods such as LIBS (Laser-Induced Breakdown Spectroscopy), magnetic separation, Eddy-current sorting (ECS), and thermal separation allow the classification of metals using an automated device. In automated sorting, material properties of metals are generally used. For instance, it is made use of properties of conductivity and density in ECS, and melting points in thermal separation<sup>16</sup>. Municipal recycling facilities (MRFs) collect various kinds of waste. The scrap can next be hand-sorted, semi-automatically sorted, or automatically sorted. Hand sorting labor expenses have prompted innovative automatic sorting techniques<sup>17, 18</sup>.

Screening can be used to eliminate microscopic or big contaminants from scrap. A few examples of oversize and undersized materials are paper and cardboard. Trommels

are frequently used for screening. Glass and steel may be separated from aluminium using an air separator. A magnetic separator may also separate ferrous from non-ferrous materials. Electrostatic separators (ES) are used to separate non-metallic contaminants from Al, such as plastics and paper<sup>19</sup>. It is summarized the typical recycled Al production pathways in Figure 2.5. After sorting and collecting the scraps, they can be recycled by using direct remelting and remelting under salt flux. A thermal pre-treatment process can be used to increase metal yield in case the scraps have an organic coating or a residue. These techniques are explained in Section 2.5.

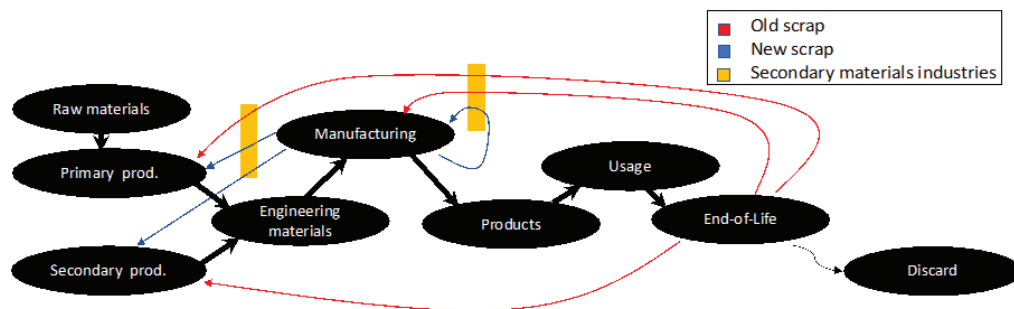


Figure 2.5. Typical recycled Al production pathways<sup>19</sup>.

### 2.1.3. Environmental and Economic Comparison between Primary and Secondary Production of Aluminium

When primary and secondary aluminium production is compared, secondary aluminium production has significant advantages in economic and environmental aspects.

In environmental aspects, the primary production of aluminium causes CO<sub>2</sub> emission in high volume due to the oxidation of carbon anodes, and high electricity consumption (in case the electricity is not produced by any renewable sources)<sup>20</sup>. CO<sub>2</sub> emission, which comes from the primary production of aluminium can be reduced by 93% by recycling aluminium scraps<sup>21</sup>. Secondary production of aluminium emits 17 times less air pollution, produces between 5 and 9 times less solid waste, and consumes 35 times less water than the primary production of aluminium. In addition, Recycling aluminium consumes 94% less carbon than producing aluminium via molten salt electrolysis. Figure 2.6 presents the difference between the CO<sub>2</sub> emission of both processes. Besides these, alumina mining and refining release toxics into the land and water. For every ton of aluminium produced, around 5 tons of red mud waste which are shown in Figure 2.7, is

created, along with  $\text{NO}_x$  and  $\text{SO}_x$ , which contributes to acid rain and smog. Also, toxic fluorides, volatile hydrocarbons, and other industrial emissions are observed<sup>22, 23</sup>.

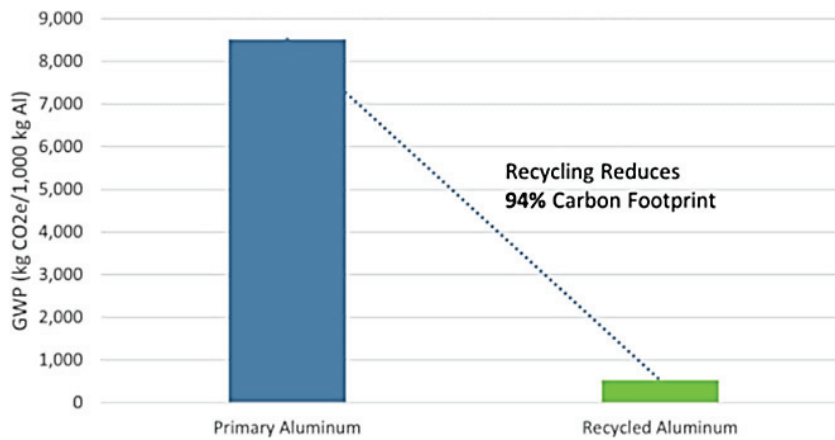


Figure 2.6. Carbon footprint Primary vs. Recycled Aluminium<sup>24</sup>.



Figure 2.7. Red mud waste<sup>25</sup>.

As mentioned before, the primary production of aluminium consists of more steps in comparison to recycling, such as alumina extraction from bauxite and electrolytic production of aluminium. The primary aluminium production needs 4-5 kgs of bauxite to produce 1 kg of aluminium. The most expensive operational costs of the primary production are the bauxite and the electricity. In addition to large  $\text{CO}_2$  emissions due to the combustion of anodes, aluminium manufacturing uses a significant amount of water due to the hydrometallurgical steps in the primary production. Red mud is generated as waste which causes environmental devastation.

Instead of 1230 kgs of CO<sub>2</sub> per tonne Al, Secondary Production emits only 75 kgs<sup>15</sup>. In short, primary production consumes more natural resources and creates more waste in comparison to secondary production. A comparison of primary and secondary aluminium production processes is shown in Table 1.

Table 1. Comparison of Primary and Secondary Aluminium Production Process<sup>26</sup>.

<b>Parameters</b>	<b>Primary Process</b>	<b>Secondary Process</b>
Consumption (GJ/t Al produced)	174	10
Atmospheric emissions (kg/t Al produced)	204	12
Solid Waste (kg/t Al produced)	2100 to 3650	400
Consumption of water (kg/ t Al produced)	57	1.6

In economic aspects, the recycling of aluminium reduces consuming of bauxite which is used as a raw material for the primary production of aluminium. When secondary production of aluminium is maintained, bauxite consumption is going to decrease. Therefore, the cost comes from bauxite mining is going to decrease too. Secondary production of aluminium needs between 10 and 15 times less energy than primary production of aluminium<sup>27</sup>. When scraps are recycled, it leads to the saving of aluminium sources in the World, and it decreases the cost of storage of wastes. The energy which is used for secondary production of aluminium is 5% of the energy which is required for primary production of aluminium<sup>28</sup>. In 2003, aluminium recycling saved more than 1.71011 kW h (0.57 quad) of energy in the United States, the equivalent of thirty-two 600 MW coal-fired power plants<sup>29</sup>.

According to these comparisons between these two types of production of aluminium, secondary production of aluminium and recycling has significant advantages on the environment and economy, as shown in Figure 2.8.

As a result of the chapter, it is obvious that recycling aluminium from secondary sources such as household wastes, packaging products, and window frames contributes positively to the environment and economy.

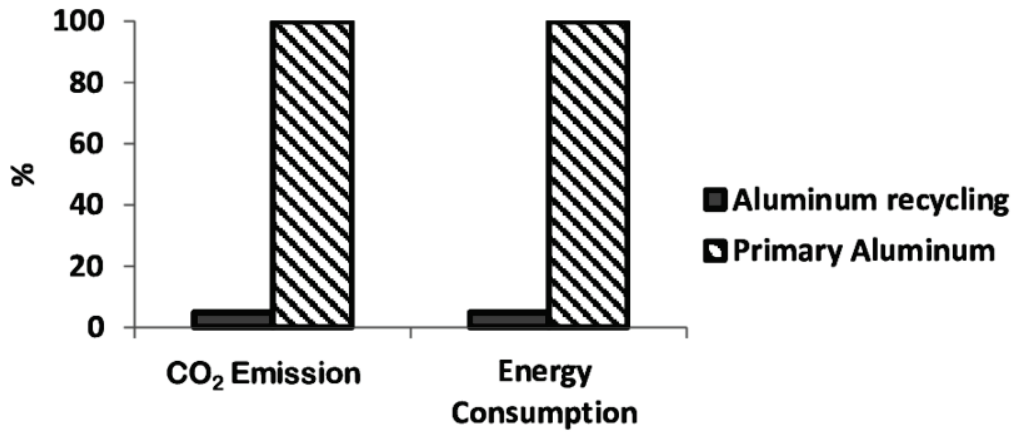


Figure 2.8. Comparison of primary and secondary aluminium production<sup>30</sup>.

## 2.2. Usage Areas and Properties of Aluminium

Aluminium is the most abundant metal in the Earth's crust (8.1%), although it is relatively rare in nature. Aluminium which has wide usage areas can be used in power lines, buildings, window frames, electronics, household and industrial appliances, aircraft, spacecraft, ships, and automotive due to its unique characteristics.

Table 2. Chemical and Physical Properties of Aluminium<sup>1,31</sup>.

<b>Atomic Mass</b>	26.98154 g.mol <sup>-1</sup>
<b>Density</b>	2.7 g cm <sup>-3</sup> at 20 °C
<b>Melting Point</b>	660.4 °C
<b>Boiling Point</b>	2467 °C
<b>Elastic Modulus</b>	70 GPa at 20 °C
<b>Tensile Strength</b>	90 MPa at 20 °C
<b>Thermal Conductivity</b>	237 W/m.K
<b>Electric Conductivity</b>	36,9 10E6 siemens/m

Aluminium is light, non-toxic, thermally conductive, corrosion-resistant, and easy to cast machine and shape. It is a highly malleable and ductile metal. Aluminium is a good electrical conductor and costs less than copper<sup>1</sup>; that's why it is used in transmission lines. Its chemical and physical properties are summarized in Table 2. The distribution of



usage areas of aluminium is shown in Figure 2.9. The transport and packaging industries have the highest portion in their usage areas.

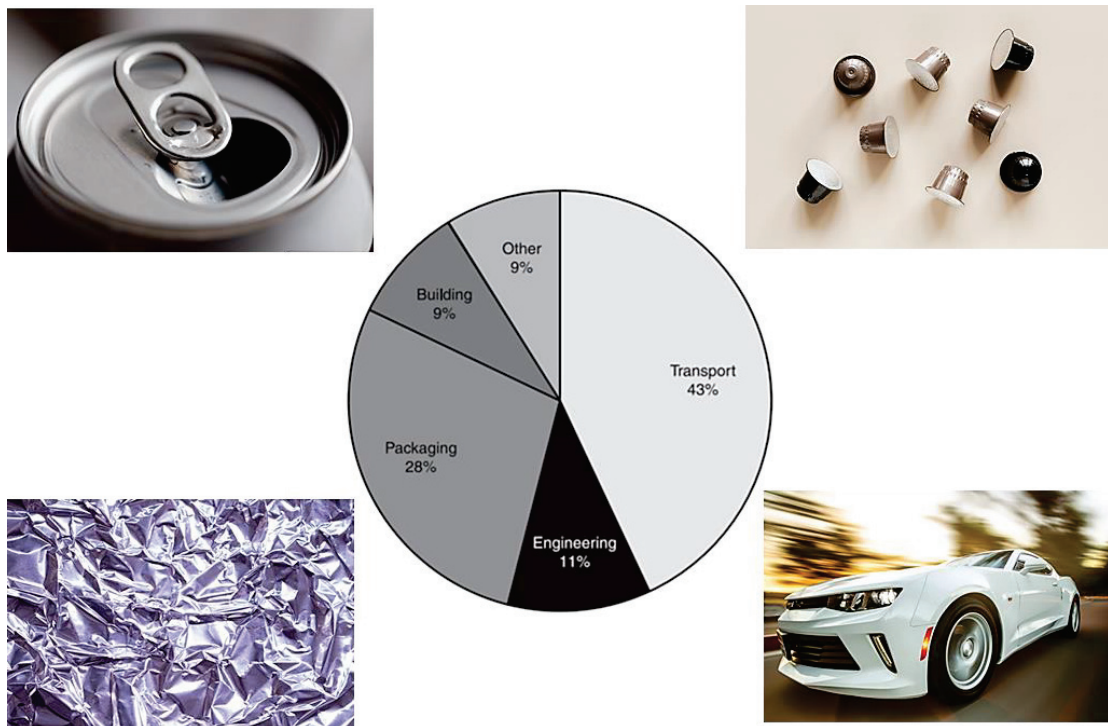


Figure 2.9. Usage areas of aluminium and Global recycled scrap by market<sup>32</sup>.

### Power Lines

Aluminium has a better conductivity to weight ratio than copper, which is one of the most often utilized materials in electrical applications. Because aluminium is 30% lighter than copper, a bare wire with the same electrical resistance weighs half as much. Aluminium is also less expensive than copper, making it more attractive from a financial point of view<sup>31</sup>.

### Buildings

Aluminium is a valuable material used in high-rise structures and skyscrapers because of its malleability, strength, and versatility. It is also a great material for front-end and back-end energy savings. Steel would also make towers heavier, requiring higher foundations and increasing construction costs<sup>31</sup>.

## **Window Frames**

Aluminium frames are a good alternative for houses and workplaces. They are also light and impact-resistant, which is important in areas prone to severe winds and storms. Windows made of aluminium are less costly and require less care than wooden windows<sup>31</sup>.

## **Electronics**

Aluminium is increasingly used in smartphones, tablets, laptops, flat-screen TVs, computer displays, and other devices. Aluminium is a versatile material that can appear classy but reliable. Aluminium has recently replaced steel and plastic in electronics. Its high heat conductivity made it perfect for cooling CPU and graphics devices. Modern devices have aluminium bodies and casings.

Aluminium is stronger and more reliable than plastic, yet lighter than steel, leading to an increase in aluminium utilization among market-leading manufacturers<sup>31</sup>.

## **Household and Industrial Appliances**

Aluminium is used in precision tubing for freezers and air conditioners, but it has additional applications. In addition to commercial appliances, many home appliances use aluminium frames. Aluminium is a great material for refrigeration and freezing because it has properties that help to cool quickly and efficiently. Modern refrigerators would be quite different without aluminium's benefits<sup>31</sup>.

## **Aircraft and Spacecraft Components**

Aluminium is utilized in aviation due to its high strength-to-weight ratio, malleability, and resistance to corrosion. Since the Wright brothers used aluminium to make the first wooden-frame aircraft's engine crankcase, humans can fly. Aluminium is stronger than steel but weighs less; therefore, utilizing it in airplane construction increases cargo and passenger capacity while decreasing fuel consumption. Aluminium's excellent corrosion resistance helps assure the safety of the aircraft and its passengers, which is a basic need for air travel. Modern spacecraft and rocket technologies rely on advanced aluminium alloys. Aluminium-lithium alloys have been used in NASA's space program since the program's beginning. Aluminium oxynitride, a transparent ceramic used to produce bulletproof materials, is one technique to make spacecraft windows<sup>31</sup>.

## **Ships**

Ships benefit from light and strong materials, especially when carrying cargo. Aluminium's low mass and high surface area allow for more surface area and less mass without compromising hull strength. This enables more products, persons, or fuel to be loaded. Aluminium is also used to build yachts, speedboats, and underwater vehicles<sup>31</sup>.

## **Automotive**

Aluminium is promoted as the most cost-effective and eco-friendly option to improve performance, fuel efficiency, and emissions while improving safety and durability. Manufacturers of automobiles are increasingly using aluminium for its strength and environmental benefits. Lighter and more nimble vehicles don't have to compromise strength or durability. Using aluminium in automobiles is also more sustainable due to the ease of recycling<sup>31</sup>.

## **Packaging Products**

This group is explained in detail in Chapter 2.3 since it is the target of this research.

### **2.3. Aluminium Packaging Products**

Aluminium is widely used in the packaging sector. Aluminium cans keep the taste and the nutritional value of drinks and food for years. Because of the long storage times, packaging-food interactions must be maintained to a minimum.<sup>33</sup> Therefore, an organic layer shields the can from food impacts and prevents chemical reactions between the can's metal and the food.

#### **Used Beverage Cans and Coffee Capsules**

Beverage can and CCs are two of the packaging products which is widely used in the world. There are two different coatings for both CC and beverage cans which are shown in Figure 2.10. One of these is an inner coating which is the layer between coffee and metal. Conversely, an outer coating that satisfies optically expectations<sup>34-36</sup>.



Figure 2.10. Coating layers of beverage can and CC.

The type of the inner coating depends on the environment, availability, and the metal. Epoxy-based coatings are currently used for 90% of all coatings applied globally. They are suitable for most foods<sup>37</sup>. Another ten percent is made up of organic chemicals such as organosols and polyesters. Organosols are industrial coatings in which polyvinyl chloride (PVC) and other resins are suspended or distributed in an organic solution<sup>38</sup>. These coatings are often created with plant-based organic compounds<sup>39</sup>. Outer coating pigments can be organic and/or inorganic. Heat can destroy organics but not inorganic coatings like  $\text{TiO}_2$ <sup>40, 41</sup>. The outer coatings are applied mostly due to optical reasons.

Chemical interactions between the metal and the food are prevented by the inner coating, which is an organic layer<sup>42, 43</sup>. Many different can coatings are available commercially, although most of them use a restricted number of chemicals. Coatings include many additives, such as lubricants, anti-foaming agents, adhesives, scavengers for hydrochloric acids, and pigments. Toxicological Research, public discussion, and recent regulatory decisions have led can producers and food businesses to abandon BPA-based epoxy coatings. The first-generation epoxy coatings were acrylic and polyester, but polyolefin and non-BPA epoxy coatings have recently been developed<sup>37, 39-41</sup>.

Moreover, the alloy composition of beverage cans and CC are different from each other. For instance, aluminium alloys AlMn1Mg1Cu (EN AW-3104) and AlMg4.5Mn0.4 (EN AW-5182) are used for the body alloy and the lid alloy (EN AW-5182), respectively. The lid alloy has more magnesium content, which affects the oxidation tendency during remelting<sup>44</sup>. The coffee capsules are produced from the 8011 series, which contains only 0-0.1% Mg content<sup>45</sup>.

## 2.4. Environmental and Economic Effects of Beverage Cans and Coffee Capsules

Coffee capsules have achieved wide popularity among consumers in recent years, as shown in Figure 2.11. The capsules are usually made of plastics or aluminium. In 2020, the market for coffee pods and capsules was valued at USD 25.07 billion, and it is predicted to increase at a CAGR of 7.07% from 2021 to 2026. Between 2018 and 2026, the global capsule coffee machines market is predicted to increase at a CAGR of 13.5 percent, from USD 5.31 billion in 2016 to USD 18.84 billion by the end of 2026<sup>46</sup>. The increasing usage of capsules generates large amounts of waste, which raises environmental concerns.

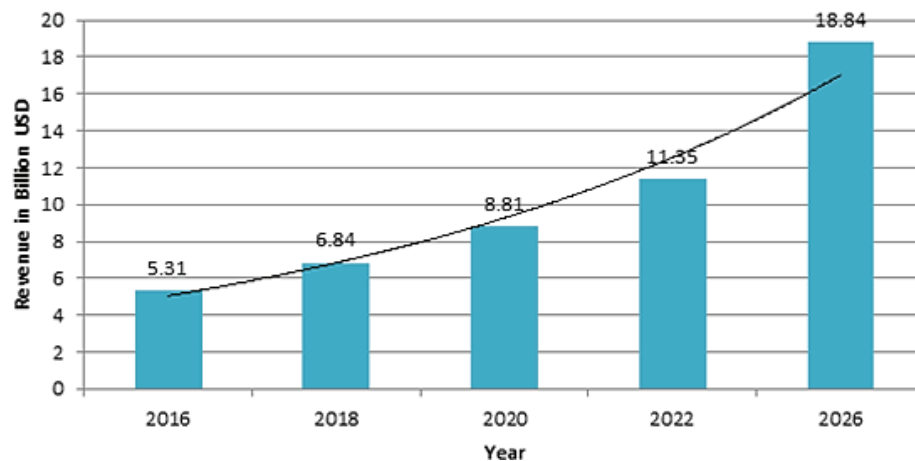


Figure 2.11. Coffee capsules machines market graph<sup>46</sup>.

The aluminium coffee capsules contain a large amount of moisture after being used as well as a coffee rest, organic coatings (inside and outside of the capsule), and metallic aluminium.

There are 3 end-of-life possibilities for the used coffee capsules: being collected by the producer, incineration, or landfilling. However, due to social behaviour, it is more likely for the capsules to end up in municipal waste. Some countries apply landfilling, and some of them incinerate their municipal solid wastes<sup>47, 48</sup>. In the case of landfilling, the metal value is completely lost. On the other hand, after incineration (temperature up to 1100 °C), the aluminium fraction may be recovered with some losses due to the high oxidation affinity and high surface area<sup>36, 49</sup>. The outer surface of CC and pods consists of mostly organic-based coatings.

Depending on the kind and origin of the scrap, additional contaminants may be present. Common contaminants in post-consumer wastes include water, oil, sand, and product residues. These are utilized in the de-coating process and aid in determining the composition of waste gases and their treatment. Because of this reason, before thermal pre-treatment, the scrap should be cleaned of contaminants<sup>34</sup>.

Moreover, cans are containers made of aluminium, low carbon steel, or plastic. It's used to store liquid refreshments, including soda, alcoholic beverages, and fruit and vegetable juices. Aluminium cans are one of the most recyclable package forms available in the market, offering several packaging benefits such as long shelf life and low weight. They are therefore earning worldwide recognition. Aluminium can packaging is becoming more prevalent in industries such as food, medicines, oil, and chemicals<sup>50</sup>. There is 3 end of life possibilities for the UBCs: being collected by using deposit, incineration, or landfilling like coffee capsules<sup>51</sup>.

Beverage cans have achieved wide popularity among consumers in recent years, like coffee capsules. The worldwide aluminium can market reached USD 50.1 billion in 2021. The market is predicted to grow at a 3.0% CAGR from 2022-2027, reaching USD 54.3 billion by 2026, as shown in Figure 2.12<sup>50</sup>.

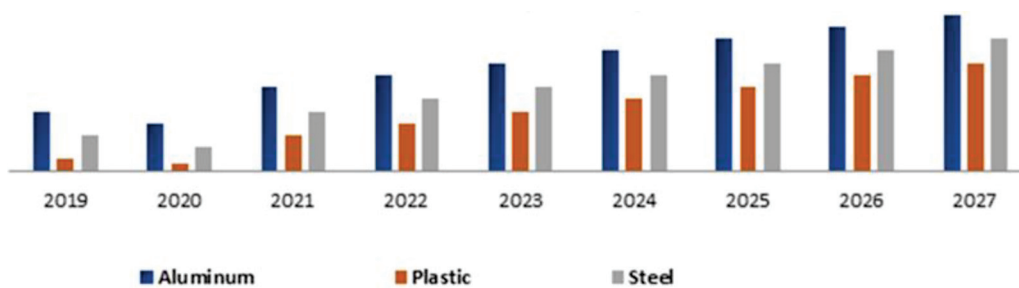


Figure 2.12. Global Beverage Cans Market<sup>50</sup>.

As a result of the graph, the increasing trend was seen until 2027 year for the global beverage cans market. It shows the necessity of recycling beverage cans. For instance, the United States discards twice as many beverage containers as it recycles.

These wastes have a significant negative impact on the ecosystem. Annual energy consumption equates to 36 million barrels of crude oil, and greenhouse gas emissions are 4.5 million tons. On the other side, wildlife is damaged to obtain minerals for primary production.

As indicated in Figure 2.13, replacing the 153 billion bottles and cans that were not recycled in 2010 caused 11.6 million tons of greenhouse gas emissions.

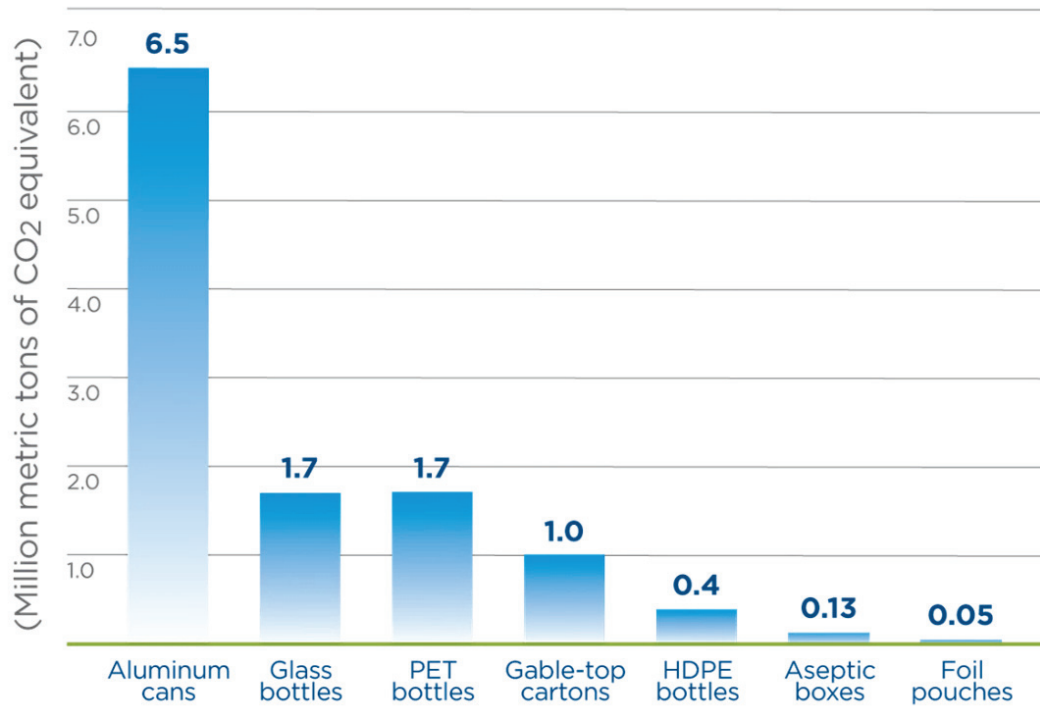


Figure 2.13. Greenhouse Gas Emissions from replacing wasted containers, 2010 (million MTCO<sub>2</sub>E)<sup>23</sup>.

While the aluminium industry has made a significant effort to reduce smelting-related greenhouse gas emissions, the worldwide amount of aluminium-related greenhouse gases has increased. This is owing to increased aluminium usage and hence increased energy output from coal, natural gas, and hydroelectric dams.

## 2.5. Industrial Recycling Techniques

Al production has one of the largest energy differences between primary and secondary production, compared to copper, zinc, magnesium, and steel, as it was shown in Figure 2.14. Al recycling reduces required energy by 95%<sup>52</sup>, the highest value compared to Mg, Cu, Zn, and steel, and emits 5% of greenhouse gas<sup>53</sup>.

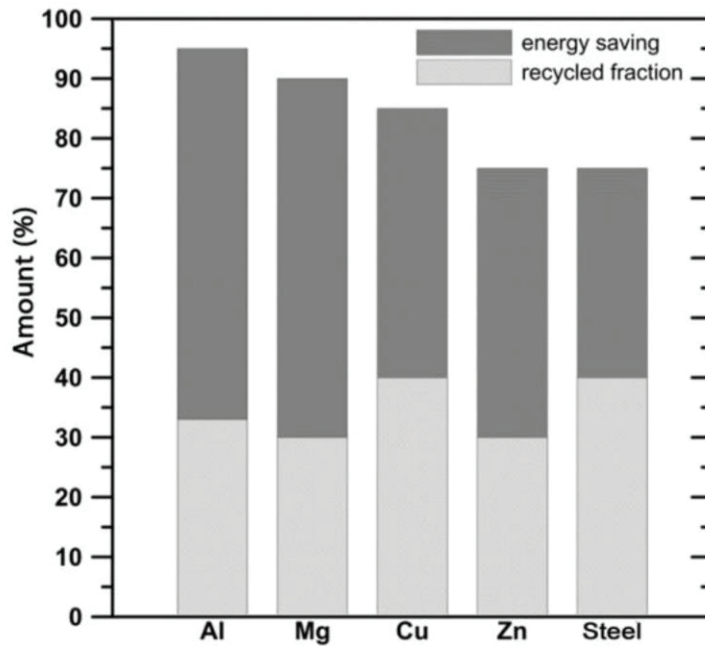


Figure 2.14. Energy savings from different metals based on production route and recycled portion<sup>54</sup>.

Metal recycling is significant for the sustainability of the world. It supplies many advantages for both economic and environmental aspects<sup>55, 56</sup>. Recycling contributes to one-third of global aluminium use<sup>57</sup>.

Sorting, shredding, and thermal pre-treatments are used during the recycling process to improve the efficiency of Al recycling in the production chain, as shown in the flow chart in Figure 2.15.

All these stages result in an increase in expense, but they also improve the quality of the scrap in terms of metal yield and recyclability.

Choosing the right melting furnace is important, and it depends on the type and amount of scrap<sup>58, 59</sup>. Each approach aims to achieve the largest melting capacity per unit volume while maximizing thermal efficiency to save fuel costs.



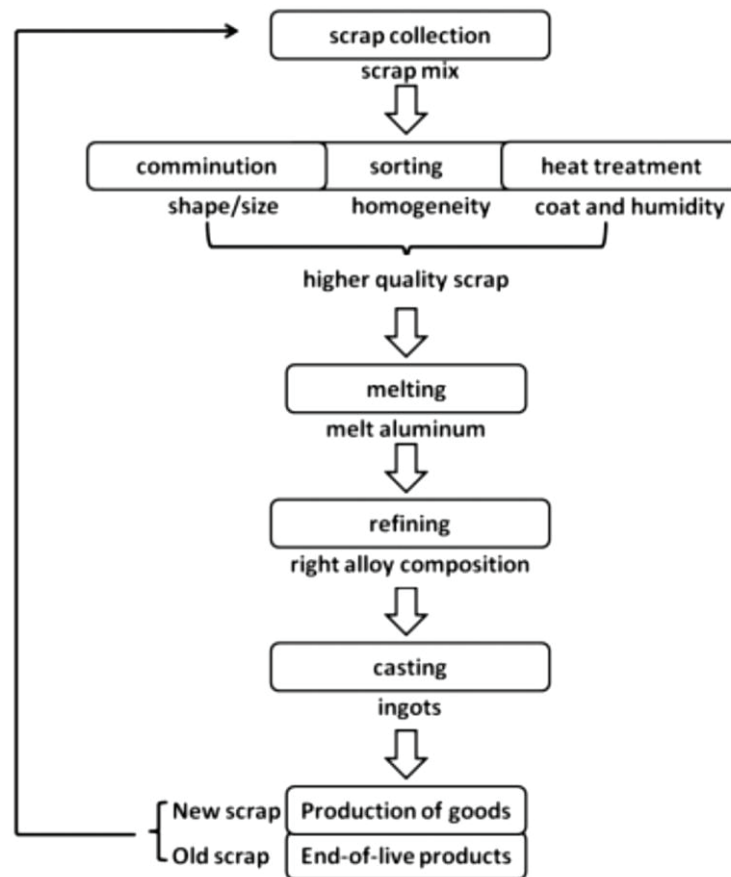


Figure 2.15. Flow chart of secondary production of aluminium<sup>54</sup>.

### 2.5.1. Pre-Treatment Methods

The various amounts of recyclable metal and impurities in aluminium scrap depend on the scrap's origin. Specific treatments can change these features before melting. The main pre-treatments for Al scrap are improving bulk density, eliminating non-aluminium scrap, and reducing impurities.

#### Mechanical Pre-Treatment

Mechanical pre-treatment is necessary prior to most recycling procedures. Mechanical treatment is mainly shredding and/or compaction of scraps.

#### *Shredding*

Shredding is performed for better sorting, which increases the recycling yield. Parts that may impede the recycling process are removed after shredding. Shredding makes the removal of unwanted parts easier<sup>19</sup>, such as magnetic separation. Due to

thermodynamic limits, metallic alloying components are difficult to extract from an Al melt, and shredding and mechanical separation of other metals are necessary prior to remelting<sup>6</sup>.

### *Compaction*

Compaction of scraps is also called bailing or briquette. Compaction is performed to improve transportation, handling, and storage, as well as to maximize recovery during remelting<sup>19</sup>. Typically, scrap processors compress UBCs into bales and new scrap turnings into briquettes. Bales are substantially bigger and less dense than briquettes. Furthermore, compaction might also reduce the recycling yield due to inefficient removal of organics during thermal pre-treatment.

### **Thermal Pre-Treatment**

Post-consumer aluminium packaging products mainly consist of organic and inorganic substances. Organic pigments are compounds based on carbon chains and rings. Organic pigments are generally used for coating the packaging products, and also some packaging products introduce organic parts inside of the scrap, such as coffee in CC drink in UBC, etc. Depending on the desired color, Cr, Co, Pb, and Mg are present in the coatings; therefore, undesired components can be introduced without de-coating the scrap<sup>54</sup>.

Organic substances of scraps lead to exothermic reactions due to combustion; because this reason, it leads to more oxidation during direct re-melting of the scraps; it also causes carbide formation due to the high soluble carbon amount in aluminium. It causes melt quality issues. Its solution is thermal pre-treatment which prevents loss of aluminium and melt quality. Thermal pre-treatment removes paint, ink, paper, plastic, and oil from a material to improve recycling by reducing metal losses during remelting. Because the molten aluminium reactivity is more than solid aluminium, therefore when samples are thermally pre-treated in a solid state, it is going to be oxidized less than direct re-melting.

Economically and environmentally, the method is beneficial. Thermal pre-treatment is categorized by its environment, which is oxygen and inert. First, scrap water is removed to prevent explosions. Increasing scrap quality increases process efficiency. This means less salt flux and dross during melting. Figure 2.16 shows a de-coating

process in an oxygen environment. The goal of thermal pre-treatment is to combust carbonaceous materials to reduce oxidation and carbon solubility. First, the coating decomposes by releasing hydrocarbons and leaving pigment residue, and then combustion occurs when surface carbon residue burns in the presence of oxygen. Inorganic material remains on the surface<sup>60</sup>.

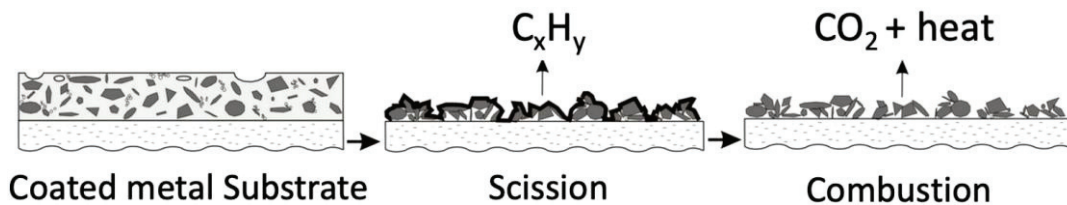


Figure 2.16. Illustration of de-coating of a coated metal substrate under an  $O_2$  gas<sup>60</sup>.

First, the hydrocarbons break down via scission, then carbon residue on the surface combusts with increasing temperatures<sup>60</sup>.

On the other hand, when thermal pre-treatment is applied to the sample in an inert environment, thermal degradation happens. Pyrolysis is described as the high-temperature decomposition of a material in the absence of oxygen. Combustion is not observed during the pyrolysis because of the absence of oxygen. Pyrolysis breaks down larger hydrocarbon molecules into smaller ones by heating them in a low oxygen atmosphere with the scission process. Smaller molecules like methane  $CH_4$  and water  $H_2O$  evaporate, forming tar.

As it was mentioned above, organic substances of scrap lead to exothermic reactions due to combustion, which increases the oxidation during direct re-melting of scraps and produces carbide formation since high soluble carbon amount in aluminium. It causes melt quality problems. Aluminium scrap with an organic content of above 5% is preferably de-coated to increase the remelting yield and metal quality, as well as operational stability and reduce dangerous and toxic gas emissions. Figure 2.17 shows the suitability of the sample for the thermal pre-treatment process according to its volatile organic content (VOC). The organic portion had to be burned prior to melting, but modern technology permits extraction without combustion.

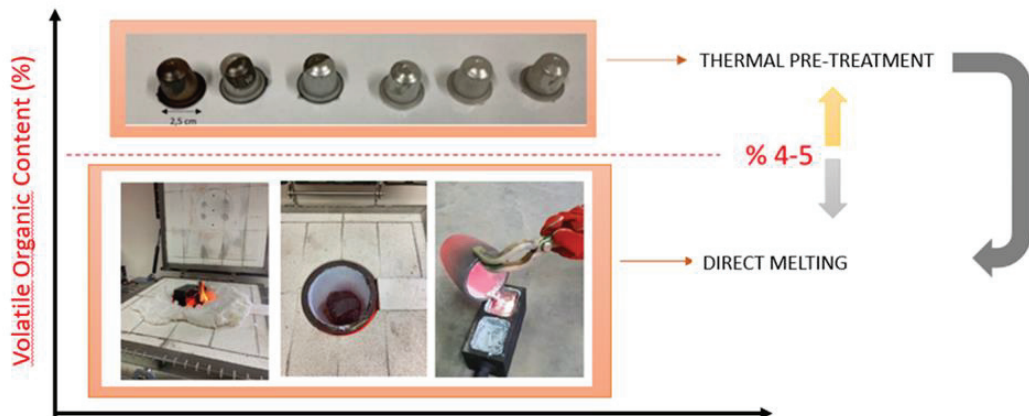


Figure 2.17. Suitability of the sample for thermal pre-treatment process according to its VOC.

Aluminium scraps can be difficult to recycle because it is commonly covered with an organic compound, usually lacquer or polymer. One of the common coatings is an epoxy-based coating for food packaging. Its TGA graph is shown in Figure 2.19, which includes four apparent degradation steps. The first step corresponds to a 7% weight loss, the second to 10%, the third (main degradation) to 44%, and the fourth (shoulder in the main degradation) to 65%. No degradation occurs between 600 and 800 °C, and the residue at 800 °C is independent of the heating rate, indicating that no competitive reactions occur during resin degradation or that all organic compounds that can be formed in competitive reactions decompose below 800 °C<sup>61</sup>.

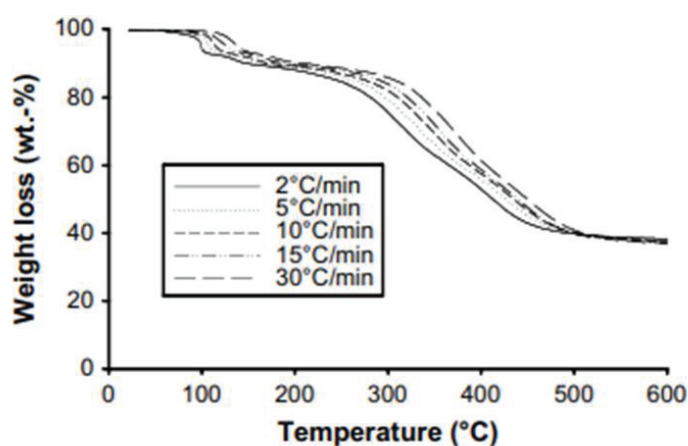


Figure 2.18. TGA curve of the epoxy-based coating with different heating rates under nitrogen gas<sup>61</sup>.

On the other hand, most of the food packaging scraps can contain organic rest inside it, like sugar rest in beverage cans. The rest also increases the VOC of the scraps. Therefore also, its thermal behavior should be investigated during the de-coating process. When you heat a sugar such as sucrose, it becomes dehydrated. Sucrose breaks down into glucose and fructose, loses water, becomes isomers, and polymerizes to form caramel, a red-orange solid at room temperature. Pure sugar caramelizes at 338°F (170 °C)<sup>62</sup>.

Cans are coated, and it contains 2–3% lacquer and paint<sup>19, 63</sup>. Emissions of smoke and soot, as well as dioxins and furans from burnt organics, are dangerous and difficult to remove. Significant increase in oxidation of waste with coatings compared to bare scrap, leading to higher metal loss. This impact transcends alloys. McAvoy et al.<sup>64</sup> discovered that melting lacquered scrap in salt flux decreased melt loss somewhat, but that lacquered scrap still lost more metal than bare scrap.

Kvithyld et al.<sup>65</sup> observed that thermal de-coating of scrap is temperature and environment-dependent. De-coating involves three steps: breaking polymer chains, forming VOCs, and oxidizing char (residue on the surface generated from the formation of VOCs). The use of an oxygen-free environment prevented char oxidation. The study found that high temperatures make autothermal operation harder (the coating is the heat source in the process). High temperatures also enhanced metal surface oxidation and metal loss. The results showed that recovery yield is based on the trade-off between a lower temperature (480-520 °C) to limit metal oxidation and the danger of coating persistence and quick heating (590-620 °C) below the melting point to remove coating but risk metal oxidation.

De-coating has further benefits. Because the scrap is heated during de-coating, remelting takes less time. This improves efficiency, allowing more scrap to be melted and recovered per time unit. Using organic compounds (VOCs) as fuel also saves energy<sup>19</sup>.

## **2.5.2. Remelting Methods**

### **Direct Remelting**

Several furnaces are used to melt Al scrap depending on the initial metal content, type and quantity of impurities, shape of the scrap, alloy composition change, operating conditions, energy cost, and desired output quality. Energy efficiency has been a long-time goal in countries such as Europe, where energy costs are high. This is why rotary

furnaces are more widespread in Europe. In the U.S., 95% of Al scrap is melted in gas reverberatory furnaces, which are less efficient (20–30%) but require less capital. Rotary furnaces are harder to operate and maintain. Metal yield and manufacturing volume are crucial furnace selection parameters. Samples are directly remelted by using a different type of furnace<sup>54</sup>. Figure 2.19 shows the criteria for choosing a suitable furnace for the melting experiment of aluminium.

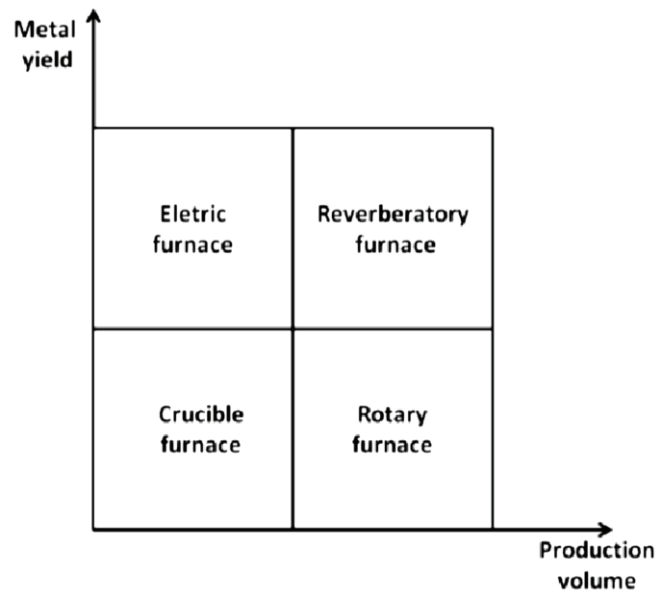


Figure 2.19. Melting furnace selection criteria for Al recycling<sup>54</sup>.

### *Reverberatory Furnace*

Reverberatory furnaces are brick-lined and have a curved roof. Depending on the application, furnaces are rectangular or round. The rectangular form allows for optimal charging and skimming access. Melted metal is heated in the furnace before tapping. Typical reverberatory furnaces have an energy efficiency of 15–39%, or the ratio of heat absorbed by the raw material to the total used fuel. High processing capacity and minimal operating and maintenance costs are reverberatory furnace advantages. High metal oxidation, low energy efficiency, and huge space needs are disadvantages.

### *Rotary Furnace*

A rotating furnace, shown in Figure 2.20, is commonly used to melt aluminium<sup>56, 66, 67</sup>. A cylindrical steel drum with refractory lining is supported by a structural steel frame. A flame of natural gas heats the furnace along the axis of the drum. Rotary furnaces

are utilized for melting scrap castings, extrusion scrap, UBC, and processing dross. This type of waste has a density to surface area ratio that is relatively low. This scrap material must be rapidly melted to prevent oxidation of the thin cross-section. They are effective for melting because they rotate the heated roof refractory directly under the melt for optimal contact and mixing. The flux and feed are then introduced into the furnace. Then, the furnace with its natural gas burner in the melting chamber rotates. The molten metal is therefore transferred to a holding furnace or casting room.

Reverberatory furnaces are less efficient than rotary furnaces. This furnace achieves reduced emissions, uniform metal composition, and decreased fuel consumption. Rotating the internal refractory increases the direct heat transfer to the charge. Installation and maintenance of rotary furnaces are expensive. They are excellent for melting dross and oxidized scrap.<sup>68</sup> A gas cleaning system extracts fumes from a chamber's furnace. The study of melting inside a rotary furnace is complex and difficult as a result of random scrap and void distribution, scrap heterogeneity (type, size, and shape), turbulence, gas combustion, mass, and energy transmission.

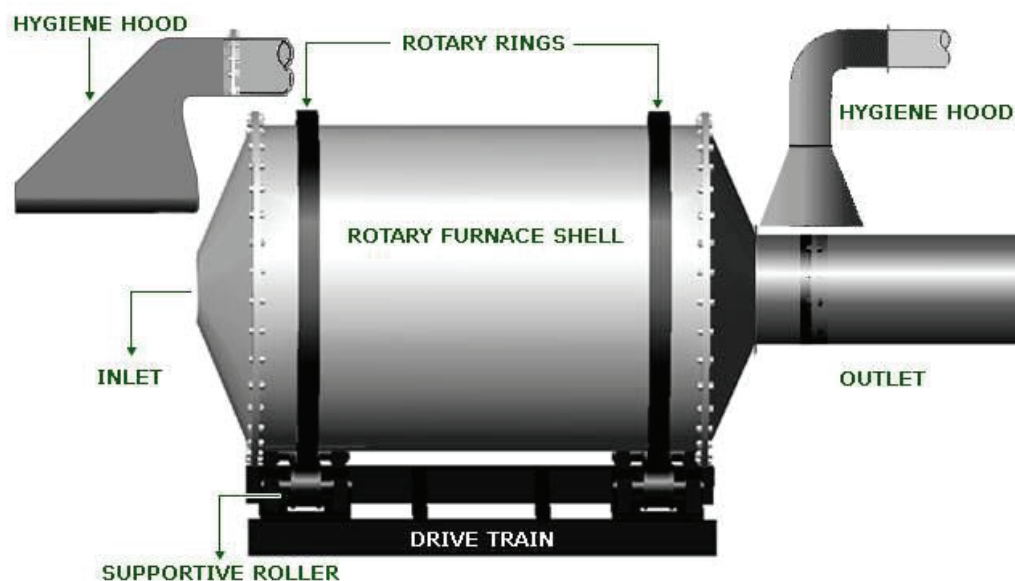


Figure 2.20. Functional diagram of a rotary furnace<sup>69</sup>.

### *Tilt Rotary Furnace*

The functions of the tilt rotary furnace shown in Figure 2.21 is similar to the rotary furnace, with the key distinction being the horizontal tilting movement, which allows for high yield and minimum maintenance cost. The move from stationary to tilting drums

represents the greatest advancement in rotary furnaces. Charging, tapping, drossing off, and cleaning needs less time due to the furnace's ability to tilt. Tilting rotary furnaces can melt high-quality scrap without fluxes.<sup>54</sup>

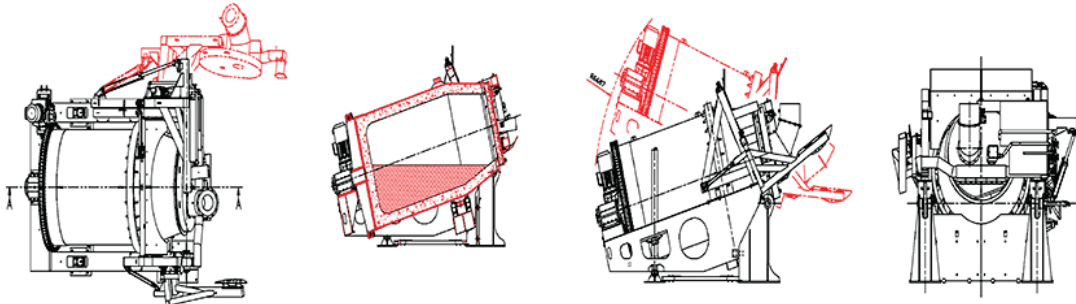


Figure 2.21. Tilt rotary furnace<sup>70</sup>.

### *Electrical Furnace*

The electrical furnace, shown in Figure 2.22, is frequently used in small processing plants to melt Al scrap. This reduces the amount of dross and improves the metal purity. Electric furnaces lose 0.5% to 3% metal compared to fossil-fuel furnaces' 5% to 8%<sup>71</sup>. A side well allows charging scrap without opening the furnace door, which prevents heat loss. Electric furnaces are more efficient and quieter than gas furnaces, especially for small scraps in terms of low metal loss<sup>72</sup>. Aluminium loses 0.49 to 0.81 kWh/kg. Induction furnaces are more than 90% energy efficient, while gas-fired crucibles are 15% to 28% efficient<sup>73</sup>.

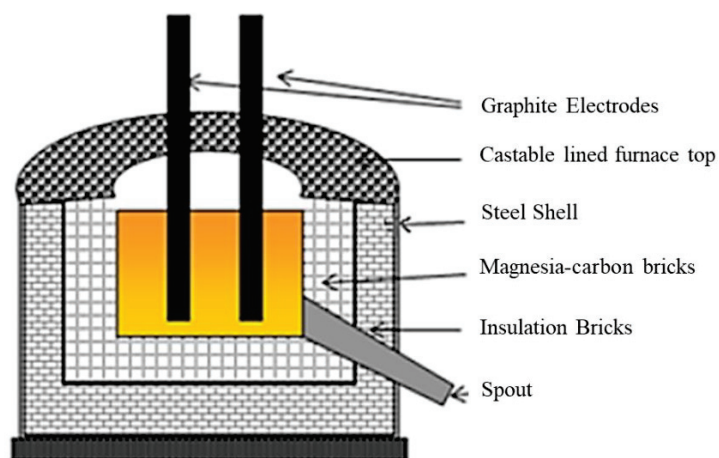


Figure 2.22. Schematic diagram of electric arc furnace<sup>75</sup>.



The churning motion of the induction furnace lowers temperature gradients, hence improving consistency. Electricity is more expensive than fossil fuels, erasing the economic advantage of fossil fuels. The melting capability of electric furnaces cannot compete with that of big fossil-fuel furnaces. When aluminium scrap is produced at home, electric furnaces are typically employed for small-scale operations<sup>74</sup>.

### **Remelting Under a Salt Flux**

Foundries must reduce the formation of dross, non-metallic inclusions, and oxides when melting and manipulating molten aluminium alloys. The issue with remelting aluminium alloy swarf and light scrap is that they possess a large oxidizable active surface area. Fluxes are utilized to address these problems. Flux is a substance added to molten metal that reacts with impurities to produce dross or slag that can be skimmed. This method is effective for cleaning metal, minimizing excessive oxide development, eliminating non-metallic impurities from the melt, and cleaning furnace walls<sup>67, 76, 77</sup>.

Coalescence is a key factor in Al recycling yield and has been researched extensively since the early 1900s<sup>78</sup>. Much research has examined Al oxide film removal and coalescence in salt flow<sup>79-84</sup>. The electrochemical process of oxide elimination by salt flow is described by Jordan, Milner, and Storchai<sup>85</sup>. Salt flux penetrates the oxide and removes it from the aluminium, while  $Al_3^+$  ions weaken it. Removal of oxide is related to changes in interfacial tension between salt, Al, and alumina, as described by Roy and Sahai<sup>80, 81, 84</sup>.

Jordan and Milner presented the following oxide removal steps:

Oxide ruptures form owing to simultaneous thermal expansion of Al and salt element assault<sup>80, 81, 85</sup>. The salt attack is used to weaken the oxide layer. Also, the spherical shape of Al droplets reduces their surface area/energy. The system's free energy is finally reduced as Al droplets coalesce or merge into one big droplet.

Surface tension defines the tendency of liquid surfaces to shrink to a minimal surface area. This is explained by opposing cohesive and adhesive forces that lead to equilibrium. Surface tension is created by the stronger attraction between liquid atoms (cohesive forces) than between liquid and gas (adhesive forces). Wetting, contact angle, and meniscus shape all influence the interaction between cohesive and adhesive forces. This also means that surface tension shapes liquid droplets. Interfacial tension is the tension between two liquids that influences the form of the Al droplet in molten salt.

According to Laplace's Law, a spherical form reduces the surface interfacial tension. Surface tension is measured in force per unit length or energy per unit area<sup>86</sup>.

Roy and Sahai<sup>80</sup> investigated the condition of the oxide layer and found that it can achieve spherical conversion when ruptured without being removed. Thermal expansion and spherical transformation of the droplets to obtain minimum free energy cannot rupture the oxide layer and promote coalescence. Rather, the activity of surface-active components is a more significant element for coalescence. Figure 2.23 shows the coalescence of several fluoride additions over time.

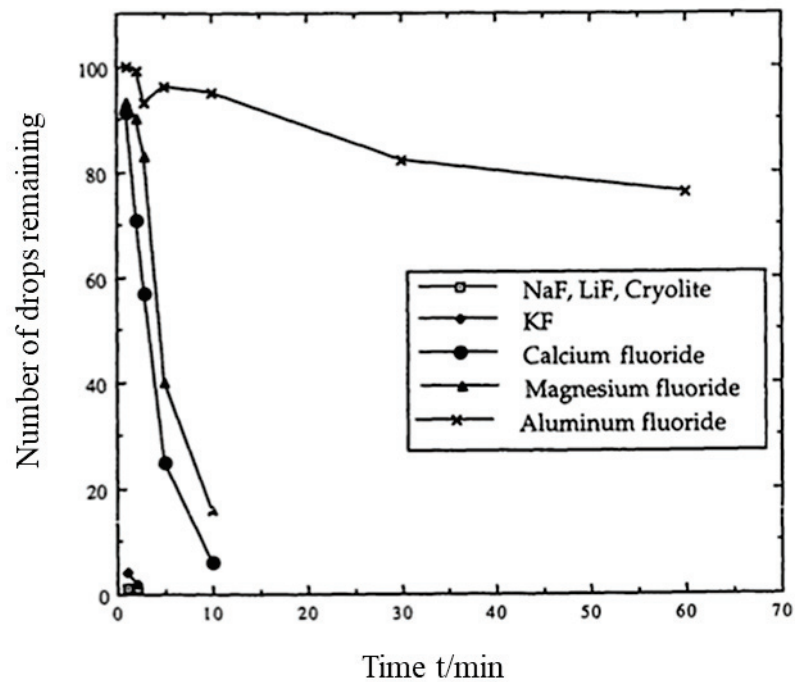


Figure 2.23. The reduction in the number of Al droplets (coalescence) with time for different fluoride additions<sup>80</sup>.

It is clear that adding fluoride chemicals promotes Al coalescence. The metal loss was 0.45% when  $\text{CaF}_2$  was introduced to equimolar NaCl-KCl, which is low compared to other fluoride compounds<sup>80</sup>. Other fluoride compounds with good coalescence caused more metal loss due to interfacial tension caused by displacement reactions.

Moreover, salt flux prevents air oxidation and contamination of metal surfaces. The salt flux features increase the oxide stripping rate, which improves coalescence. Metal recovery in Europe typically uses the ratio of 70/30 NaCl/KCl salt fluxes with minor amounts of  $\text{CaF}_2$ . The ternary phase diagram of NaCl, KCl, and  $\text{CaF}_2$  salts is shown in Figure 2.24  $\text{CaF}_2$  is inexpensive, and it is frequently used in concentrations of 2-5

wt%<sup>87</sup>. Also, NaCl KCl binary phase diagram is given in Figure 2.25. When the binary phase diagram of NaCl KCl salts is analyzed, the eutectic point (lowest melting point) of the diagram was observed at 44 wt% NaCl and 645 °C. Pure NaCl has a melting point of 801 °C, which is only 36 °C higher than the melting point of salt mixtures used by European recyclers (725 °C). On the diagram, it can be seen how adding NaCl raises the melting point<sup>88</sup>.

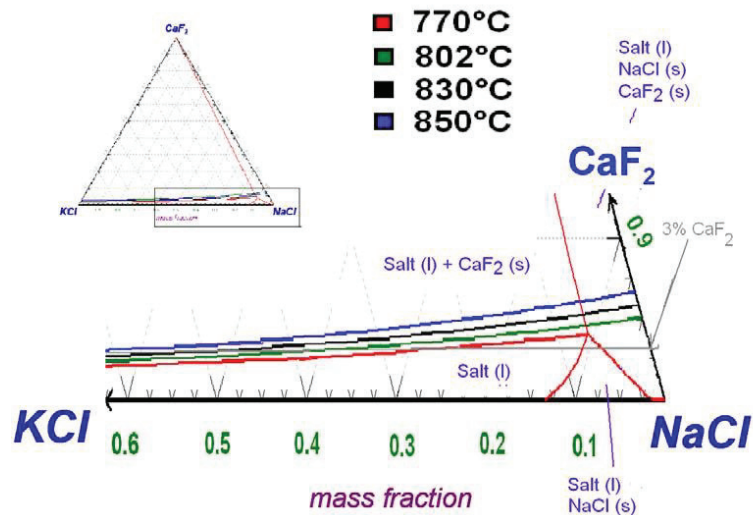


Figure 2.24. Equilibrium ternary diagram of CaF<sub>2</sub> -NaCl-KCl<sup>88</sup>.

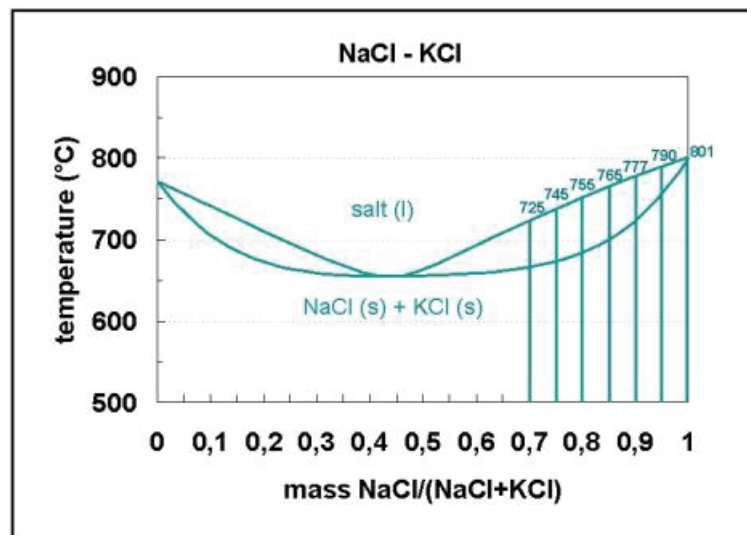


Figure 2.25. NaCl KCl binary phase diagram<sup>88</sup>.

Only dissolved fluoride ions increased oxide removal, according to Milke et al. Higher amounts increase salt flow viscosity and reduce interfacial tension, increasing melt loss. Dispersed oxide layers in the salt flux also enhance viscosity. Solubility over 730 °C is much lower than the only available phase diagram by Bukhalova and Bergman. Figure 2.26 shows that higher Al/salt ratios cause increased metal loss. Al-dispersion goes down when there is more salt to scrap, which means there is more Al in the salt. However, the amount of Al lost is greater when there is more salt than scrap (Figure 2.25).

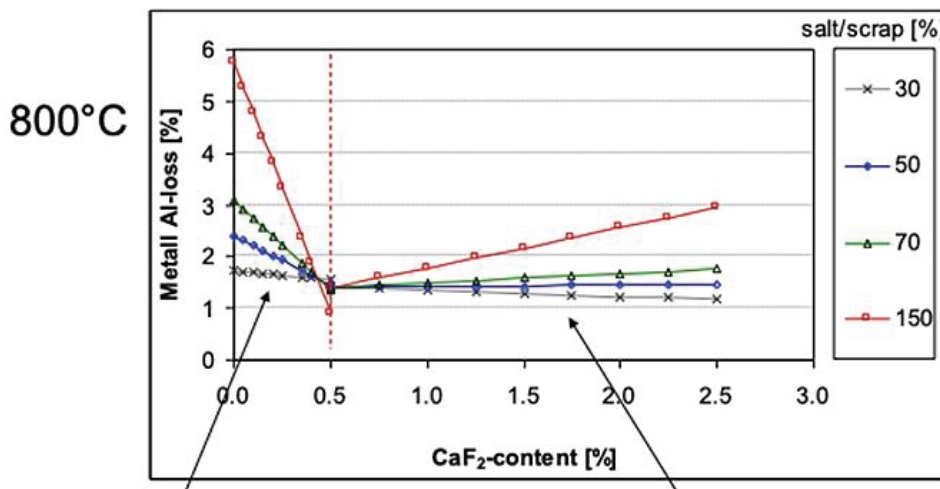


Figure 2.26. The relationship between metal loss and CaF<sub>2</sub> addition for different salt/Al ratios<sup>87</sup>.

Influences include the fact that at low CaF<sub>2</sub> contents, fluorides cannot remove the oxide layer from Al-pieces, so they stay in the melt and can't combine. With more CaF<sub>2</sub>, the salt-Al surface tension goes down, which lets more Al-droplets spread out. Stripped oxides improve salt slag viscosity, preventing coalescence. 30% salt/scrap had the lowest Al-losses. To maximize recovery, it should be added minimum amount of salt flux to cover the Al<sup>87</sup>.

### 2.5.3. Metal Losses During Recycling

To maximize aluminium recycling effectiveness, coatings should be removed from the metal surface<sup>89</sup>. When heated, the organic coating on coated aluminium samples begins to burn and emits CO and CO<sub>2</sub>. Aluminium oxide is formed when it is oxidized by heat and oxygen<sup>90</sup>. Organic substances of scraps lead to exothermic reactions due to combustion; because this reason, it leads to more oxidation during direct re-melting of

the scraps; it also causes carbide formation due to high soluble carbon in aluminium. It causes melt quality issues. On the other, hand alloy composition of the sample affects melt quality. The alloy composition of the sample, which includes a high amount of Mg content, tends to oxidize more. These scenarios affect the recycling effectiveness of aluminium. The aluminium sample should be oxidized as little as possible during the thermal pre-treatment to maximize efficiency<sup>91</sup>. All the reactions on the metal surface are shown in Equations 9-13.



## CHAPTER 3

### MATERIALS, CHARACTERIZATION, AND METHODS

In this chapter of the thesis, experimental setup and procedure are given for the recycling of the CC and UBC samples.

#### 3.1. Materials

Used beverage cans and coffee capsules were used for this study. The samples were categorized as pressed and unpressed. NaCl, KCl, and CaF<sub>2</sub> mixture were used as the salt flux for remelting experiments.

#### 3.2. Experimental Setup

Memmert drying oven (Universal oven UN 30) was used for drying the samples before experiments (Figure 3.1(a)). A laboratory-scale resistance chamber furnace that can heat up to 1600 °C was used for thermal pre-treatment and remelting experiments for coffee capsules and beverage cans (Figure 3.1(b)) (Protherm Furnaces PLF series 140-160 max temp: 1600 °C). A clayed-bonded graphite crucible in A2 (95x109x61 in mm) and A5 (124x152x86 in mm) volume was used for the remelting experiments. The casting furnace (Protherm, which is shown in Figure 3.1(c)), was used in the remelting experiments of the UBC samples.

Casting mould made from iron was used for the casting of remelted UBC samples. A graphite rod was used to stir the molten metal and skimming-off the slag. Figure 3.2 shows the materials which were used for the re-melting experiments.



(a)



(b)



(c)

Figure 3.1. (a) Memmert drying oven (b) Protherm laboratory-scale electrical resistance chamber furnace (c) Protherm tiltable casting furnace.

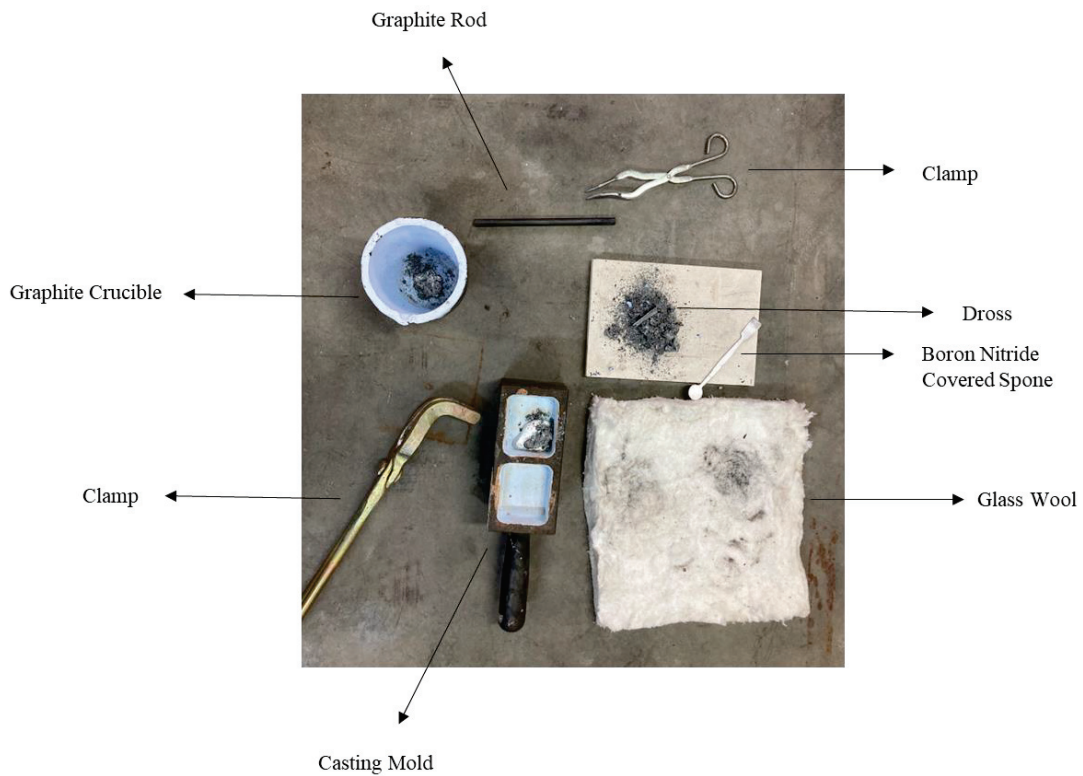


Figure 3.2. Set up of re-melting procedure.

### 3.3. Experimental Procedure

#### 3.3.1. Thermal Pre-Treatment Experiments

The coating of the samples was characterized using Scanning Electron Microscopy (FEI QUANTA 250 FEG) and Energy Dispersive Spectroscopy (SEM/EDS). In this study, the effect of the thermal pre-treatment was investigated by using pressed and unpressed beverage cans and coffee capsules. Firstly, the furnace optimization was maintained to observe the correlation between the temperature of the furnace and samples as a function of holding time. The temperature difference was tracked in a range of 30 and 50 °C, corresponding to holding times up to 90 minutes.

All the samples were cleaned from the residues by using water and ethanol before the thermal pre-treatment; after the cleaning process, the samples were dried at 100 °C, and their coating behaviours during heating were investigated using a lab-scale resistance heating chamber furnace at temperatures between 400 °C and 650 °C. After the samples cooled down, they were weighed by using an analytical balance.



The temperature-dependent mass change was investigated by thermogravimetric analysis (Perkin Elmer Diamond TG/DTA) under a nitrogen and oxygen environment. In addition, the effect of the holding time in the furnace on the efficiency of the de-coating process was discussed. Experimental parameters of this procedure which were applied for both CC and UBC samples are given in the following sections.

Table 3 presents the thermal pre-treatment experimental parameters for CC samples, which are from 400 to 650 °C and 0 to 15 min. holding time.

Table 3. Experimental parameters of thermal pre-treatment trials of CCs.

Experiment Number	Temperature (°C)	Holding Time (min.)
1	550	15
2	600	
3	650	
4	550	30
5	600	
6	650	
7	400	0
8	450	
9	500	
10	550	
11	600	
12	650	

Table 4 presents the thermal pre-treatment experimental parameters for UBC samples which is from 500 to 630 °C and 0 to 90 min. holding time. Some of the experiments were repeated.

Table 4. Experimental parameters of thermal pre-treatment trials of UBCs.

Experiment Number	Condition of the Sample			Temperature (°C)	Holding Time (min.)
13-14	Clean	Pressed	Single Pressed (International Brand)	500	0
15				550	0
16-22				600	0
23-24				600	15
25-26				600	30
				600	

(cont. on next page)

**Table 4. (cont.)**

27					60		
28-29		Unpressed		500	0		
30-32	Clean	Unpressed	International Brand	550	0		
33					15		
34					30		
35					45		
36					90		
37-39				600	0		
40				630	30		
41-50				With Drink Residue	Pressed	Bales (Mix of brands)	600
51-53	15						
54-60	Unpressed	Sugar-free (International Brand)	600		600	0	
61-70				Sugared (International Brand)			600
71-80							

Thermal pre-treatment results of CCs and UBCs in detail are given in Attachment section.

### 3.3.2. Remelting Experiments

The second part of the work includes remelting experiments for both types of samples. All samples were not cleaned before remelting experiments to observe the residue effect on the efficiency of aluminium recycling. Samples were sorted as de-coated, coated, pressed, and unpressed. After this categorization, CC samples that have a higher coating/metal thickness ratio were remelted under salt flux because of preventing

oxidation and metal loss. End of the remelting experiment, salt was removed by using water from the metal. Moreover, UBC samples were remelted directly at 750 °C. Dross on the molten metal was skimmed off at the end of the remelting procedure. After it skimmed off, it was cast to mold, and the dross was remelted under salt flux to obtain exact metal yield. At the end of the remelting under salt flux experiment, salt was removed by washing with water from the metal.

### Coffee Capsules

The samples were remelted under the salt flux at 750 °C. CaF<sub>2</sub>, NaCl, and KCl were used at 2%, 68.6%, and 29.4% concentration, respectively, and the salt factor (SF), which is the ratio between the non-aluminium content in the scrap and the quantity of salt<sup>92</sup>, was selected as 1:3. All the experiments were performed in an open atmosphere. Table 5 shows the parameters of all remelting experiments. Also, the sample definitions are given in Table 5.

Table 5. Remelting Experiments and Sample Definitions for Coffee Capsule.

Exp. Number	Sample			Salt Composition (wt%)	Salt Factor
	Pressed	De-coated prior to melting	Remelting		
1-5	yes	Yes	Under a salt flux	CaF <sub>2</sub> : 2% NaCl: 68.6% KCl: 29.4%	1:3
6	no	Yes			1:3
7-8	yes	No			1:3
9-11	yes	No	Direct		1:3

### Used Beverage Cans

The samples were categorized as clean-pressed (first cleaned from the residues, then manually pressed), clean-unpressed (only cleaned from residues), residue-pressed (only pressed), and residue-unpressed. Also, different brands, which are international and local unpressed samples, were categorized as sugar-free (international brand), sugared (International brand), and sugared (local brand). The samples were dried in a drying oven at 100 °C for 2 hours. The samples were remelted directly at 750 °C under two heating conditions (gradually heating and rapid heating). For the first case, the crucible was heated up gradually, and samples were de-coated without combustion before the melting. On the other hand, the rapid heating resulted in combustion before melting; thus, the

flame effect on the oxidation tendency was observed. After it reached 750 °C, the sample was casted into a casting mould after skimming off the slag. In the second step of the experiment, the dross of the sample was remelted under the salt flux at 750 °C. CaF<sub>2</sub>, NaCl and KCl with concentrations of 2%, 49% and 49% respectively. The salt factor was selected as 1:2 for the under salt flux re-melting experiment. The experimental parameters for the experiments are shown in Table 6. All the experiments were performed in an open atmosphere.

Table 6. Remelting Experiments and Sample Definitions for UBC.

Exp. Number	Sample			Salt Composition (wt%)	Salt Factor
	Pressed	Gradually Heated	Remelting		
12-14	No	No	Under salt flux	CaF <sub>2</sub> : 2%	1:2
15-17	Yes	No		NaCl: 49%	1:2
18-25	Yes	Yes		KCl: 49%	1:2

Summary of the experimental procedure is given in Figure 3.3.

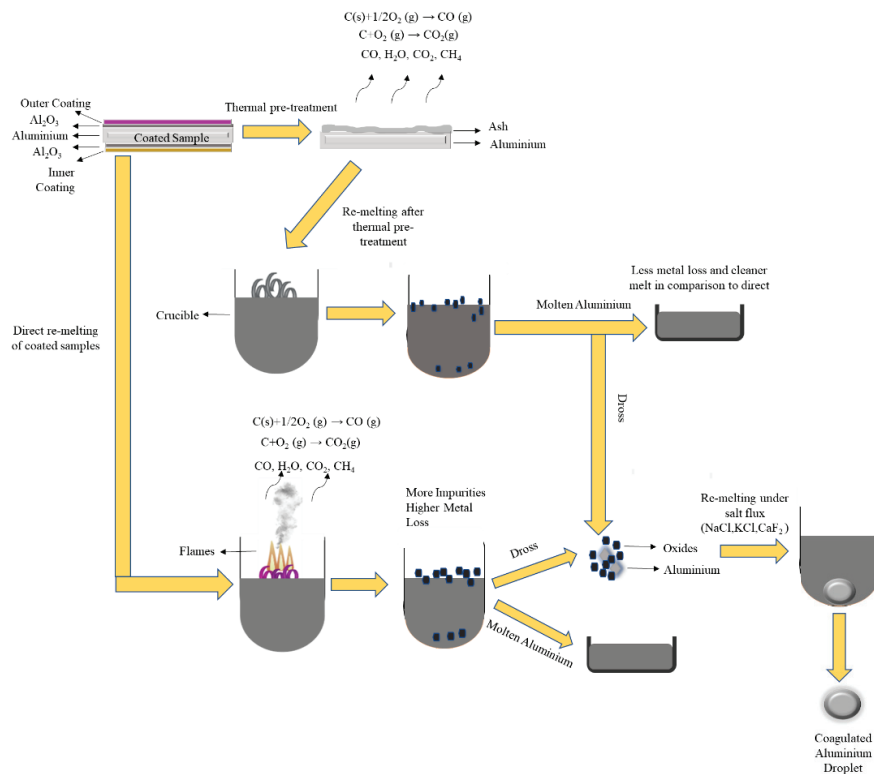


Figure 3.3. Summary of the experimental procedure.

## CHAPTER 4

### RESULT AND DISCUSSION

In this chapter of the thesis, the results of characterization, thermal pre-treatment, and re-melting experiments were given for both UBC and CC samples. Results were compared and evaluated with results in the literature. The parameters of holding time, temperature, pressing effect, and VOC of the samples were discussed.

#### 4.1. Characterization Results

In this section of the study used, beverage can and coffee capsule samples' coatings were characterized by using EDS and SEM analysis. Also, the mass distribution of their components was analyzed.

##### 4.1.1. Used Beverage Cans

Used beverage cans introduce not only drink rest and metal but also introduces inner coating and organic coating on the metal surface. The Figure 4.1 shows the mass distribution of UBC content. A UBC introduces 95.54 wt% metal, 2.43 wt% coating, and 2.02 wt% drink residue.

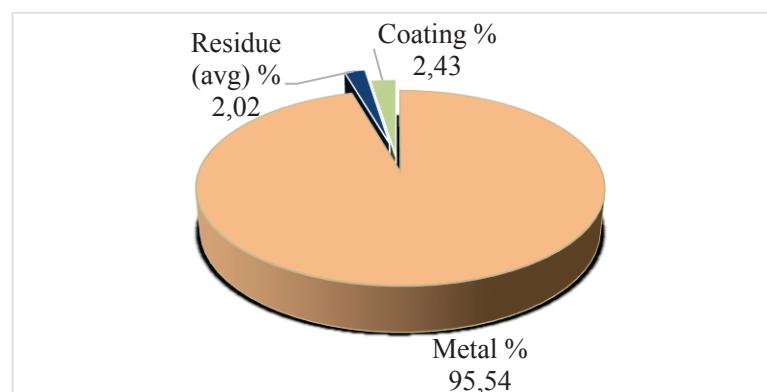


Figure 4.1. Mass Distribution of UBC component.

The cross-section of a beverage can be characterized by SEM. The wall thickness of the sample was measured with “ImageJ” image analysis software. The average wall thickness of the samples was measured as  $94.136 \pm 7.015 \mu\text{m}$  for beverage cans, and the total coating thickness was  $19.19 \pm 3.42 \mu\text{m}$ . The SEM image of the cross-section of a beverage can sample shown in Figure 4.2. Total coating thickness corresponds to 20 vol% of the cross-section.

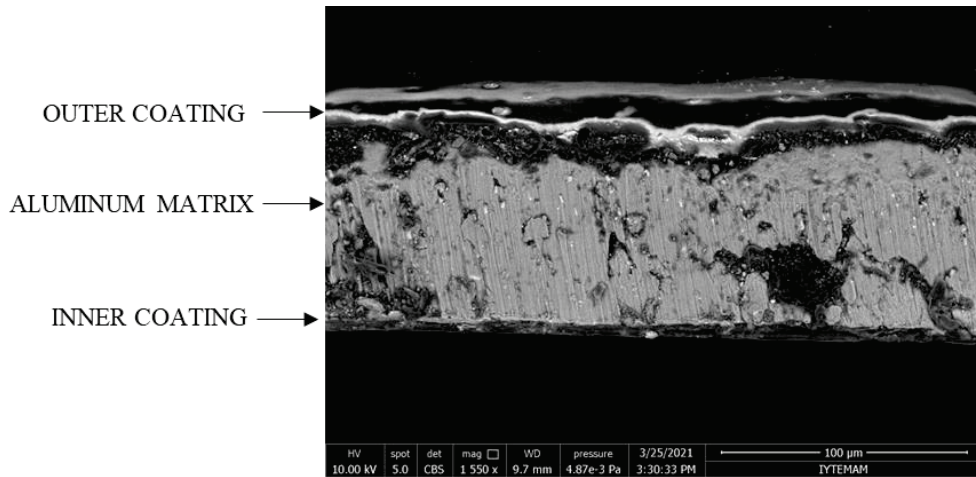


Figure 4.2. SEM image of the cross-section of a beverage can.

As it was mentioned in Chapter 2, the coatings of the aluminium products can be organic or inorganic. The inorganic pigments cannot be removed by heat treatment, but organic coatings degrade or combust by heat<sup>40, 41</sup>. A regular can was held in the furnace at 500 °C for 90 minutes, and the white written area on the surface was analyzed by using EDS. Figure 4.3 presents the EDS analysis after the thermal treatment. Ti presence on the de-coated sample is seen in the result, which is evidence of the inorganic TiO<sub>2</sub> pigment on the cans. It also shows that the inorganic pigments cannot be removed by using thermal pre-treatment. Carbon peaks that come from VOC on the sample are also evidence of the existence of organic pigments on the surface of the beverage can even after the thermal treatment<sup>40, 41, 60</sup>. Moreover, Al and Mg peaks are seen in the EDS analysis, which comes from EN AW-5182 alloy of the beverage can body<sup>44</sup>.

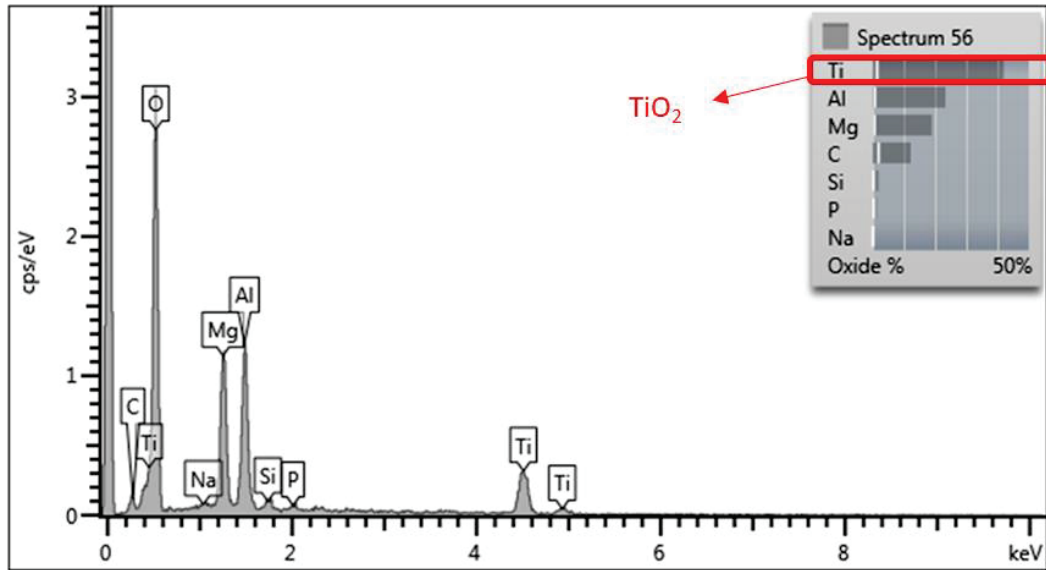


Figure 4.3. EDS result of the body part of a beverage can sample which held in the furnace at 500 °C for 90 minutes.

#### 4.1.2. Coffee Capsules

The coffee capsule introduces not only coffee and metal but also introduces filter paper and organic coating on the metal surface. Figure 4.4 shows the mass distribution of CC content. A CC introduces 85.19 wt% coffee, which is a significant organic rest amount. Also, it introduces 1.08 wt% organic coating on the metal surface and 0.3 wt% filter paper.

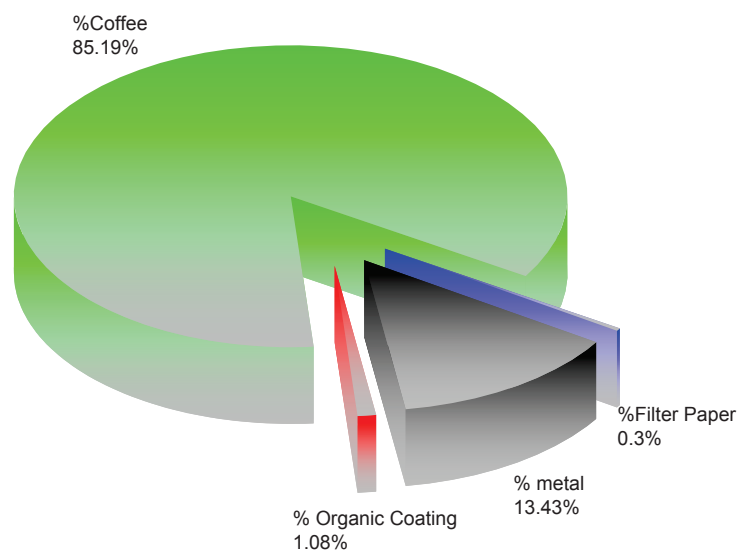


Figure 4.4. Mass distribution of CC component.

The cross-section of the coffee capsules was characterized by using SEM before the de-coating procedure. The cross-section of the sample is presented in Figure 4.5. The wall thickness of the sample was measured from different locations by using “ImageJ” image analysis software. The average wall thickness of the sample was  $95 \pm 6.022 \mu\text{m}$ . In addition, the average thickness of the outer coating was  $16 \pm 2.66 \mu\text{m}$ , and the inner coating was  $12 \pm 2.30 \mu\text{m}$ . The total coating thickness was measured as  $28 \mu\text{m}$ , which corresponds to 29 vol% of the cross-section. The coating part of the CC samples has a larger portion in comparison with the beverage cans.

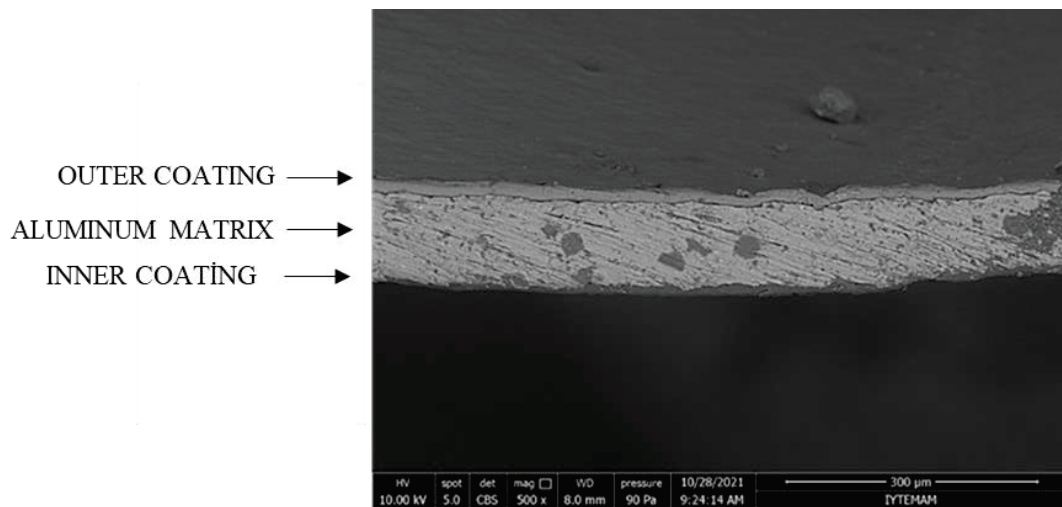


Figure 4.5. SEM image of the cross-section of a CC.

The coating material of ccs was characterized without any thermal pre-treatment by using EDS to understand the coating composition. In Figure 4.6, it was observed that the coating of the capsules mainly consists of C, Cl, and N, which are signs of organic coating<sup>93</sup>. Some weak peaks such as Si, Fe, Ti, and Zn come from the chemical alloy composition of 8011 aluminium alloy<sup>45</sup>. One of the main structures which are used to get red pigment is  $\text{C}_{23}\text{H}_{15}\text{Cl}_2\text{N}_3\text{O}_2$ , and Cd is used as an additive to change the shade of the red color.

The results also support that the pigments which were used in the coating of the CC are organic<sup>40, 41, 94, 89</sup>.



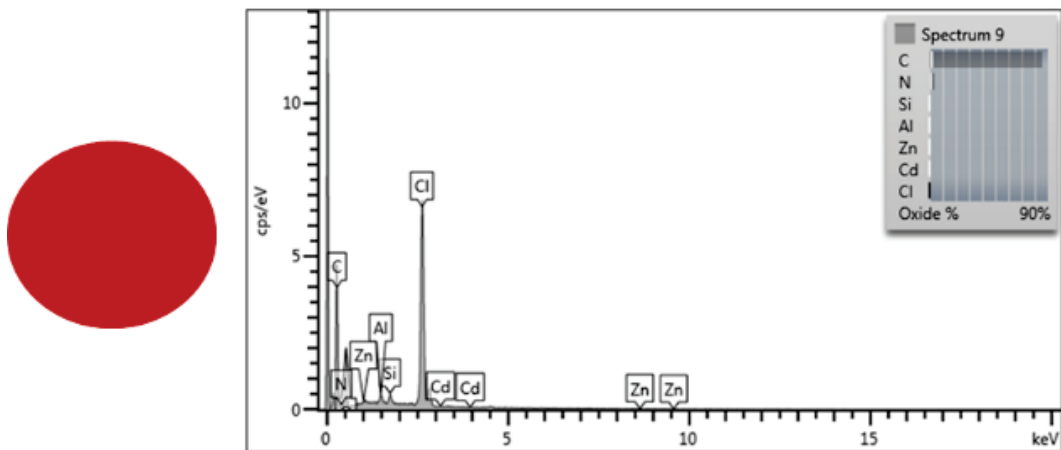


Figure 4.6 EDS result of the red coating material of CCs.

It was observed that signs of organic coating which comes from C, Cl, and N like in the red CC EDS result (Figure 4.7). One of the main structures to get orange color is  $C_{32}H_{24}Cl_2N_8O_2$ . Aluminium alloy 8011 series elemental composition peaks also were observed in the orange CC coating EDS result.<sup>40, 41, 94, 89</sup>

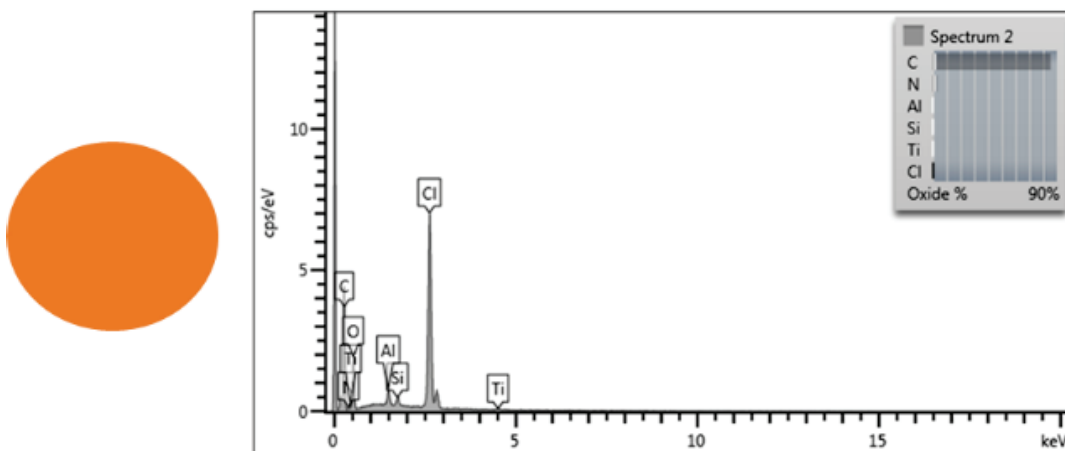


Figure 4.7 EDS result of the orange coating material of CCs.

Boron-based organic pigments are used to get violet shades in organic pigments. One of the main structures of boron-based organic pigment is  $C_{50}H_{36}O_8B$ . Also, other peaks come from aluminium alloy elemental composition can also be observed in this EDS result (Figure 4.8).<sup>40, 41, 94, 89</sup>

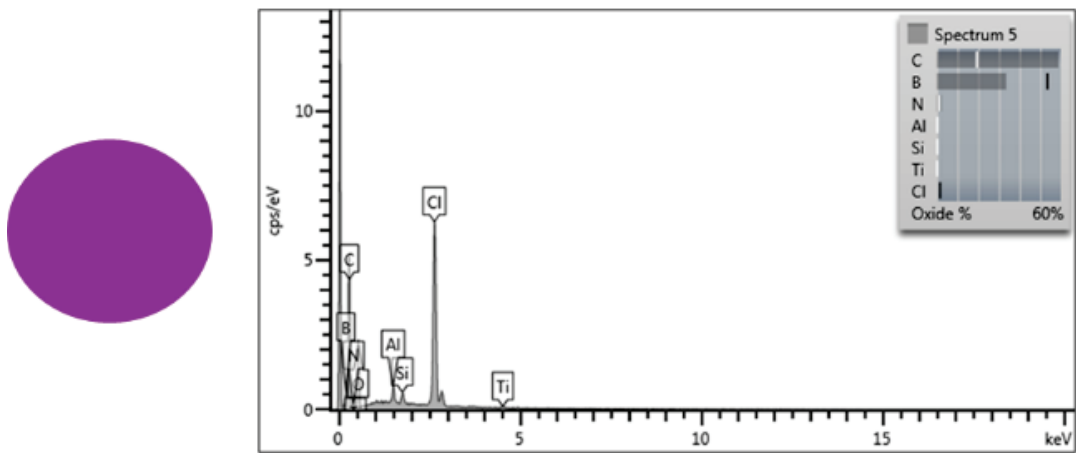


Figure 4.8 EDS result of the purple coating material of CCs

One of the main chemical structures to get organic brown pigment is  $C_{16}H_{10}ClN_3O_3$ , and Fe is used to change the shade of the brown color in organic pigments (Figure 4.9).<sup>40, 41, 94, 89</sup>

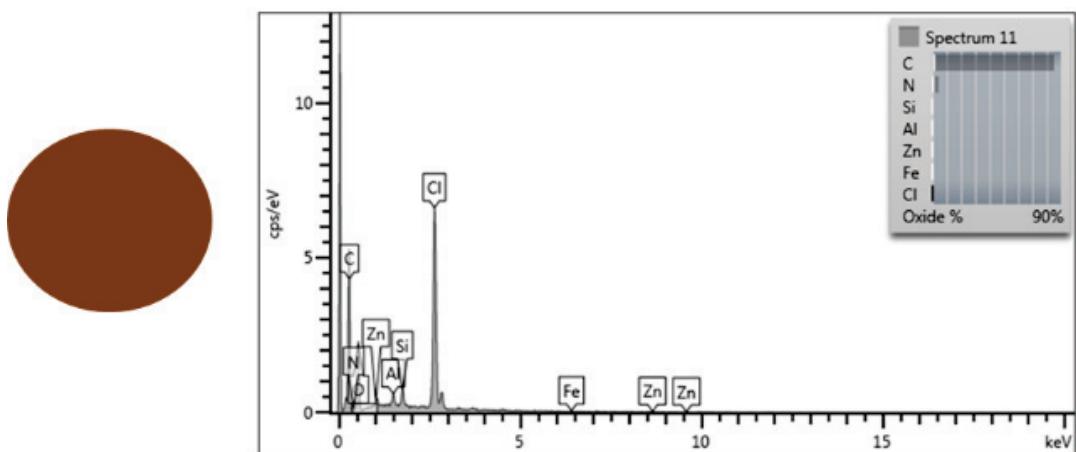


Figure 4.9 EDS result of the brown coating material of CCs.

The mass balance of the CC components as-fabricated was performed by separating and weighing each component. The results are listed in Table 7. The calculations indicate that an unused CC contains 84.83 wt% of coffee, 1.7 wt% of coating, and 13.47 wt% of the aluminium alloy. The sheet aluminium product also has a certain amount of oxide on its surface as usual. It shows the VOC wt% of CC is much higher than the critical VOC wt% limit for direct remelting, which was 5% that is mentioned in Section 2.5.1.<sup>89</sup> Therefore, thermal pre-treatment becomes reasonable for CC samples.

Table 7. Mass of organic coating and metal for CC.

Mass (g)	Capsule	Capsule without coffee	Coffee	Metal	Coatings	Filter paper in the capsule
1	6.53	0.957	5.573	0.868	0.069	0.02
2	6.437	0.970	5.467	0.882	0.068	0.02
3	6.502	0.979	5.523	0.89	0.069	0.02
4	6.48	0.963	5.517	0.868	0.075	0.02
Medium	6.48±0.03	0.967±0.008	5.52±0.04	0.873±0.009	0.070±0.003	0.02
wt%	-	14.80	85.18	13.47	1.08	0.3

VOC wt% of the UBC and Cc were found from the thermal pre-treatment experiments at 2.5% and 9%, respectively, as shown in Figure 4.10. In literature, the thermal pre-treatment process is sensible when the volatile organic content in scraps is more than 5%<sup>89</sup>. Otherwise, thermal pre-treatment is not necessary way because of the high metal / volatile organic content ratio, as it is discussed above<sup>89</sup>. While thermal pre-treatment is sensible for CC with 9 wt% VOC, it does not seem sensible for beverage can sample with less than the critical limit of wt% VOC. However, there is one more critical parameter to determine the pathway of the recycling procedure. Alloy composition, which has a high oxidation tendency (high Mg content), also affects metal yield. Because Mg has a high tendency to oxidize, and when it is directly remelted oxidation tendency of the alloy is going to increase because of uncontrolled temperature during the combustion of the VOC on the surface of the beverage can<sup>89</sup>.

EN AW-5182 and EN AW-3104 high magnesium content alloy composition<sup>44</sup> of UBCs have a high oxidation tendency. Therefore, both CC and UBC scraps should be thermally pre-treated since ccs have a high amount of VOC, and although UBCs have less organic content, direct remelting can significantly increase the metal losses due to the high Mg content of the can alloys.

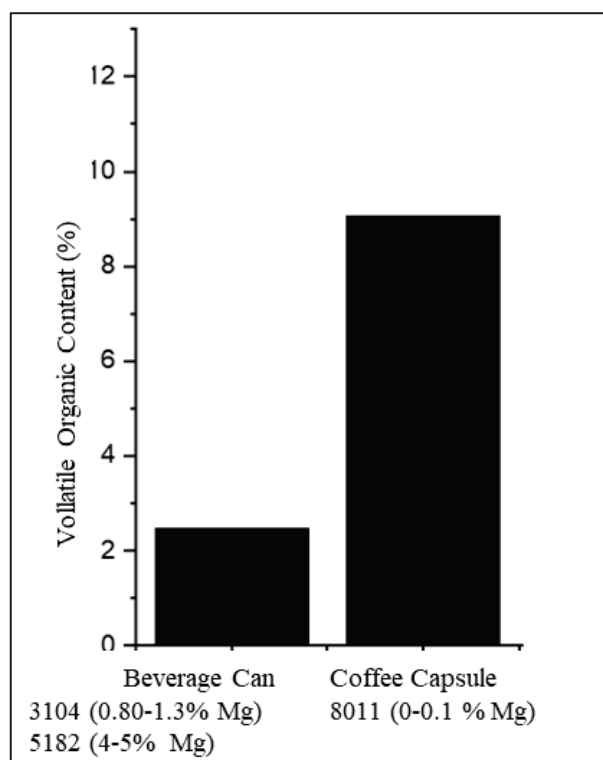


Figure 4.10. VOC of cleaned coffee capsule and beverage can samples.

## 4.2. Thermal Pre-Treatment Results

In this section of the study, used beverage can and coffee capsule samples which were thermally pre-treated at different temperatures and holding times, were analyzed. The samples were categorized as clean, with drink residue, pressed and unpressed. Also, different brands and drink residue effects on mass loss during thermal pre-treatment were investigated.

### 4.2.1. Used Beverage Cans

After beverage cans were cleaned with ethanol and water, they were subjected to a thermal pre-treatment temperature from 500 to 600 °C. Some samples were pressed before the treatment to observe the effect of compaction, and some samples were not cleaned before the thermal pre-treatment to observe the effect of the residues. Figure 4.11 shows pressed and unpressed samples after thermal pre-treatment.



Figure 4.11. Pressed and unpressed UBC samples after thermal pre-treatment.

Figure 4.12 presents pictures of the inside surface of unpressed and pressed UBC samples after holding at 500 °C for 15 minutes holding at 5°C/min. rate. The samples were cut after thermal pre-treatment, and thermal decomposition residues were observed inside. The residues in unpressed samples did not combust completely with O<sub>2</sub>, and its carbonaceous residue could be seen in the sample in addition to less amount of thermal decomposition of heavy hydrocarbons (Figure 4.12(a)). This situation can be explained as less amount of O<sub>2</sub> which entire from the hole on the lid of the beverage can with time<sup>60</sup>. Thermal decomposition or thermolysis is a chemical decomposition caused by heat in an O<sub>2</sub> or N<sub>2</sub> environment. Thermal decomposition in an inert environment is called pyrolysis. On the other hand, the inner wall of the UBC sample seems oily, and there is pyrolysis observation on the inner wall. Figure 4.12(b) presents thermal decomposition observation in the pressed sample after the thermal pre-treatment process. Residue starts to decompose in an oxygen-free environment; because of this reason, pyrolysis residue was observed in the pressed type of samples as shown in studies in the literature<sup>95, 89, 96, 97</sup>.



(a)



(b)

Figure 4.12. The inner surface of the UBC samples after thermal pre-treatment (a) Unpressed and (b) Pressed.

In this section, the different components of the coatings, their tendency to separate from the metal depending on temperature, and their residues were examined. Figure 4.13 shows the SEM-EDS analysis of the body of an unpressed beverage can be heated up to 520-550 °C and held at this temperature range for 90 minutes the significant presence of carbon, magnesium and titanium were observed in the EDS analysis; other elements getting from result can be negligible because of EDS precision. This situation is considered in all EDS results in this thesis.

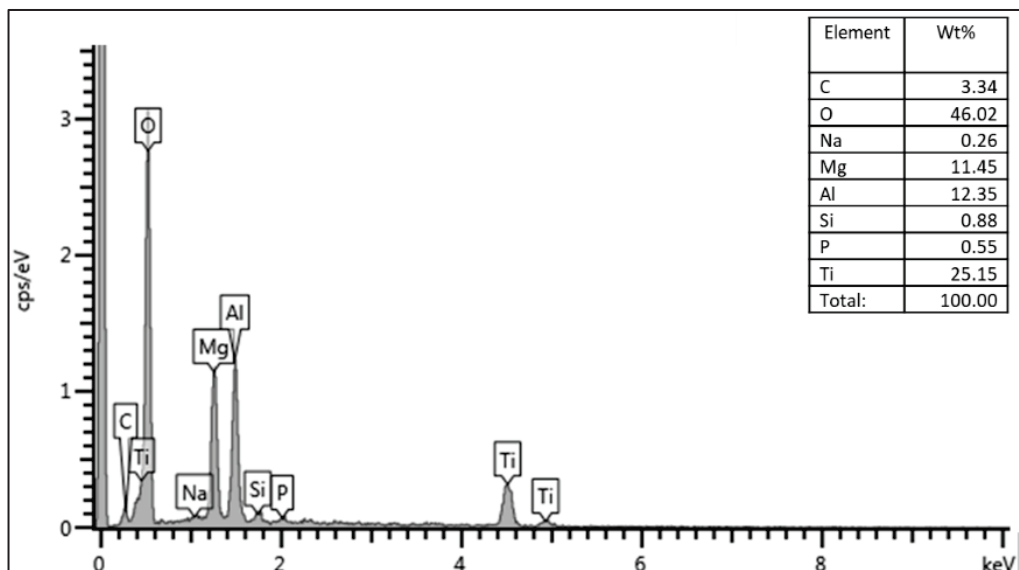


Figure 4.13. EDS result of UBC sample kept in the oven from 520 to 550 °C for 90 minutes.

The presence of titanium was seen in the white areas where a text is placed on the cans after the thermal pre-treatment. The widespread use of  $\text{TiO}_2$  (titanium (IV) oxide) as a white pigment explains the presence of titanium seen in EDS results<sup>40, 41</sup>. The carbon residue represents the presence of non-combusted VOC on the surface of the sample. The magnesium peak originates from the EN AW 3104-magnesium-containing aluminium alloy used in the can bodies<sup>44, 45</sup>.

Figure 4.14 shows the EDS analysis of the body of the beverage can after thermal pre-treatment at 615 °C. It is obvious that the alloy composition consists of magnesium and aluminium that comes from EN AW-3104 alloy composition of the body of beverage can<sup>44</sup>. The sample which was held in the furnace temperature of 520-550 °C has higher carbon residue than that of the temperature of 615-630 °C.

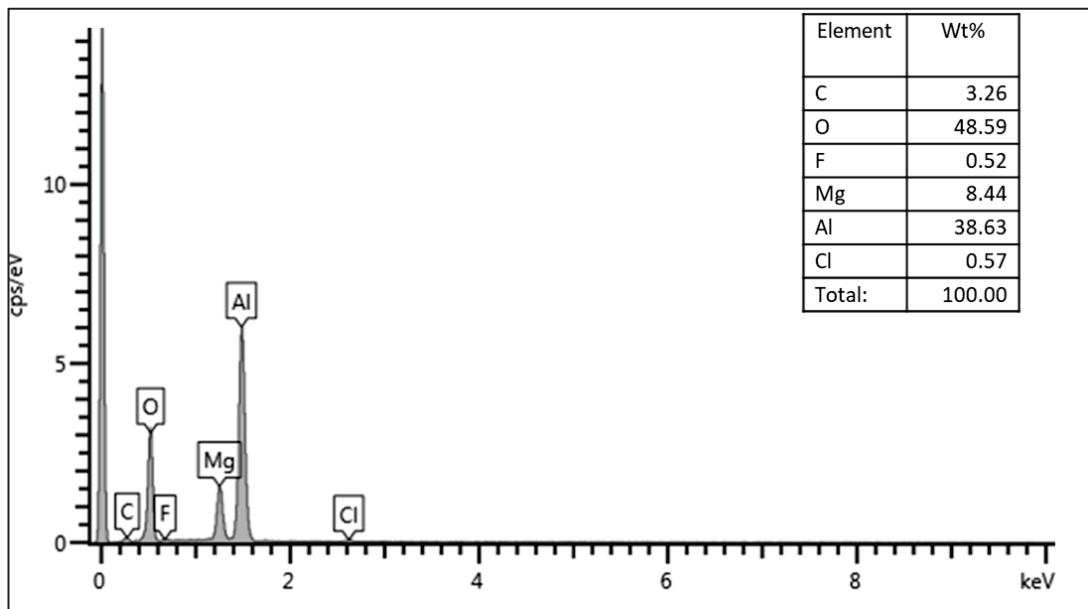


Figure 4.14. EDS result of the sample taken from the body of the UBC which was kept in the oven at 615-630 °C for 30 minutes.

This result indicates that most of the coating is removed with the rising temperature. On the other hand, it shows that a higher temperature than optimum thermal pre-treatment temperature increases the tendency of the oxidation considered oxygen wt%. It is also evidence of the significance of choosing a suitable temperature and holding time for the de-coating process<sup>14, 89, 98</sup>.

Figure 4.15 shows the EDS result of the lid alloy of the beverage can sample thermally pre-treated at 615-630 °C for a period of 30 minutes. Aluminium, magnesium, and carbon elements were observed in EDS results as a high-intensity peak. Lids of

beverage cans are made of magnesium-rich EN AW 5182 alloy<sup>44</sup>. The reason for the difference between the body and lid alloys of the beverage can is the different mechanical properties of these alloys.

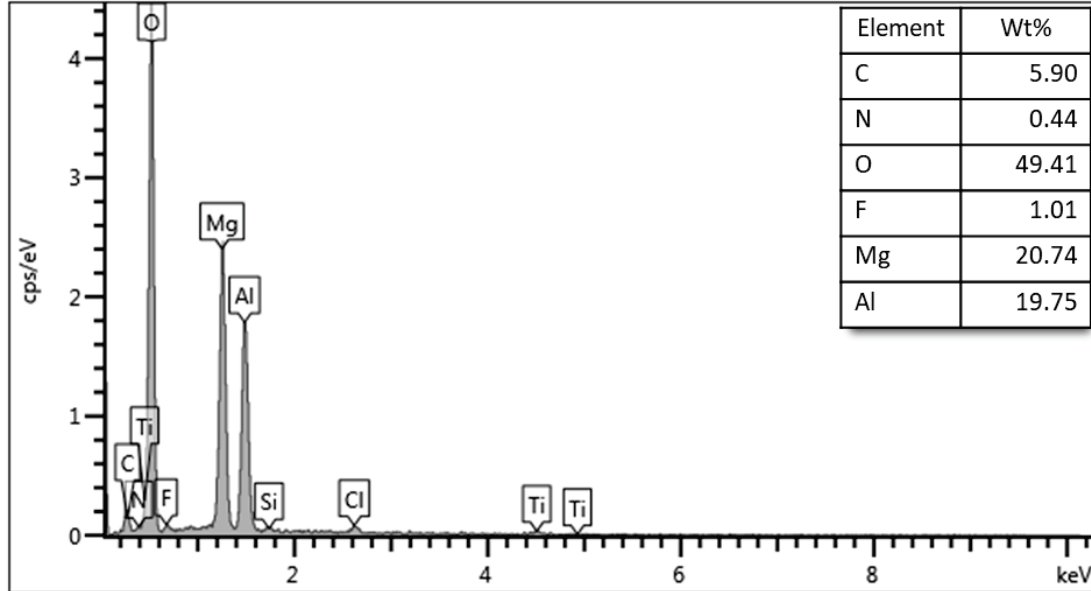


Figure 4.15. EDS result of lid alloy of a UBC, which was kept in the oven at 615-630 °C for 30 minutes.

It is observed that the amount of oxidation increases as the temperature increases, according to Figure 4.13 and Figure 4.14. In Figure 4.14 and Figure 4.15, the oxidation tendency of samples consisting of different alloys was investigated, and it was observed that the lid of the beverage can, which is rich in magnesium, was more oxidized at the same test parameters. Oxidation on the surfaces of magnesium-rich alloys was observed with the naked eye in the form of spots or flakes. In Figure 4.16, the behaviour of different alloys on the beverage can sample against thermal pre-treatment is given.

The percentage of mass loss was calculated using Eq. 14 to understand the behaviour of mass change depending on temperature with time.

$$\text{Mass Loss (\%)} = \frac{(\text{the initial mass of sample} - \text{final mass of the sample})}{\text{the initial mass of the sample}} \times 100 \quad (\text{Eq.14})$$



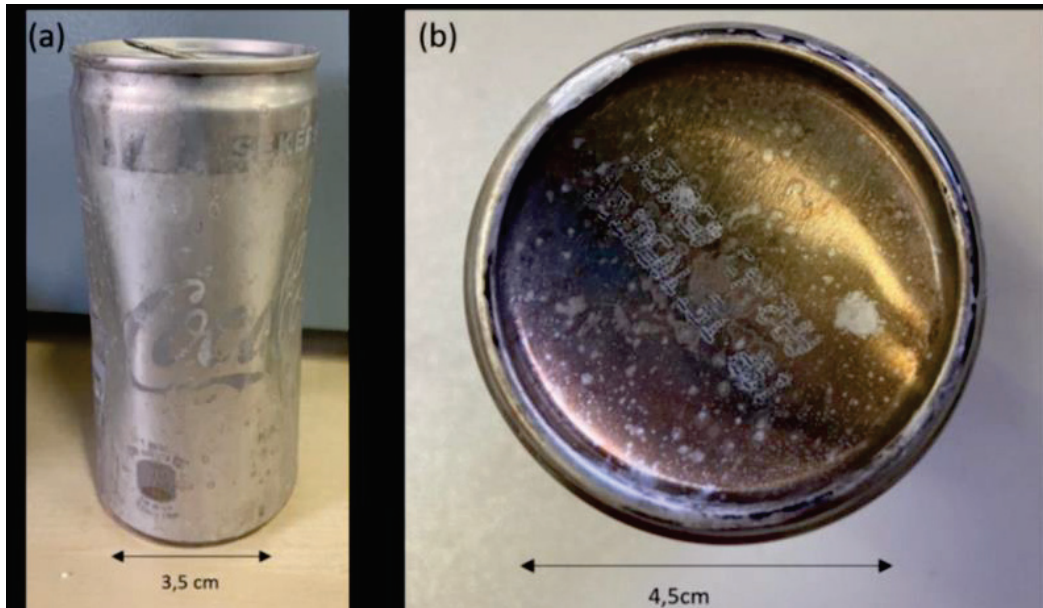


Figure 4.16. Thermal pre-treatment behaviour of different alloys on the UBC sample  
a) Body b) Base.

In Figure 4.17, mass loss of the international brand beverage can be subjected to heat pre-treatment for different holding times at 550, and 600 °C are given. Increasing in mass was observed after 30 minutes at 550 °C, which was estimated to be due to oxidation<sup>99</sup>. On the other hand, it was observed that the samples which were kept in the furnace at 600 °C without holding time were less exposed to oxidation.

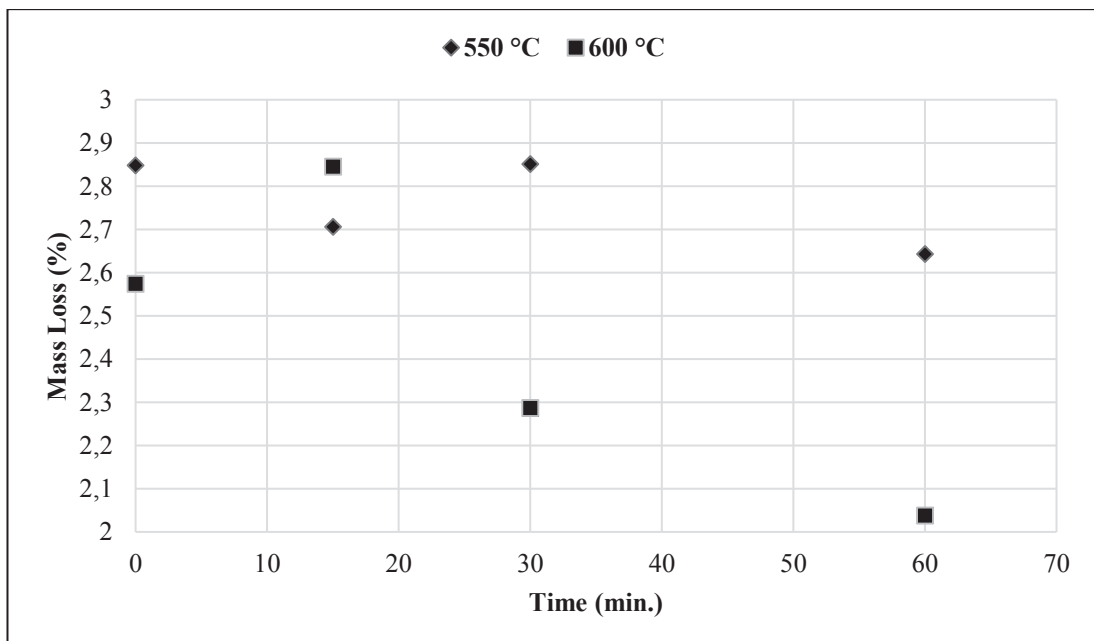


Figure 4.17. Mass loss of UBC sample at 550 and 600 °C.

Figure 4.18 shows the mass loss graph of bales, local brand UBC sample, and international brand UBC sample. It can be said that mass loss of cleaned unpressed UBC sample shows higher mass loss than cleaned pressed sample because of pressing shape. Moreover, when uncleaned unpressed and industrial pressed (bale) UBC sample's mass loss after thermal pre-treatment were compared, unpressed samples showed higher mass loss at the end of the experiments because volatile organic content (VOC) on/in unpressed samples can remove at the end of the experiment. However, when it was pressed, VOC on/in the pressed UBC sample could not remove because of the pressing shape. When it starts to decompose, it can only consume oxygen in the pressed area. Whenever oxygen is finished inside of it, the burning of the VOC also stops<sup>100</sup>. The effect of residue on mass loss is shown in Figure 4.18, which are two different unpressed samples that were cleaned from the residues inside by using ethanol and water, while the other was subjected to pre-heat treatment with the residues in it. It is clearly seen that in the samples that were not cleaned of the residues, an increase in mass loss was observed in direct proportion to the amount of residue. The reason for this is that the residue in it is removed with the heat pre-treatment. Organic residue in the scraps increases the VOC of scrap; thus, mass loss is higher than in cleaned samples. The standard deviation for the uncleaned sample is more than the cleaned one in consequence of the different amounts of residue in scraps.

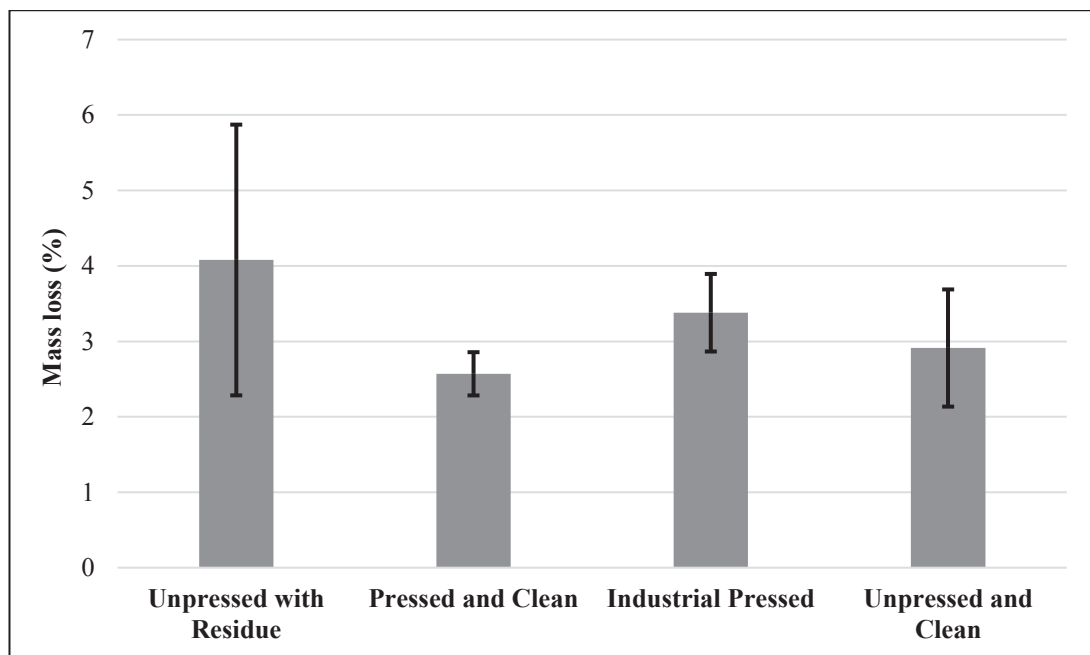


Figure 4.18. Mass loss of pressed, unpressed, and industrial pressed UBC samples

In Figure 4.19, the graph of the mass loss behaviour of the pressed and unpressed samples that have the same volume at different temperatures without being kept in the furnace is given. It was observed that the mass loss of the pressed samples was higher when pre-treatment was applied at 550 and 600 °C. The reason for this can be shown that the surface areas of the unpressed samples in contact with the oxygen in the atmosphere are much more than the pressed sample. In fact, this shows the advantage of pressing over oxidation<sup>101</sup>.

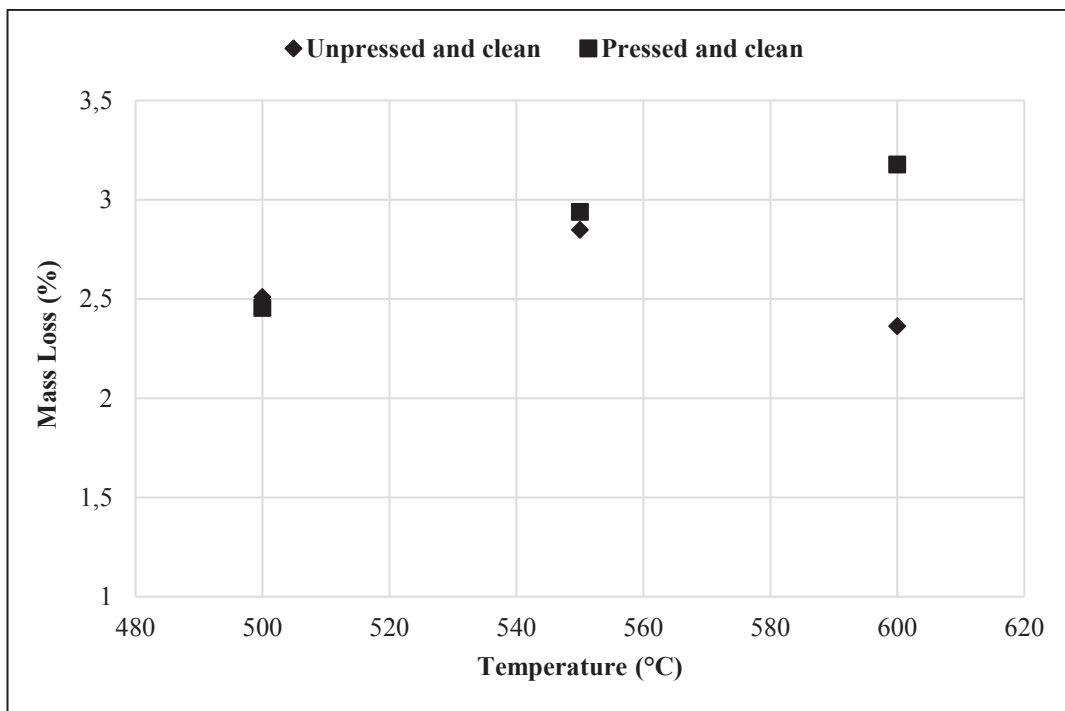


Figure 4.19. Mass loss of pressed and unpressed UBC samples at different temperatures.

The Figure 4.20 shows the mass loss between sugar-free drinks and sugared drinks during the thermal pre-treatment process. Sugared one has more VOC because it introduces sugar<sup>102</sup>. Because of this reason, mass loss is higher than in sugar-free drink samples. Its standard deviation is more than sugar-free drink because of the different sugar content inside it. In large-scale recycling, according to the industrial aspect, more metal can be bought when sugar-free UBC scraps are chosen because of lower VOC.

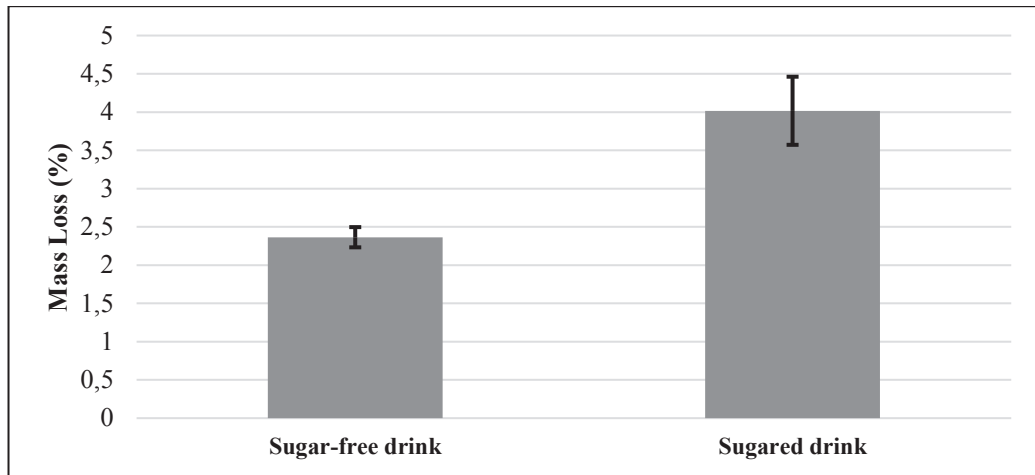


Figure 4.20. Mass loss comparison of UBC samples which have a sugar-free and sugared drink.

The Figure 4.21 shows the mass loss comparison of UBC samples, which have different brands and different drink residues after being thermally pre-treated at 600 °C. It was seen that the lowest mass loss % belongs to the International Brands-sugar free sample because of its lower VOC in the residue. On the other hand, when the samples which have sugar-containing residue were compared, Local Brand 1 showed 1% lower mass loss than International Brand sugar and Local Brand 2 samples because of different types of drink rest inside of it.

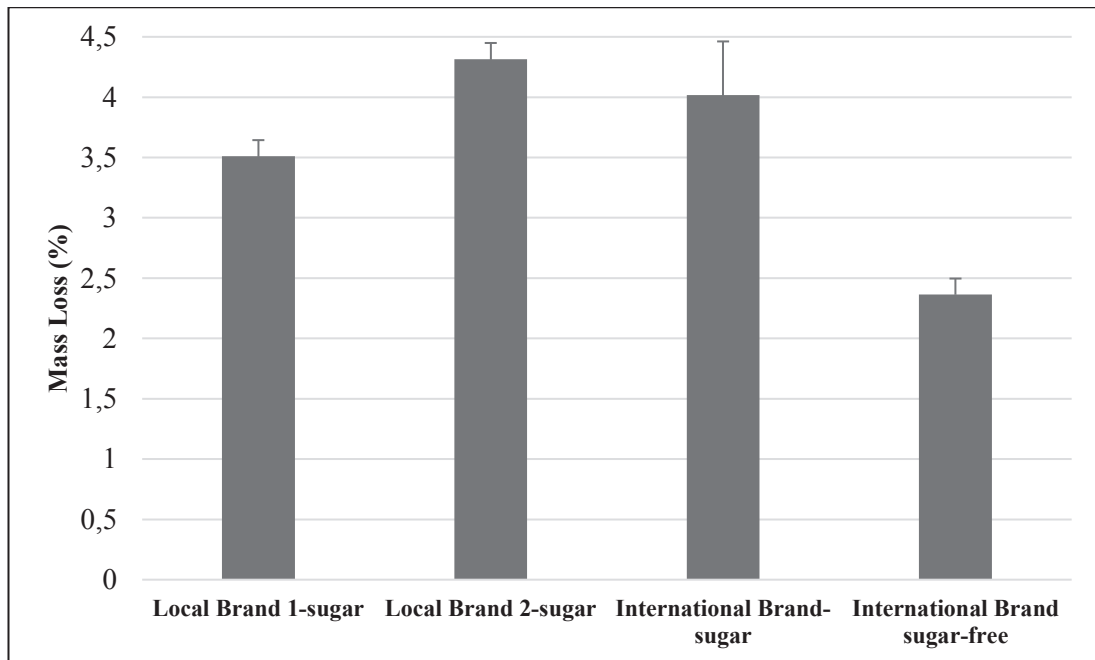


Figure 4.21. Mass Loss comparison of UBC samples which have different brands and different drink residue.

O<sub>2</sub> effect on the thermal pre-treatment process was investigated, and TGA analysis was maintained under both O<sub>2</sub> and N<sub>2</sub> gas. The processes of combustion and pyrolysis are both thermochemical reactions. Hydrocarbons burn in the presence of oxygen to produce heat, carbon dioxide, and water. In contrast, pyrolysis happens in the absence of oxygen or under inert conditions to generate gaseous, liquid, and solid residues (chars). TGA analysis result of beverage can sample under oxygen and nitrogen environment was shown in Figure 4.22 and Figure 4.23, respectively. In their research, Alade et al. observed low-temperature devolatilization of light organic components and high-temperature decomposition of the heavy fraction. In terms of three stages of weight loss and/or conversion, they described the thermal decomposition of their sample: volatilization of moisture and light hydrocarbon (20–227 °C), combustion of heavy hydrocarbon (227–527 °C), and oxidative decomposition of carbonaceous organic matter (502 – 877 °C)<sup>95</sup>. In Figure 4.23, volatilization of moisture and light hydrocarbon until 200 °C were emerged. After this temperature, combustion was observed as two peaks that come with different hydrocarbon compositions between 200-300 and 300-400 °C. When TGA results are examined, the mass increase is observed after 500 °C, which indicates that oxidation has started in an oxygen environment as depicted in <sup>14, 89, 98,95</sup>.

In Figure 4.22, it was observed that the initial volatility started at about 250 °C and continued up to 400 °C since the sample was dry in a nitrogen environment.

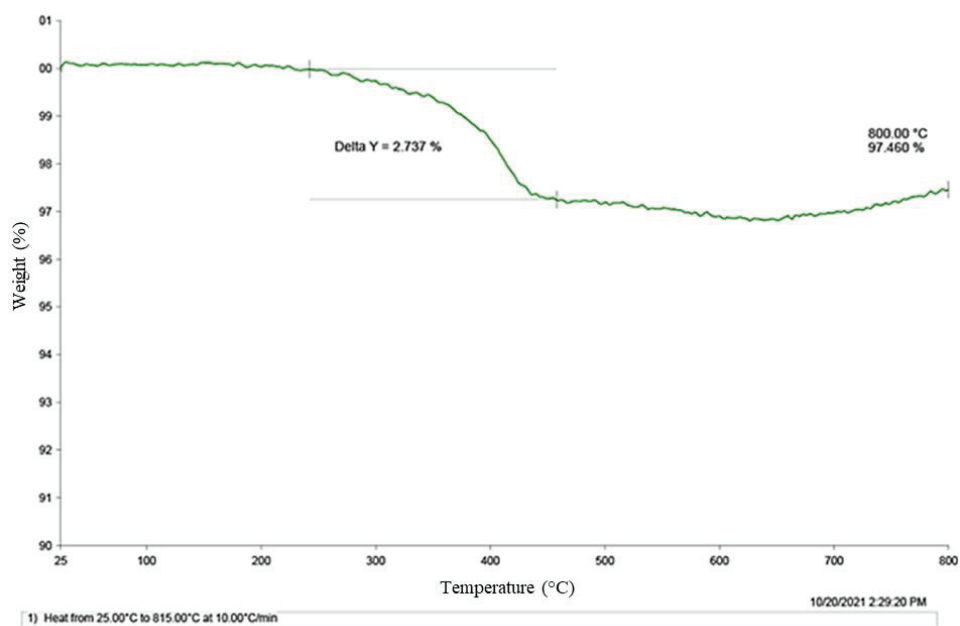


Figure 4.22. TGA analysis of UBC-body sample (international brand) under nitrogen gas.

After 400 °C, it is predicted that the small increase in mass seen in the sample may be oxidation caused by the trace amount of oxygen in the environment. A further increase in mass after 700 °C is a sign of increased oxidation. The reason for this is that the liquid kinetics is higher than the solid kinetics, and therefore it is more prone to oxidation<sup>103</sup>. This can be explained by the fact that the aluminium in the liquid phase at 700 °C is more easily oxidized.

TGA analyses were maintained for thermally untreated body and lid part of the UBC sample for different brands. Figure 4.23 and Figure 4.24 show the TGA analysis result of UBC, which is an international brand in the O<sub>2</sub> environment. In Figure 4.23, combustion of organic coating on the surface was observed between 250 and 450 °C, and oxidation was not observed significantly until 600 °C. The mass increase was observed after 600 °C as a sign of oxidation, and this result coincides with the evaluation given in Figure 4.17. Also, it was observed that the body part of the sample starts to oxidize earlier than the lid part because of the difference between the melting point of these.

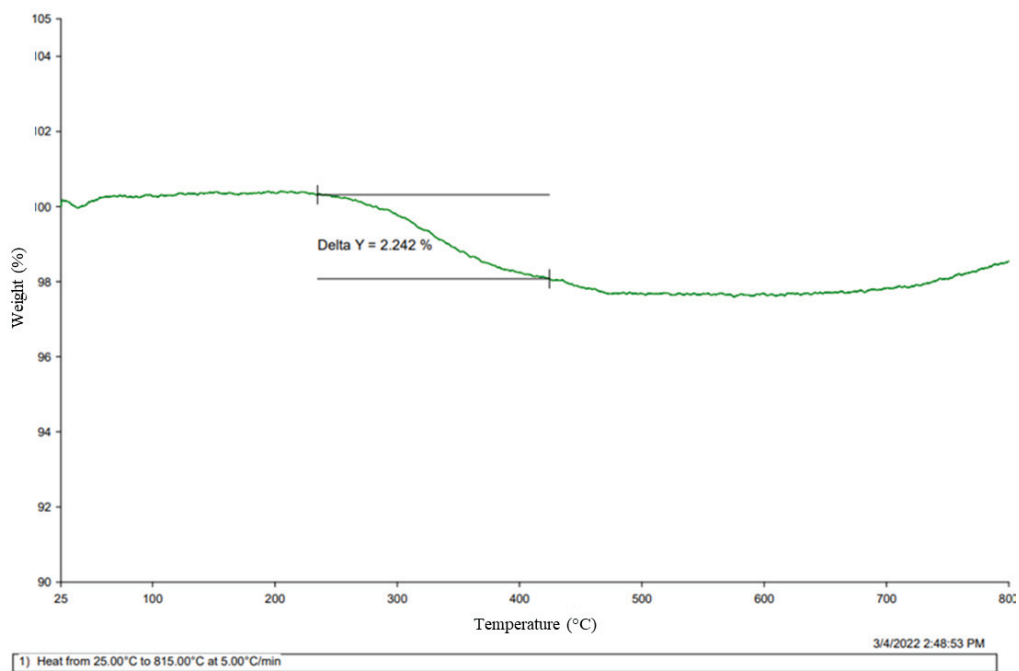


Figure 4.23. TGA analysis of UBC-body sample (international brand) under oxygen gas.

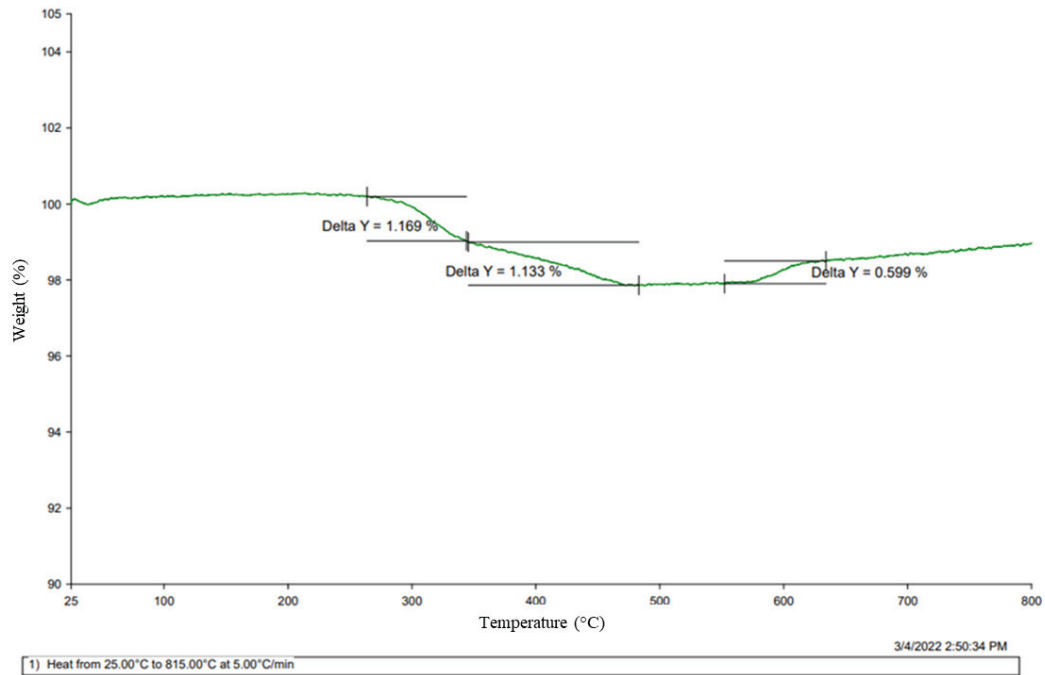


Figure 4.24. TGA analysis graph of UBC- lid sample (international brand) under oxygen gas.

Moreover, combustion of plastic coatings on the lid part was observed between 250 and 500 °C as depicted in<sup>35</sup>. A significant increase in mass was not observed until 580 °C after this temperature. However, the mass of the lid part of the beverage can starts to increase with high acceleration after 580 °C. Its reason is that body and lid parts of UBC are made of different alloy compositions, which are AlMn1Mg1Cu (EN AW-3104), and AlMg4.5Mn0.4 (EN AW-5182) is used for the body alloy, and the lid alloy (EN AW-5182) respectively. The lid alloy has more magnesium content, which affects the oxidation tendency during remelting<sup>44</sup>. The mass of the lid part of the beverage can increase more than the body part of the beverage can because of its higher Mg content in its alloy composition.

UBC sample, which is a local brand, was analyzed by using TGA. Figure 4.25 and Figure 4.26 show the body and lid part of the local brand UBC sample's TGA results in an O<sub>2</sub> environment. It can be seen that the lid part of the sample gains more mass than the body part, similar to the international brand UBC sample, because of the more oxidation. However, when the international brand and local brand's TGA results were compared, it can be seen that both the lid and body part of the local brand UBC sample gained more mass than the international brand UBC sample because of the more oxidation. The oxidation difference between them could come from the difference in the alloy composition.

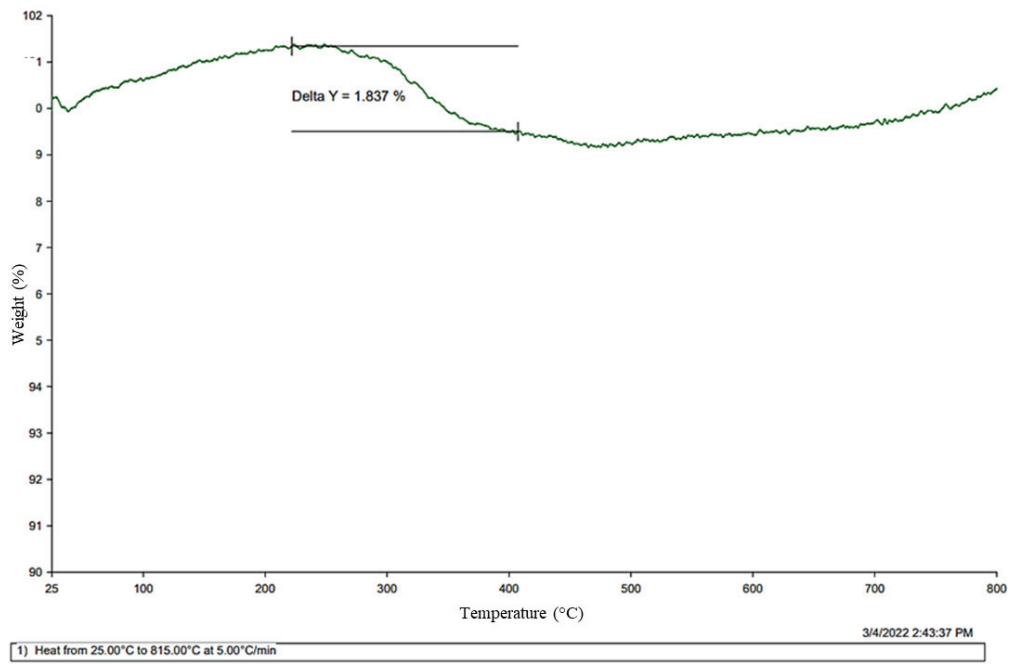


Figure 4.25. TGA analysis of UBC-body sample (local brand) under oxygen gas.

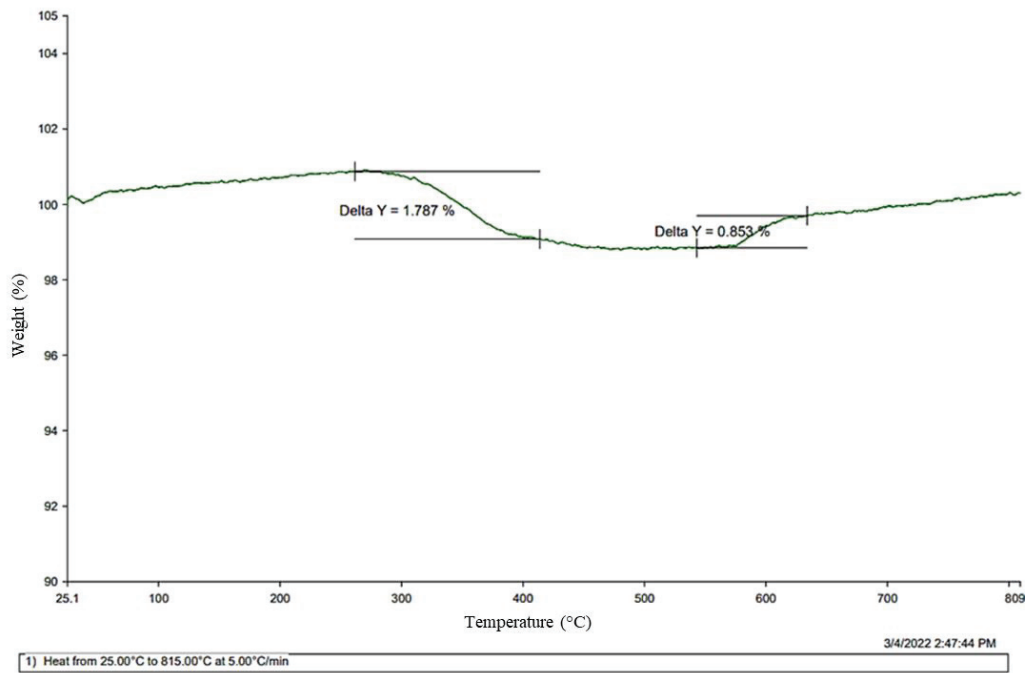


Figure 4.26. TGA analysis of UBC-lid sample (local brand) under oxygen gas.



## 4.2.2. Coffee Capsules

Coffee capsule samples that have the same color was thermally pre-treated at different temperatures from 350 to 600 °C. The entire coating on the surface before 550 °C could not be removed, as shown in Figure 4.27. The steps which are mentioned in Figure 2.16 could also be observed. These results support the literature results<sup>60</sup>.



Figure 4.27. Coffee capsule samples after pre-heat treatment at 350, 400, 450, 500, 550, and 600 °C (from left to right).

Figure 4.28 shows the mass loss graph of thermally pre-treated samples at different temperatures and holding times in the furnace. In Figure 4.28, the highest mass loss was observed at 550 °C for 30 minutes holding time. After this temperature, a decrease in mass loss was observed because of oxidation. As seen in Figure 4.28, it was observed that increasing on holding time shows an increase in the mass of the sample because of increasing in oxidation tendency after 550 °C.

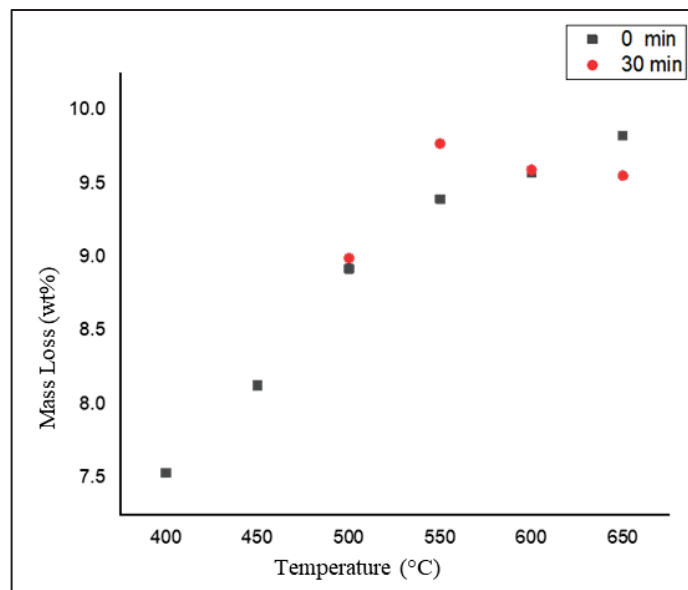


Figure 4.28. Mass loss of thermally pre-treated coffee capsule samples at different temperatures and holding times.

On the other hand, it was observed that mass loss increased with temperature increasing for no-holding time. It shows the effect of holding time and temperature on oxidation<sup>14, 89, 98</sup>. It was observed that when the holding time in the furnace was increased to 30 minutes, the suitable temperature for thermal pre-treatment was 550 °C and a decrease in mass loss occurred after 550 °C. When the holding time in the furnace was increased to 650 °C, a decrease in mass loss was again observed.

Figure 4.29 shows the SEM-EDS analysis of the CC heated from 520 to 550 °C without holding. The presence of carbon, magnesium, and titanium was observed. When the EDS results were taken from different parts of the sample were examined, it was observed that the 8011 series, which are alloy composition of CC, contains less amount of Mg, Si, and Ti content<sup>45</sup>.

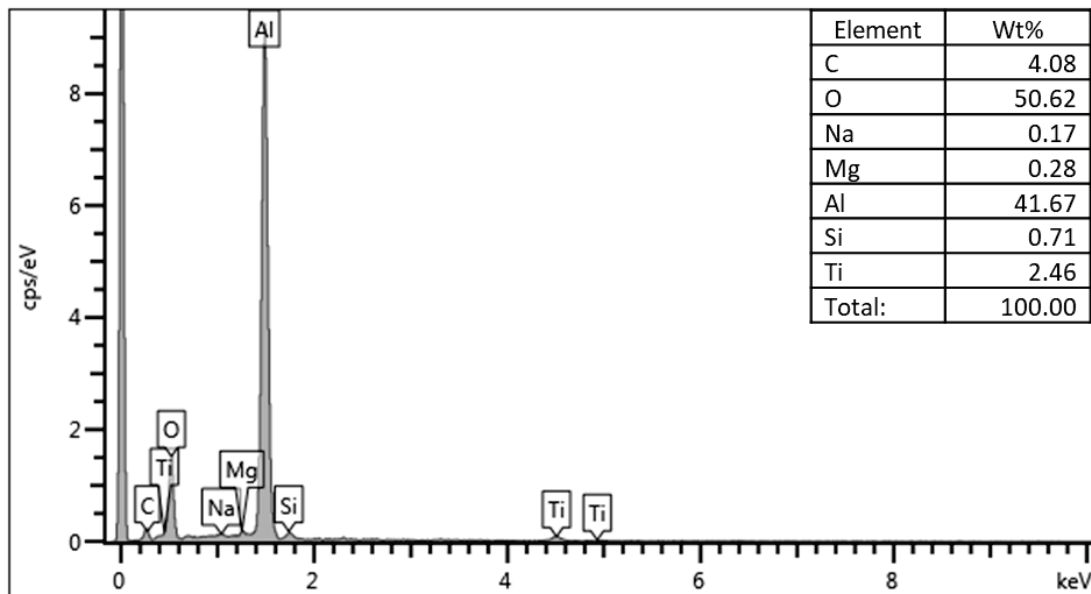


Figure 4.29. EDS result of CC sample kept in the oven from 520 to 550 °C for no-holding time.

EDS result of CC, which was heated from 520 to 550 °C and held for 15 minutes, was shown in Figure 4.30. When EDS results are compared in Figure 4.29 and Figure 4.30, it can be clearly observed that increasing on holding time decreases carbon content on the surface. A more successful de-coating process was observed with less oxidation. It shows the importance of holding time during thermal pre-treatment.

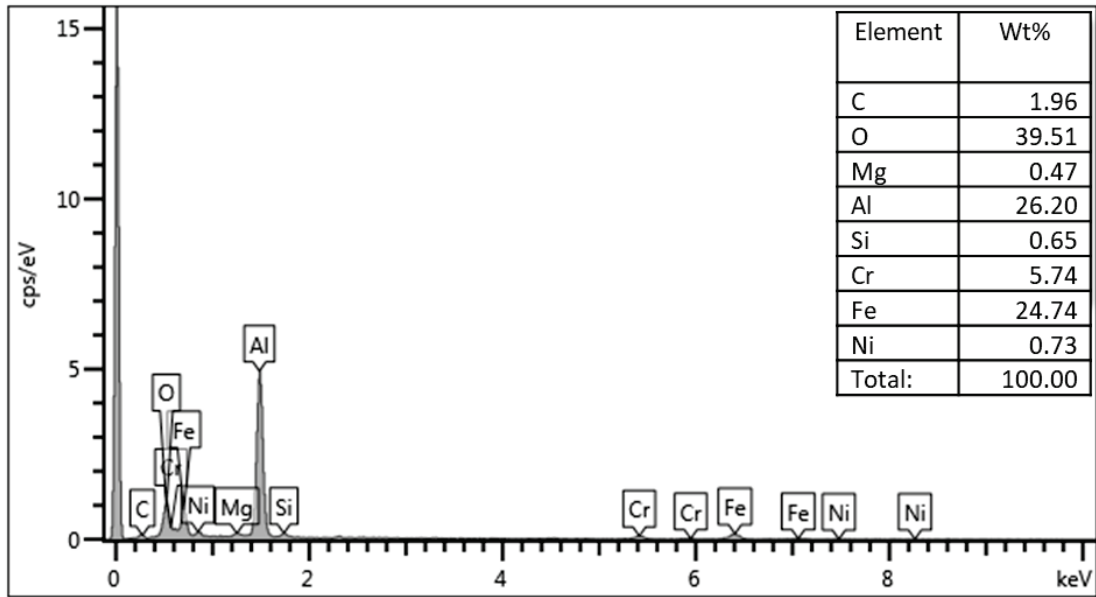


Figure 4.30. EDS result of CC sample kept in the oven from 520 to 550 °C for 15 minutes.

One of the two unpressed samples was cleaned from residues using ethanol and water, while the other was exposed to pre-heat treatment with residues, and the impact of these two conditions on the percent mass loss was plotted (Figure 4.31). It is obvious to see that in samples that were not cleaned of residues, mass loss increased in direct proportion to the amount of residue. This is because the residue in it is removed during the heat pre-treatment process.

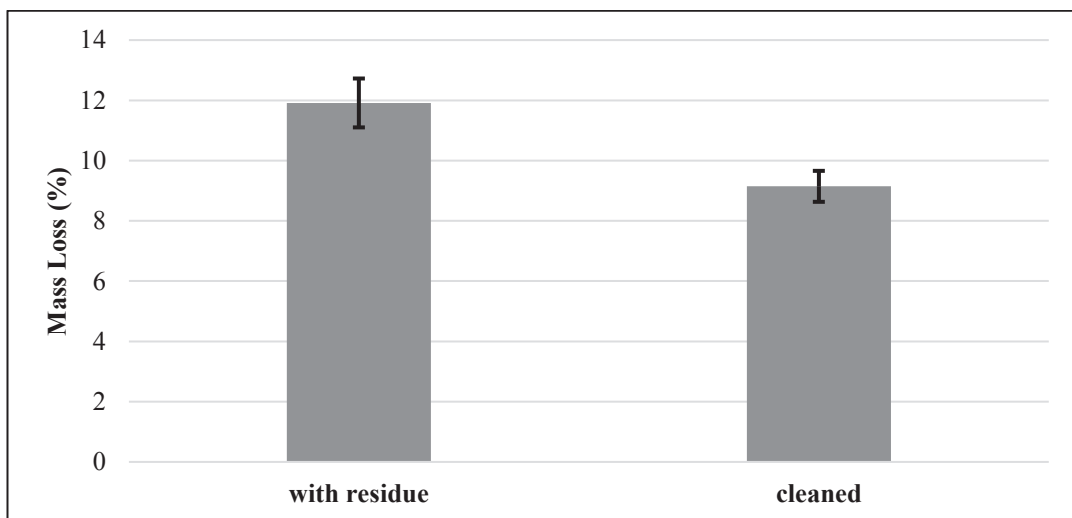


Figure 4.31. Mass loss of cleaned and uncleaned CC samples.

Figure 4.32 and Figure 4.33 show the TGA analysis result of the CC sample, which was heated up to 800 °C with 5 °C/min. Under O<sub>2</sub> and N<sub>2</sub> gas to understand the effect of O<sub>2</sub> on oxidation. In Figure 4.32, a decrease in mass is observed until 500 °C because of the combustion of different chemical compositions. When TGA results of CCs were analyzed, a percentage of mass increase was not significantly observed after 500 °C for the O<sub>2</sub> medium. Its reason is the alloy composition of the CC sample. The alloy composition of CC is 8011 series which contains only 0-0.1% Mg content<sup>45</sup>. Figure 4.33 also shows the TGA analysis result of the CC sample, which was heated up to 800 °C with 5 °C/min. Under an N<sub>2</sub> gas. Due to the absence of oxygen, combustion was not observed in the TGA analysis. Degradation of the coating of the sample could be detected after 200 °C due to the decreases in mass as explained in literature<sup>89, 96, 97</sup>. The mass of the coating can be understood in virtue of this graph because there is no oxidation. 7% mass loss is observed in the TGA that comes from the de-coating process. Different chemical compositions on the sample pyrolysis can be seen at different 3 rates, which are shown between 200 and 500 °C.

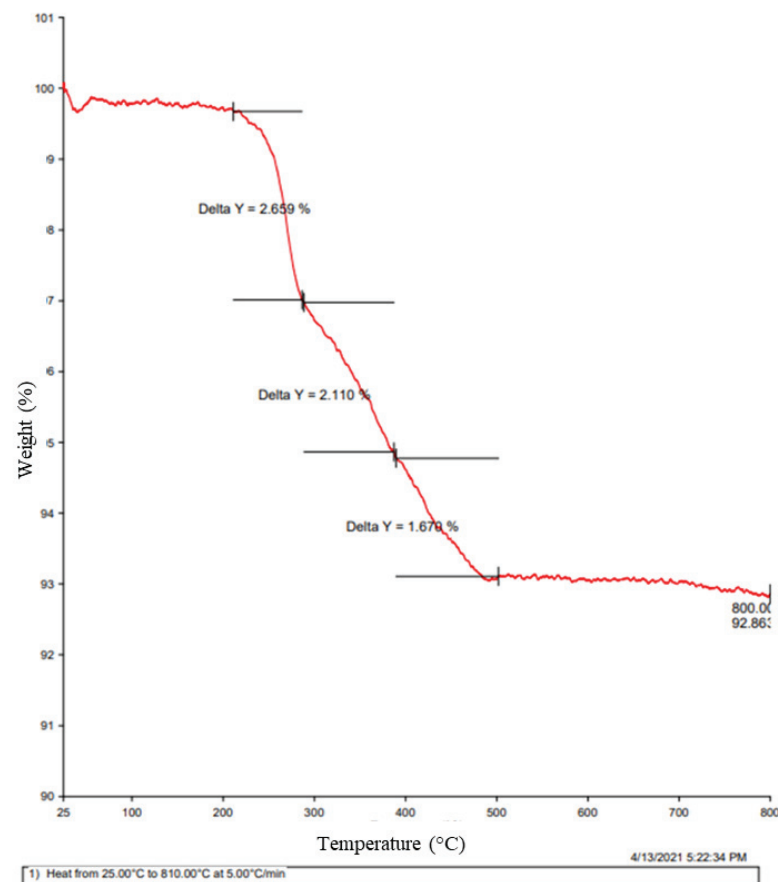


Figure 4.32. TGA analysis of CC sample under oxygen gas.

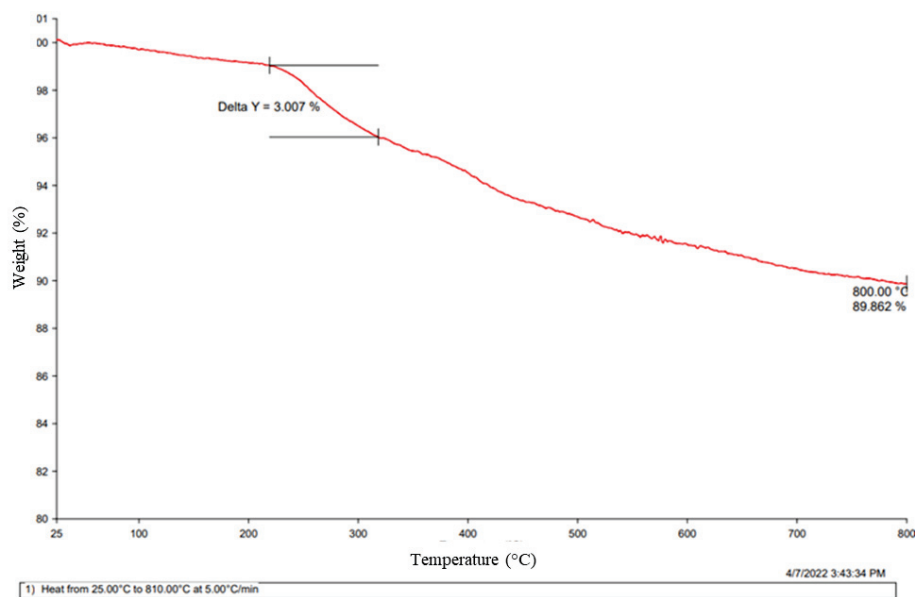


Figure 4.33. TGA analysis of CC sample under nitrogen gas.

### 4.3. Re-melting Results

In this section of the study, the de-coating effect was investigated on the metal yield of the used beverage can and coffee capsule samples which have different conditions (pressed, unpressed).

#### 4.3.1. Used Beverage Cans

The samples were directly remelted by using two different methods. In the first method, the crucible was heated up without any samples inside of it, and then after it was heated up, samples were put into the crucible. In the second method, the crucible was heated up gradually, and samples were de-coated.

UBC samples were directly remelted rapidly without a de-coating process after they dried at 100 °C for 2 hours in a drying oven. After the crucible was heated up, it was put into the crucible, and the flame was observed after putting it into the crucible because of the sudden combustion of organics on the beverage can. Figure 4.34 shows the flame after it is put into the crucible for rapid heating. The flame effect on metal yield could be observed by making this experiment.



Figure 4.34. Flame observation during the burning of organics on the sample surface.

The samples were heated up gradually with a crucible, and the samples were de-coated. Steps of the gradually heating of the pressed UBC samples are shown in Figure 4.35.

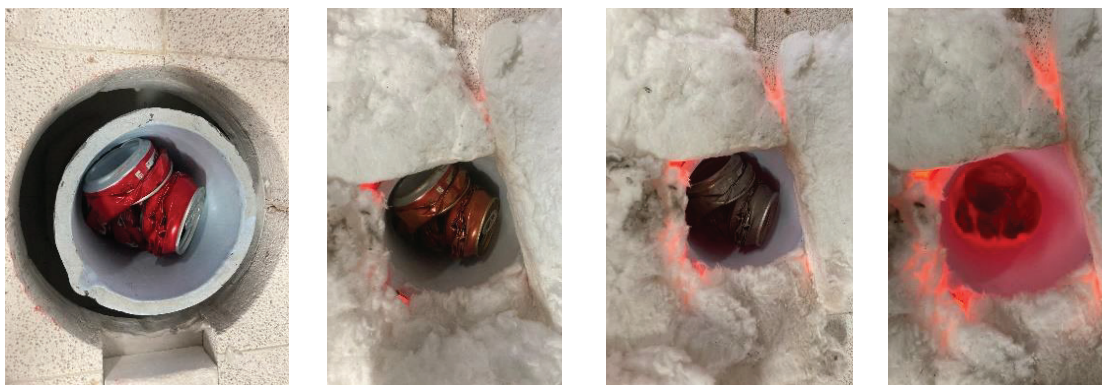


Figure 4.35. Steps of the slow heating of the UBC samples.

In the final step, dross was remelted under salt flux to determine the exact metal yield at the end of the procedure. Figure 4.36 is shown dross remelting under salt flux. Salt increases the coagulation of molten metal because salt melt prior to the metal, and it covers the metal; therefore, metal to oxygen contact is prevented<sup>104</sup>.

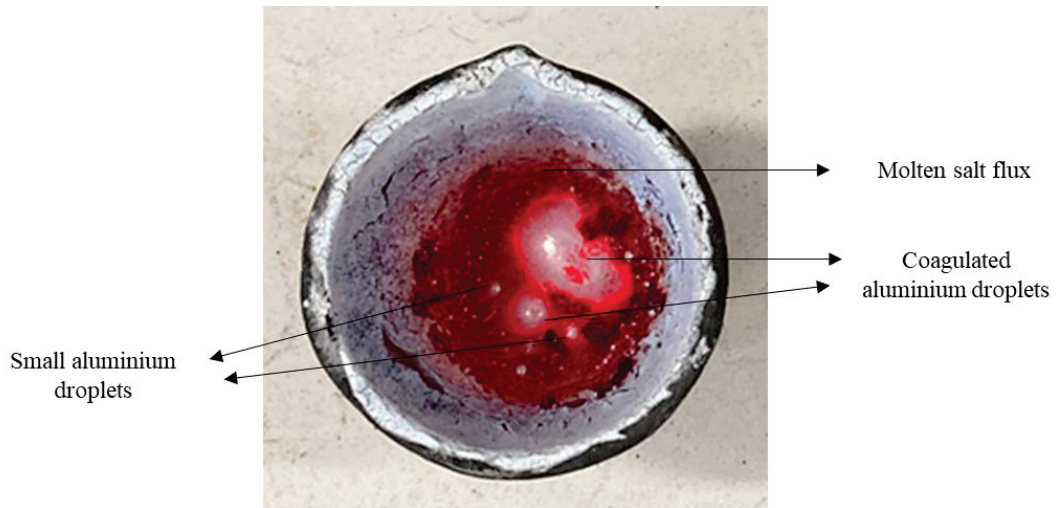


Figure 4.36. Coagulation of aluminium droplets in salt flux.

Figure 4.37 shows the slag mass graph for all the samples, and it can be observed that flame increase the formation of the dross because of uncontrolled temperatures during the rapid heating of the samples<sup>65</sup>. Therefore, samples should be de-coated to prevent flame's negative effect and decrease the dross amount.

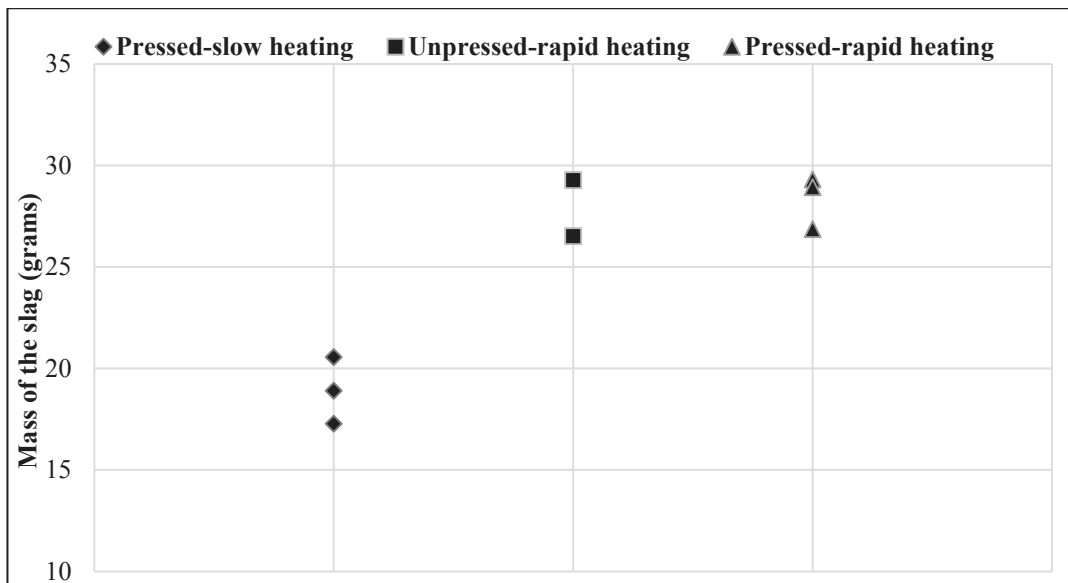


Figure 4.37. Slag mass after direct melting of UBC samples which have different conditions and heating rates.

Recycling of different types of beverage cans which are unpressed-rapid heating, pressed-slow heating, and pressed-rapid heating, was performed as an accompanying metal yield calculation. The percentage of metal yield was calculated using Eq. 15.

$$\text{Metal Yield} = \frac{\text{Total recovered metal (g)}}{\text{The initial mass of the sample (g)}} \times 100 \quad (\text{Eq. 15})$$

Figure 4.38 shows the metal yield of the samples at the end of the experiment. In the graph, the total recovered metal mass standard deviation is large for a pressed and de-coated sample because of the different pressing shapes of the sample. The standard deviation of the pressed and de-coated sample seems with a broad range because coated samples were pressed, and it was thermally pre-treated after the pressing step. Therefore, the percentage of VOC on the sample could be different because of different pressing shapes. It could affect metal yield. If the unpressed sample were firstly de-coated, then pressed and remelted, the standard deviation is going to decrease, whereas metal yield is going to increase because of less VOC. High temperatures also enhanced metal surface oxidation and metal loss<sup>65</sup>.

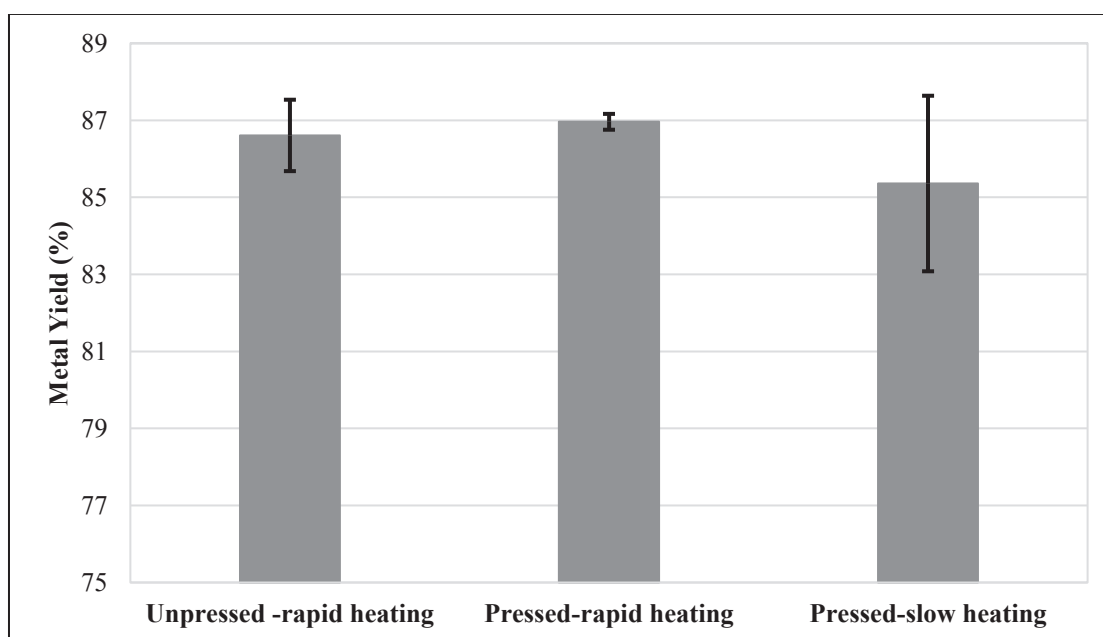


Figure 4.38. Effect of heating rate on metal yield for unpressed and pressed UBC samples.

The final step of the UBC remelting experiments includes different brands of UBC samples which are of the same volume. Three different brands of UBC sample, which introduces sugar, and one of the sugar-free samples were pressed and remelted with gradually heating. The results are shown in Figure 4.39. The results of the UBC sample, which has sugar-free residue of the international brand, show a slightly higher metal yield because of its lower VOC. High VOC leads to more oxidation. When compared with the



UBC sample, which has sugar residue, it can be seen that 3.5% difference in metal yield. When the same experiment was maintained on a local brand, it can be said that the metal yield of the sample decreased by about 2% and 1%, respectively. It is related to the organic content amount in the drink residue. If it introduces more organic content, it decreases metal yield at the end of the experiment.

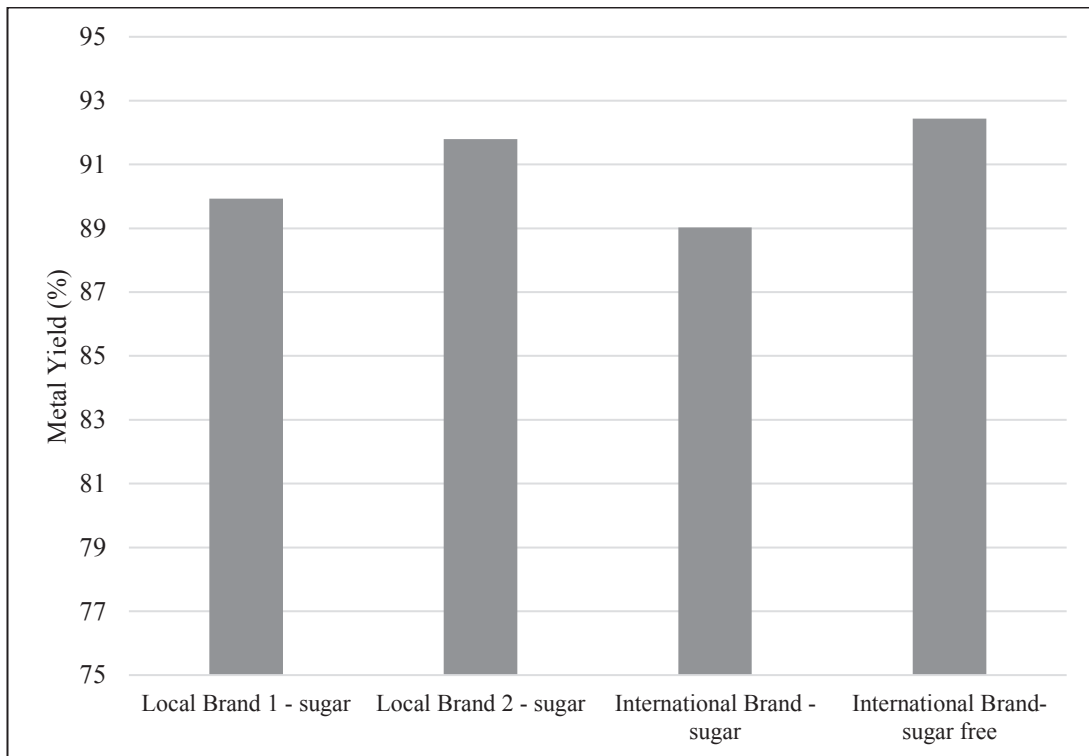


Figure 4.39. The metal yield of different brand UBC samples.

### 4.3.2. Coffee Capsules

Pressed and unpressed CC samples were remelted under salt flux with a 1:3 salt ratio by using NaCl, KCl, and CaF<sub>2</sub> because of the surface area of the sample and its low wall thickness. The thin walls tend to be more oxidation<sup>5</sup>. Figure 4.40 shows the remelted CC sample under salt flux to obtain coagulated metal at the end of the remelting experiment<sup>105</sup>.



Figure 4.40. Coagulated coffee capsule samples after re-melting under salt flux

Figure 4.41 represents the ratio of recovered metal mass and the number of CCs which was used in remelting experiment. It gives information about metal yield. The highest metal yield belongs to remelting of the de-coated then pressed sample re-melting under salt flux. It was firstly de-coated, then pressed; thus, the fold coming from pressing can be prevented as it was seen clearly that its standard deviation is lower than the metal yield of re-melting of the pressed sample under salt flux.

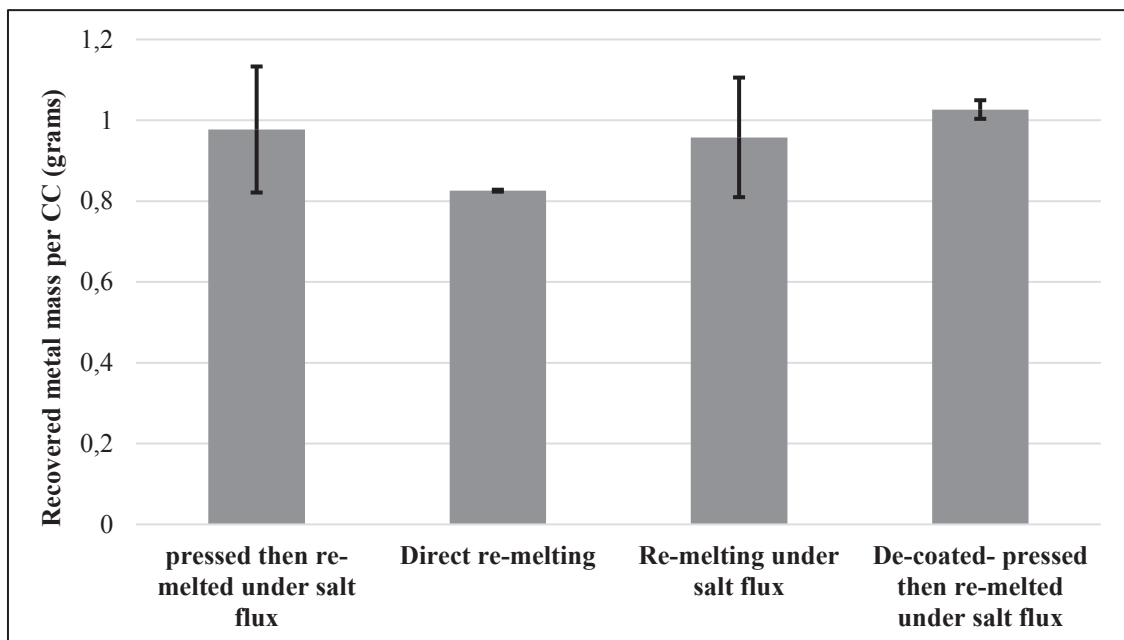


Figure 4.41. Metal yield comparisons of different pre-treated and melting combinations of CC samples.

The lowest metal yield belongs to direct remelting of the unpressed sample because the oxidation of the sample and metal loss are going to increase without using salt. Remelting experiments under salt flux for pressed sample did not increase metal yield significantly when compared with unpressed samples, and it could be seen because using salt prevent oxidation<sup>79-84</sup>. Due to the fact that salt melt prior to the metal and covers the metal thus, it removes metal contact with oxygen<sup>80, 81, 84, 86</sup>. As a result of this, it decreases the oxidation of the metal and metal loss.

## CHAPTER 5

### CONCLUSIONS

Recycling aluminium used in packaging products can be challenging due to short life cycles, low wall thicknesses, and coating materials on the surface. In this thesis, the characteristic properties and recyclability of aluminium beverage cans and coffee capsules were investigated. As deduced from detailed experimental investigations, the specific conclusions related to performed study can be drawn:

- Thermal pre-treatment temperature is more critical for alloys that have high Mg content due to their oxidation tendency (UBC lid).
- It was observed that UBCs and CCs contain 2.2% and 9% volatile organic content, respectively.
- Suitable thermal pre-treatment temperature was observed as keeping in the oven from 520 to 550 °C for 90 minutes for beverage can sample, 550 °C for 15-30 minutes was observed as a suitable condition for thermal pre-treatment of CC sample.
- Organic rest in food packaging can affect the metal/organic ratio and the metal yield accordingly. The metal yield can differ up to 3.5% due to the drink residues (sugar).
- Pressing the sample prior to the decoating process increases the amount of the entrapped carbonaceous materials and decreases the decoating efficiency.
- Samples with low wall thicknesses should be remelted under a salt flux to prevent oxidation and allow coalescence.
- Alloy quality differences might determine the oxidation and the metal yield. Cans with different brands showed a difference of up to 30% due to oxidation.
- Rapid heating of scraps might result in flaming, which promotes oxidation due to local overheating of the surface. Therefore, samples should be gradually de-coated to prevent the flame effect on the metal yield.

## CHAPTER 6

### FUTURE WORKS

- Alternative salts which can be used in salt flux for re-melting of thin-wall structure scraps can be searched instead of NaCl, KCl, and CaF<sub>2</sub> salt mixture to decrease salt cake formation.
- Metal quality could be tested by using RPT (Reduced Pressure Test) after recycling aluminium.
- Alloy quality differences of scraps and their effects on metal yield can be investigated deeper. The elemental composition of alloys can be determined by using XRF (X-Ray Fluorescence Spectroscopy) or OES (Optical Emission Spectroscopy).
- Toxic fume gases which emit during thermal pre-treatment can be analyzed by using Gas Chromatography.
- The critical temperature for oxidation of the scraps can be observed in detail by using DTA (Differential Thermal Analysis)

## REFERENCES

1. Aluminum.  
[http://amkay.com.hk/?page\\_id=81](http://amkay.com.hk/?page_id=81).
2. Khaji, K.; Al Qassemi, M., The role of anode manufacturing processes in net carbon consumption. *Metals* 2016, 6 (6), 128.
3. Millbank, P., Aluminium recycling vital to global supply chain. *Aluminium International Today* 2004, 16 (5), 44.
4. Aluminum Cans Recycling.  
[https://www.wastecare.com/Articles/Aluminum\\_Cans\\_Recycling.htm](https://www.wastecare.com/Articles/Aluminum_Cans_Recycling.htm).
5. Stacey, M., *Aluminium and Durability: Towards Sustainable Cities*. Cwningen Press: 2015.
6. Tabereaux, A. T.; Peterson, R. D., Aluminum production. In *Treatise on process metallurgy*, Elsevier: 2014; pp 839-917.
7. Manufacturing of alumina through Bayer process.  
<https://www.worldofchemicals.com/591/chemistry-articles/manufacturing-of-alumina-through-bayer-process.html>.
8. Hind, A. R.; Bhargava, S. K.; Grocott, S. C., The surface chemistry of Bayer process solids: a review. *Colloids and surfaces A: Physicochemical and engineering aspects* 1999, 146 (1-3), 359-374.
9. Birinci, M.; Ramazan, G., Ön Desilikasyon Amaçlı Boksit Zenginleştirme İşlemleri Üzerine Güncel Bir Değerlendirme. *Bilimsel Madencilik Dergisi* 2018, 57 (3), 197-218.
10. Habashi, F., Bayer's process for alumina production--a historical perspective. *Cahiers d'Histoire de l'Aluminium* 1994, 13.
11. Balomenos, E.; Pantias, D.; Paspaliaris, I., Energy and exergy analysis of the primary aluminum production processes: a review on current and future sustainability. *Mineral Processing & Extractive Metallurgy Review* 2011, 32 (2), 69-89.
12. Hall-Héroult Prosesi. <https://9lib.net/article/hall-h%C3%A9roult-prosesi-boksitten-al%C3%BCminyum-%C3%BCretimi.4yrd9d7q>.
13. Obaidat, M.; Al-Ghandoor, A.; Phelan, P.; Villalobos, R.; Alkhalidi, A., Energy and exergy analyses of different aluminum reduction technologies. *Sustainability* 2018, 10 (4), 1216.
14. Totten, G. E.; MacKenzie, D. S., *Handbook of Aluminum: Volume 2: Alloy production and materials manufacturing*. CRC press: 2003.

15. Asif, M.; Muneer, T.; Kubie, J., Sustainability analysis of window frames. *Building Services Engineering Research and Technology* 2005, 26 (1), 71-87.
16. Bauer, A.; Laska, C., LIBS for Automated Aluminum Scrap Sorting. *Application Note LIBS-028 (US)* 2018, 2018.
17. Glenn, J., Innovations in processing and sorting recyclables. *Biocycle* 1991, 32 (10), 35-39.
18. Arimoto, M.; Akiu, K.; Takuwa, T.; Oshida, E.; Yoshinaga, Y.; Asano, M., Pre-sorting technologies in a waste recycling system. *NKK TECH REV* 1998, (78), 39-43.
19. Schlesinger, M. E., *Aluminum recycling*. CRC press: 2006.
20. Kvande, H.; Haupin, W., Inert anodes for AI smelters: Energy balances and environmental impact. *Jom* 2001, 53 (5), 29-33.
21. *Bureau of International Recycling (BIR) Annual report 2019*; 3 March 2021.
22. Baker, M. D.; Moore, S. E.; Wise, P. H., The impact of 'Bottle Bill' legislation on the incidence of lacerations in childhood. *American journal of public health* 1986, 76 (10), 1243-1244.
23. All About Beverage Container Waste-Environmental Consequences of Beverage Container Waste.  
<https://www.container-recycling.org/index.php/all-about-beverage-container-waste/272-environmental-consequences-of-beverage-container-waste->.
24. Association, T. A. Increased Recycling Reduces Carbon Impact.  
<https://www.aluminum.org/aluminum-carbon-footprint-cut-half-over-30-years>.
25. R&D Around Driving Value From Red Mud Increases. <https://feeco.com/driving-value-from-red-mud/>.
26. Gil, A., Management of the salt cake from secondary aluminum fusion processes. *Industrial & engineering chemistry research* 2005, 44 (23), 8852-8857.
27. Green, J. A., *Aluminum recycling and processing for energy conservation and sustainability*. ASM International: 2007.
28. Kammer, C., *Aluminum Handbook, Vol. 1: Fundamentals and Materials*, Aluminium-Verlag. Inc: 1999.
29. Efficiency, E., *US Energy Requirements for Aluminum Production*. 2007.
30. Gerber, J., *Global aluminium recycling: a cornerstone of sustainable development*. International Aluminium Institute: 2006.
31. Flagel, J. Top 10 Uses of Aluminium in the Industry Today.  
<https://matmatch.com/resources/blog/top-10-uses-of-aluminium-in-the-industry-today/>.

32. Lumley, R., *Fundamentals of aluminium metallurgy: production, processing and applications*. Elsevier: 2010.
33. Barnes, K.; Sinclair, R.; Watson, D., *Chemical migration and food contact materials*. Woodhead publishing: 2006.
34. Gökelman, M.; Diaz, F.; Öner, I. E.; Friedrich, B.; Tranell, G., An assessment of recyclability of used aluminium coffee capsules. In *Light Metals 2020*, Springer: 2020; pp 1101-1109.
35. Kvithyld, A., Thermal decoating of aluminium scrap. 2003.
36. Biganzoli, L.; Gorla, L.; Nessi, S.; Grosso, M. J. W. m., Volatilisation and oxidation of aluminium scraps fed into incineration furnaces. 2012, 32 (12), 2266-2272.
37. LaKind, J. S., Can coatings for foods and beverages: issues and options. *International Journal of Technology, Policy and Management* 2013, 13 (1), 80-95.
38. Organosol.  
<https://www.corrosionpedia.com/definition/5754/organosol>.
39. Robertson, G. L., *Food packaging: principles and practice*. CRC press: 2005.
40. Debeaufort, F., Metal Packaging. *Packaging Materials and Processing for Food, Pharmaceuticals and Cosmetics* 2021, 75-104.
41. Brody, A. L., Taking a Closer Look at BPA and Its Alternatives Packaging.
42. Bomgardner, M., No clear winner in race to find non-BPA can linings. *Chem Engin News* 2013, 91 (6), 24-25.
43. Authority, E. F. S., Guidelines on submission of a dossier for safety evaluation by the EFSA of active or intelligent substances present in active and intelligent materials and articles intended to come into contact with food. *EFSA Journal* 2009, 7 (8), 1208.
44. Steglich, J.; Dittrich, R.; Rosefort, M.; Friedrich, B., Pre-treatment of beverage can scrap to increase recycling efficiency. *Journal of Materials Science and Engineering A* 2016, 3 (3-4), 57-65.
45. Aluminum 3104.  
[https://www.matweb.com/search/datasheet\\_print.aspx?matguid=aaaabe41a20a4ed2b48270f7f2ef1b2d](https://www.matweb.com/search/datasheet_print.aspx?matguid=aaaabe41a20a4ed2b48270f7f2ef1b2d).
46. *Capsule Coffee Machines Market by Product (Closed Source System, Open Source System ) by Application (Household, Commercial ) by Industry Analysis, Volume, Share, Growth, Challenges, Trends and Forecast 2018-2026*; PSMR-PSMR-01227; 2021; p 159.



47. Peter Lee, E. S., Olivia Bertham, Harry Symington, Nia Bell, Lucie; Sjögren., P. a. P. *Towards a circulareconomy – Waste management in the EU*; European Parliamentary Research Service, September 2017.
48. Gökelma, M.; Meling, I.; Soylu, E.; Kvithyld, A.; Tranell, G., A Method for Assessment of Recyclability of Aluminum from Incinerated Household Waste. In *Light Metals 2019*, Springer: 2019; pp 1359-1365.
49. Hu, Y.; Bakker, M.; De Heij, P. J. W. m., Recovery and distribution of incinerated aluminum packaging waste. 2011, *31* (12), 2422-2430.
50. *Global Beverage Cans Market Overview: 2020-2027*; 82879; February 2021.
51. Europe hits record beverage can recycling rate spurred by deposit return system. <https://www.packaginginsights.com/news/europe-hits-record-beverage-can-recycling-rate-spurred-by-deposit-return-systems.html>.
52. Blomberg, J.; Söderholm, P., The economics of secondary aluminium supply: An econometric analysis based on European data. *Resources, Conservation and Recycling* 2009, *53* (8), 455-463.
53. Sevigné-Itoiz, E.; Gasol, C. M.; Rieradevall, J.; Gabarrell, X., Environmental consequences of recycling aluminum old scrap in a global market. *Resources, conservation and recycling* 2014, *89*, 94-103.
54. Capuzzi, S.; Timelli, G., Preparation and melting of scrap in aluminum recycling: A review. *Metals* 2018, *8* (4), 249.
55. Khoei, A.; Gethin, D.; Masters, I. In *Design optimisation of aluminum recycling process using the Taguchi approach*, Proceedings of the Second International Conference on Intelligent Processing and Manufacturing of Materials. IPMM'99 (Cat. No. 99EX296), IEEE: 1999; pp 513-518.
56. Khoei, A.; Masters, I.; Gethin, D., Design optimisation of aluminium recycling processes using Taguchi technique. *Journal of Materials Processing Technology* 2002, *127* (1), 96-106.
57. Association., E. A. [www.eaa.net](http://www.eaa.net), .
58. Schwarz, H.-G., Aluminum production and energy. 2004.
59. Emes, C. B., Improvements in metal quality and operating efficiency through furnace design. *Aluminium International Today* 2002, *14* (1), 25.
60. Kvithyld, A.; Meskers, C.; Gaal, S.; Reuter, M.; Engh, T. A., Recycling light metals: Optimal thermal de-coating. *JOM* 2008, *60* (8), 47-51.
61. Jimenez, M.; Duquesne, S.; Bourbigot, S., Kinetic analysis of the thermal degradation of an epoxy-based intumescent coating. *Polymer Degradation and Stability* 2009, *94* (3), 404-409.

62. Ashish Why Does Sugar Turn Brown When Melted?  
<https://www.scienceabc.com/pure-sciences/sugar-turn-brown-melted-caramelization-maillard-reaction.html>.
63. Cui, J.; Kvithyld, A.; Roven, H. J., Degreasing of aluminum turnings and implications for solid state recycling. *Light Metals 2010* 2010.
64. McAvoy, B.; McNeish, J.; Stevens, W. In *The Alcan decoater process for UBC decoating*, International Symposium Recycling of Metals and Engineered Materials, 1990; p 2037214.
65. Kvithyld, A.; Engh, T. A.; Illés, R. In *Decoating of aluminum scrap in various atmospheres*, Light Metals-Warrendale-Proceedings-, TMS: 2002; pp 1055-1060.
66. Davies, S. B.; Masters, I.; Gethin, D. T., Numerical modelling of a rotary aluminum recycling furnace. *Recycling of Metals and Engineered Materials* 2000, 1113-1121.
67. Ünlü, N.; Drouet, M. G., Comparison of salt-free aluminum dross treatment processes. *Resources, conservation and recycling* 2002, 36 (1), 61-72.
68. Velasco, E.; Nino, J., Recycling of aluminium scrap for secondary Al-Si alloys. *Waste management & research* 2011, 29 (7), 686-693.
69. Lead Melting Furnace.  
<https://faridabadfurnacemanufacturer.wordpress.com/category/lead-melting-furnace/>.
70. Tilting rotary furnaces for non-ferrous metals and alloys recycling. <https://sa-foundry.com/product/modern-tilting-rotary-furnaces/?lang=en>.
71. Rooy, E., Aluminum Dross-Liability into Opportunity. *LIGHT METAL AGE-CHICAGO-* 1995, 53, 40-40.
72. Butnariu, I.; Butnariu, I.; Butnariu, D. In *Technological Researches Concerning a Decrease in the Losses Due to the Oxidation of Remelted Scrap from Aluminium Alloys*, Materials Science Forum, Trans Tech Publ: 2010; pp 71-74.
73. Choate, W. T.; Green, J. A., *US energy requirements for aluminum production: historical perspective, theoretical limits and new opportunities*. US Department of Energy, Energy Efficiency and Renewable Energy: 2003.
74. Whiteley, P. In *A historical perspective of aluminium casthouse furnace developments*, Materials Science Forum, Trans Tech Publ: 2011; pp 73-79.
75. Jana, R.; Randhawa, N. In *Production of silicomanganese alloy from low manganese containing leached sea nodules residue*, Eighth ISOPE Ocean Mining Symposium, OnePetro: 2009.
76. GALLO, R., Development evaluation and application of solid fluxes. *Modern casting* 2002, 92 (10), 30-33.

77. Gallo, R. In *Development, Evaluation, and Application of Granular and Powder Fluxes in Transfer Ladles, Crucible, and Reverberatory Furnaces*, 6th International Conference on Molten Aluminum Processing, 2001; pp 55-69.
78. Kamp, J.; Villwock, J.; Kraume, M., Drop coalescence in technical liquid/liquid applications: A review on experimental techniques and modeling approaches. *Reviews in Chemical Engineering* 2017, 33 (1), 1-47.
79. Van Linden, J.; Stewart, D., Molten salt flux composition effects in aluminum scrap remelting. In *Essential Readings in Light Metals*, Springer: 2016; pp 173-180.
80. Roy, R. R.; Sahai, Y., Coalescence behavior of aluminum alloy drops in molten salts. *Materials transactions, JIM* 1997, 38 (11), 995-1003.
81. Roy, R. R.; Sahai, Y., Interfacial tension between aluminum alloy and molten salt flux. *Materials transactions, JIM* 1997, 38 (6), 546-552.
82. Tenorio, J. A. S.; Carboni, M. C.; Espinosa, D. C. R., Recycling of aluminum—effect of fluoride additions on the salt viscosity and on the alumina dissolution. *Journal of Light metals* 2001, 1 (3), 195-198.
83. Tenorio, J. A. S.; Espinosa, D. C. R., Effect of salt/oxide interaction on the process of aluminum recycling. *Journal of light metals* 2002, 2 (2), 89-93.
84. Ye, J.; Sahai, Y., Interaction and interfacial tension between aluminum alloys and molten salts. *Materials transactions, JIM* 1996, 37 (9), 1479-1485.
85. Roy, R. R.; Sahai, Y., Wetting behavior in aluminum-alumina-salt systems. *Materials Transactions, JIM* 1997, 38 (6), 571-574.
86. Berry, M., The molecular mechanism of surface tension. *Physics Education* 1971, 6 (2), 79.
87. Milke, E.; Friedrich, B.; Sydykov, A.; Arnold, A. In *Solubility of CaF<sub>2</sub> in NaCl-KCl salt flux for Al-recycling and its effect on Al-loss*, Proceedings of EMC, 2005; pp 1537-1548.
88. Bolivar, R.; Friedrich, B., The influence of increased NaCl: KCl ratios on Metal Yield in salt bath smelting processes for aluminium recycling. *World of Metallurgy—ERZMETALL* 2009, 62, 366-371.
89. Evans, R.; Guest, G. J. S. A. S. L., *The aluminium decoating handbook*. 2002.
90. Perry, D. L., *Handbook of inorganic compounds*. CRC press: 2016.
91. Dispinar, D.; Campbell, J., Porosity, hydrogen and bifilm content in Al alloy castings. *Materials Science and Engineering: A* 2011, 528 (10-11), 3860-3865.
92. Capuzzi, S.; Timelli, G.; Capra, L.; Romano, L., Study of fluxing in Al refining process by rotary and crucible furnaces. *International Journal of Sustainable Engineering* 2019, 12 (1), 38-46.

93. Pigment.  
[https://www.chemicalbook.com/ProductCatalog\\_EN/1612.htm](https://www.chemicalbook.com/ProductCatalog_EN/1612.htm).
94. Organic pigments. [http://chemart.rice.edu/Organic\\_Pigments.html](http://chemart.rice.edu/Organic_Pigments.html).
95. Alade, O. S.; Mahmoud, M.; Al Shehri, D.; Ganiyu, S. A.; Al-Nakhli, A.; Bataweel, M., Kinetics of thermal decomposition of tar in the presence of air and nitrogen gas. *Energy & Fuels* 2019, 33 (10), 10167-10175.
96. UBC and Aluminium Scrap Decoaters.  
<https://www.presezzixtrusion.com/product/melting-technology/ubc-scrap-decoaters.html>.
97. Ceba de-coating unit for aluminium scrap.  
<https://www.cebasrl.com/products/aluminium/de-coating-unit-for-aluminium-scrap>.
98. Schmitz, C., *Handbook of aluminium recycling*. Vulkan-Verlag GmbH: 2006.
99. Echsler, H.; Hattendorf, H.; Singheiser, L.; Quadackers, W., Oxidation behaviour of Fe - Cr - Al alloys during resistance and furnace heating. *Materials and Corrosion* 2006, 57 (2), 115-121.
100. Steglich, J.; Friedrich, B.; Rosefort, M., Dross Formation in Aluminum Melts During the Charging of Beverage Can Scrap Bales with Different Densities Using Various Thermal Pretreatments. *JOM* 2020, 72 (10), 3383-3392.
101. Vallejo-Olivares, A.; Høgåsen, S.; Kvithyld, A.; Tranell, G., Effect of Compaction and Thermal De-coating Pre-treatments on the Recyclability of Coated and Uncoated Aluminium. In *Light Metals 2022*, Springer: 2022; pp 1029-1037.
102. Ask the experts: Diet Coke vs Coke Zero. <https://www.healthyfood.com/ask-the-experts/diet-coke-vs-coke-zero/>.
103. Zhang, J.; Li, N., Analysis on liquid metal corrosion–oxidation interactions. *Corrosion Science* 2007, 49 (11), 4154-4184.
104. Thoraval, M.; Friedrich, B. In *Metal entrapment in slag during the aluminium recycling process in tilting rotary furnace*, Proceedings of the European Metallurgical Conference, Dusseldorf, Germany, 2015; pp 14-17.
105. Besson, S.; Pichat, A.; Xolin, E.; Chartrand, P.; Friedrich, B. In *Improving coalescence in Al-Recycling by salt optimization*, Proceedings of EMC, 2011; p 1.

## ATTACHMENT

Table 8. Experimental parameters and results of thermal pre-treatment trials of CCs.

Experiment Number	Temperature (°C)	Holding Time (min.)	Avg. Mass Loss (%)
1	550	15	9.57
2	600		9.63
3	650		9.50
4	550	30	9.78
5	600		9.59
6	650		9.55
7	400	0	7.53
8	450		8.12
9	500		8.92
10	550		9.39
11	600		9.57
12	650		9.82

Table 9. Experimental parameters and results of thermal pre-treatment trials of UBCs.

Experiment Number	Condition of the Sample			Temperature (°C)	Holding Time (min.)	Avg. Mass Loss (%)
20-21	Clean	Pressed	Single Pressed (International Brand)	500	0	2.67±0.21
22				550	0	2.94
23-28				600	0	2.61±0.12
29-30				600	15	2.61±0.23
31-32				600	30	2.35±0.065
33		600	60	2.03		
34-36		Unpressed	International Brand	500	0	2.68±0.14

(cont. on next page)

**Table 9.(cont.)**

37-39	Clean	Unpressed	International Brand	550	0	2.69±0.15
40					15	2.70
41					30	2.85
42					45	2.60
43					90	3.16
44-46				600	0	2.31±0.05
47				630	30	5.67
48-57		Pressed	Bales (Mix of brands)	600	0	3.42±0.54
58-60					15	3.12±0.33
61-64	With Drink Residue	Unpressed	Sugar-free (International Brand)	600	0	2.36±0.13
65-71			Sugared (International Brand)	600		4.02±0.44
72-81			Sugared (Local Brand)	600		3.99±0.41